



1 Global Observations and Modeling of Atmosphere-Surface Exchange of Elemental  
2 Mercury – A Critical Review

3 W. Zhu<sup>1,2</sup>, C.-J. Lin<sup>1,3,\*</sup>, X. Wang<sup>1</sup>, J. Sommar<sup>1</sup>, X. W. Fu<sup>1</sup>, X. Feng<sup>1,\*</sup>

4 <sup>1</sup> State Key Laboratory of Environmental Geochemistry, Institute of Geochemistry, Chinese Academy of  
5 Sciences, Guiyang 550002, China

6 <sup>2</sup> Department of Chemistry, Umeå University, SE-901 87 Umeå, Sweden

7 <sup>3</sup> Center for Advances in Water and Air Quality, Lamar University, Beaumont, Texas 77710, United States

8

9 *Correspondence to:* C.-J. Lin ([jerry.lin@lamar.edu](mailto:jerry.lin@lamar.edu)) and X. Feng ([fengxinbin@vip.skleg.cn](mailto:fengxinbin@vip.skleg.cn))

10 C.-J. Lin, phone: +1 409 880 8761; fax: +1 409 880 8121; e-mail: [jerry.lin@lamar.edu](mailto:jerry.lin@lamar.edu)

11 X. Feng, phone: +86 851 85895728, fax: +86 851 85895095, e-mail: [fengxinbin@vip.skleg.cn](mailto:fengxinbin@vip.skleg.cn)

12

13 *Manuscript for the Special issue of “Data collection, analysis and application of speciated atmospheric mercury”*  
14 *in Atmospheric Chemistry and Physics (2015)*

15

16

17 **Abstract**

18       Reliable quantification of air-surfaces flux of elemental Hg vapor ( $\text{Hg}^0$ ) is crucial for understanding  
19 mercury (Hg) global biogeochemical cycles. There have been extensive measurements and modeling efforts  
20 devoting to estimating the exchange fluxes between the atmosphere and various surfaces (e.g., soil, canopies,  
21 water, snow, etc.) in past three decades. However, large uncertainty remains due to the complexity of  $\text{Hg}^0$   
22 bi-directional exchange, limitations of flux quantification techniques and challenges in model parameterization.  
23 In this study, we provide a comprehensive review on the state of science in the atmosphere-surface exchange of  
24  $\text{Hg}^0$ . Specifically, the advancement of flux quantification techniques, mechanisms in driving the air-surfaces Hg  
25 exchange, and modeling efforts are presented. Due to the semi-volatile nature of  $\text{Hg}^0$  and redox transformation of  
26 Hg in environmental media, Hg deposition and evasion are influenced by multiple environmental variables  
27 including seasonality, vegetative coverage and its life cycle, temperature, light, moisture, atmospheric  
28 turbulence, presence of reactants (e.g.,  $\text{O}_3$ , radicals, etc.) that drives the physicochemical process of Hg in the  
29 media where  $\text{Hg}^0$  exchange occurs. However, effects of these processes on flux have not been fundamentally and  
30 quantitatively determined, which limits the accuracy of flux modeling.

31       In this study, we compile an up-to-date global observational flux database and discuss the implication of  
32 flux data on global Hg budget. Mean  $\text{Hg}^0$  flux obtained by micrometeorological measurement did not appear to  
33 be significantly greater than the flux measured by dynamic flux chamber methods over unpolluted surfaces  
34 ( $p=0.16$ , one-tailed, Mann-Whitney  $U$  test). The spatio-temporal coverage of existing  $\text{Hg}^0$  flux measurements is  
35 highly heterogeneous with large data gaps existing in multiple continents (Africa, South Asia, Middle East,  
36 South America and Australia). The magnitude of evasion flux is strongly enhanced by human activities,  
37 particularly at contaminated sites.  $\text{Hg}^0$  flux observations in East Asia are comparatively larger in magnitude than  
38 the rest of the world, suggesting substantial reemission of previously deposited mercury from anthropogenic  
39 sources.  $\text{Hg}^0$  exchange over pristine surfaces (e.g., background soil and water) and vegetation need better  
40 constrains for global analysis of atmospheric Hg budget. The existing knowledge gap and the associated research  
41 needs for future measurements and modeling efforts for the air-surface exchange of  $\text{Hg}^0$  are discussed.

42



## 43 1. Introduction

44 Mercury (Hg) is a global pollutant of broad concerns due to its toxicity, bioaccumulation characteristics and  
45 adverse health effects (Driscoll et al., 2013), especially in its methylated forms such as monomethyl-mercury  
46 ( $\text{CH}_3\text{Hg}$ ) species and dimethyl-mercury ( $(\text{CH}_3)_2\text{Hg}$ ) (Clarkson and Magos, 2006). Fish consumption has been  
47 identified as the primary pathway for human exposure to  $\text{CH}_3\text{Hg}$  (Mergler et al., 2007; Mason et al., 2012), while  
48 the exposure through rice cultivated in areas with Hg pollution (e.g. mining and smelting areas) also poses a risk  
49 (Feng et al., 2008a; Zhang et al., 2010). To protect human health and the environment from the adverse effects of  
50 mercury, a global treaty “Minamata Convention for Mercury” that regulates Hg emission reduction from  
51 anthropogenic sources has been signed by 128 countries since October 2013 (UNEP Minamata Convention,  
52 2014). Emission of Hg into the atmosphere occurs from both natural processes and human activities. The release  
53 of Hg from natural surfaces has been estimated to account for two thirds of global emissions (Fig. 1). However,  
54 this estimate is subject to large uncertainty because of the challenges in quantifying the flux and in understanding  
55 the mechanisms involved in the exchange process of elemental mercury vapor ( $\text{Hg}^0$ ) (Selin, 2009; Zhang et al.,  
56 2009; Gustin, 2011; Zhang et al., 2012a).

57 Hg emitted from the anthropogenic sources include all atmospheric species: gaseous elemental Hg ( $\text{Hg}^0$ ,  
58 GEM), gaseous oxidized Hg (GOM), and particulate bound Hg (PBM) (Pacyna et al., 2006; AMAP/UNEP,  
59 2013), while evasion derived from the Earth’s surfaces is dominated by GEM (Gustin, 2011). Owing to the high  
60 deposition velocity of GOM and PBM (~1-2 orders higher than GEM) (Zhang et al., 2009), GOM and PBM are  
61 readily deposited locally and regionally while GEM is subject to long-range transport (e.g., hemisphere scale)  
62 and can deposit remotely from the emission sources (Lindberg et al., 2007; Gustin and Jaffe, 2010). Atmospheric  
63 Hg continuously goes through the deposition and re-emission cycle while undergoing physical and chemical  
64 transformations (Lin and Pehkonen, 1999).

65 Extensive efforts have been devoted to understanding the spatial and temporal pattern of  $\text{Hg}^0$  exchange flux.  
66 Geogenically Hg-enriched surfaces and anthropogenically polluted sites are strong Hg emission sources  
67 (Kocman et al., 2013). Emissions from natural sources and from previously deposited  $\text{Hg}^0$  on substrate surfaces  
68 are not analytically distinguishable using current measurement techniques (cf. Section 2). Direct measurement of  
69  $\text{Hg}^0$  flux from the background surfaces is difficult due to small vertical  $\text{Hg}^0$  concentration gradient (therefore low



70 flux) (Zhu et al., 2015a). Since the first application of a stainless steel dynamic flux chamber for  $\text{Hg}^0$  flux  
71 measurement over background lakes and soils in 1980s (Schroeder et al., 1989; Xiao et al., 1991), significant  
72 advancement in the experimental approaches (e.g., dynamic flux chamber, micrometeorological methods,  
73  $\text{Hg}^0/^{222}\text{Rn}$  flux ratio, enriched isotope tracer methods, open-path laser optical spectroscopic method, and  $\text{Hg}^0/\text{CO}$   
74 ratio) have been made (Sommar et al., 2013a). However, a standard protocol for  $\text{Hg}^0$  flux quantification does not  
75 exist (Gustin, 2011; Zhu et al., 2015b), which complicates the comparison and interpretation of flux data  
76 reported in the literature (cf. Section 4).

77 In this study, we present a comprehensive review on the global observation of  $\text{Hg}^0$  flux in the peer-reviewed  
78 literatures, and provide a state-of-the-science assessment on the air-surface exchange of  $\text{Hg}^0$ . Specifically, the  
79 advancement of flux quantification techniques, physicochemical factors driving the exchange process, existing  
80 field data of  $\text{Hg}^0$  flux, and modeling efforts for scaling up the measured flux for global assessment are  
81 synthesized. Furthermore, the spatial and temporal characteristics of  $\text{Hg}^0$  flux, as well as the underlying  
82 influencing factors are investigated. Key knowledge gaps, future directions for field measurements, and  
83 development of new-generation air-surface exchange model for  $\text{Hg}^0$  flux are discussed.

84

## 85 2. Advances in $\text{Hg}^0$ flux quantification methods

86 The theory and application of  $\text{Hg}^0$  flux measurement techniques have been documented extensively (Zhang  
87 et al., 2009; Gustin, 2011; Sommar et al., 2013a). Here we focus on the developments, advantages and  
88 disadvantages, and comparability and uncertainties of different flux quantification techniques. DFCs,  
89 micrometeorological techniques (MM), and bulk methods (e.g.,  $\text{Hg}^0/^{222}\text{Rn}$  flux ratio, enriched isotope tracers)  
90 are the mostly widely applied approaches for surface-atmosphere  $\text{Hg}^0$  flux quantification (Schroeder et al., 1989;  
91 Xiao et al., 1991; Kim and Lindberg, 1995; Kim et al., 1995; Cobos et al., 2002; Amyot et al., 2004; Olofsson et  
92 al., 2005; Obrist et al., 2006; Bash and Miller, 2008; Lin et al., 2012; Slemr et al., 2013; Zhu et al., 2013c), of  
93 which DFCs and MM techniques accounted for >95% of all observations documented to date (cf. Section 4).  
94 Open-path laser optical spectroscopic (LIDAR) method and  $\text{Hg}^0/\text{CO}$  ratio were applied to estimate Hg emission  
95 from area/regional sources (e.g. LIDAR: mining areas, industrial plants, geothermal sites;  $\text{Hg}^0/\text{CO}$  ratio:  
96 continental level atmospheric Hg transport) (Aldén et al., 1982; Edner et al., 1991; Sjöholm et al., 2004; Jaffe et



97 al., 2005; Fu et al., 2015a). There has not been a standardized protocol for any of the techniques (e.g.,  
98 instrumentation set-up, operation parameters) (Gustin, 2011; Zhu et al., 2015b). Recent collocated  
99 measurements and uncertainties analysis emphasized the importance of method standardization and processing  
100 of field data acquired by the measurement systems (Fritsche et al., 2008b; Converse et al., 2010; Zhu et al.,  
101 2015a). Application of appropriate flux measurement technique depends on the scalar detection accuracy, sensor  
102 response frequency and level of automation (Sutton et al., 2007). The traditional standard procedure of sampling  
103 ambient air  $\text{Hg}^0$  is by enhancement collection onto traps containing gold (Fitzgerald and Gill, 1979; Slemr et al.,  
104 1979). A wide-spread continuous  $\text{Hg}^0$  monitor is the automated dual channel, single amalgamation, cold vapor  
105 atomic fluorescence analyzer (Model 2537, Tekran Instruments Corp.), which relying on this principle. The  
106 certified detection limit is  $< 0.1 \text{ ng m}^{-3}$ . However, the pre-concentration procedure takes  $\geq 2.5$  min and therefore  
107 real-time, high-frequency data acquisition is not possible (Gustin, 2011; Fu et al., 2012b; Gustin et al., 2013;  
108 Gustin et al., 2015). Monitoring ambient air  $\text{Hg}^0$  with a higher frequency ( $\leq 1\text{Hz}$ ) can be achieved by using  
109 Lumex RA-915+ Zeeman atomic absorption spectrometry (AAS) analyzer operating without trap  
110 pre-concentration. However, the instrument has a detection limit  $\sim 1 \text{ ng m}^{-3}$  and therefore is preferred for  
111 industrial level studies but applicable under ambient  $\text{Hg}^0$  concentration (Holland K., 2005). More recently, high  
112 frequency (25 Hz) cavity ring-down spectroscopy (CRDS) sensor has been deployed for  $\text{Hg}^0$  concentration  
113 measurement, but it has a higher detection limit ( $> 0.35 \text{ ng m}^{-3}$ ) and suffers from sensor's baseline drifting and  
114 interferences with  $\text{O}_3$  (Fain et al., 2010; Pierce et al., 2013). Another laser technique, laser-induced fluorescence  
115 sensor, has been designed and successfully applied for up to one day continuous measurement with improved  
116 detection limit ( $\sim 15 \text{ pg m}^{-3}$ ) (Bauer et al., 2002; Bauer et al., 2014). However, both methods have not been yet  
117 proved to apply for long-term field measurement. The coupling with a commercial instrument (e.g. Tekran<sup>®</sup>  
118 2537) renders continuous and unattended flux measurements by DFC or MM techniques to be accomplished and  
119 are most widely deployed over various surfaces (cf. Section 4). However, this implementation is associated with  
120 a significant cost, for which the expense of the  $\text{Hg}^0$  analyzer is normally exciding that of the essential flux  
121 system.

122

123 **2.1 Dynamic flux chambers**



124 The DFC method (footprint generally  $<0.1 \text{ m}^2$ ) is a frequently used  $\text{Hg}^0$  flux measurement technique over  
125 soils, water surfaces, and low-stand grass due to its relatively low cost, portability, and versatility (Sommar et al.,  
126 2013a). DFCs operating under steady-state (Xiao et al., 1991; Carpi and Lindberg, 1998) and non-steady-state  
127 conditions (Rinklebe et al., 2009) are used in Hg research with the former configuration by far the most common.  
128 Dynamic flux bag (DFB) has been applied for flux measurement over tall grass and tree branches (Zhang et al.,  
129 2005; Graydon et al., 2006; Poissant et al., 2008). Laboratory mesocosms probing whole ecosystem Hg  
130 exchange have also been attempted; a  $180 \times 10^3 \text{ L}$  chamber ( $7.3 \times 5.5 \times 4.5 \text{ m}^3$ ) was deployed for quantifying  
131 soil-plant-atmosphere flux (Gustin et al., 2004; Obrist et al., 2005; Stamenkovic and Gustin, 2007; Stamenkovic  
132 et al., 2008). Construction materials such as fluorinated ethylene propylene (FEP) films and quartz have been  
133 recommended for DFCs due to its high actinic light transmittance and low blank (Kim and Lindberg, 1995; Carpi  
134 et al., 2007; Lin et al., 2012). DFCs volumes and flushing flow rates reported ranged from 1 to 32 L and 1.5 to 20  
135  $\text{L min}^{-1}$ , resulting a turnover time (TOT) ranging from 0.1 to 14 min (Eckley et al., 2010; Zhu et al., 2011). Using  
136 DFCs,  $\text{Hg}^0$  flux is calculated as:

$$137 \quad F = \frac{Q(C_{out} - C_{in})}{A} \quad (1)$$

138 where  $F$  is  $\text{Hg}^0$  flux ( $\text{ng m}^{-2} \text{ h}^{-1}$ ),  $Q$  is DFC internal flushing flow rate ( $\text{m}^3 \text{ h}^{-1}$ ),  $A$  is DFC footprint,  $C_{out}$  and  
139  $C_{in}$  are the  $\text{Hg}^0$  concentrations at the DFC outlet and inlet, respectively. Eq. (1) relies on mass balance  
140 calculation of two  $C_{out}$  and two  $C_{in}$  measurements alternately and assumes that the surface shear velocity over  
141 the DFC footprint is uniform and therefore results in a constant flux spatially over the wetted surface. Distinct  
142  $\text{Hg}^0$  fluxes have been observed using DFCs of different designed shapes under similar environmental conditions  
143 (Eckley et al., 2010). Lin et al. (2012) investigated the internal flow field and  $\text{Hg}^0$  concentration distribution in  
144 two commonly designed DFC (i.e. rectangular and dome-shaped chambers) showed that the airstream inside the  
145 DFCs is not uniform and the surface shear flow is divergent over the footprint, resulting in a non-uniform  $\text{Hg}^0$   
146 concentration gradient over the substrate surface. Eckley et al. (2010) systematically investigated effects of  
147 fabrication material, footprint, chamber dimensions including port positions and flushing flow rates on the  
148 measured  $\text{Hg}^0$  flux by DFCs. Consistent with previous studies, flushing flow rate is among the most influential



149 factor that if varied may induce up to one order of magnitude differences in the observed fluxes (Gustin et al.,  
 150 1999; Wallschläger et al., 1999; Gillis and Miller, 2000a; Lindberg et al., 2002c; Zhang et al., 2002).  
 151 Computational fluid dynamic modeling of DFC mass transfer indicated that smaller diffusion resistance at  
 152 higher flushing flow rate yielded higher measured flux. However, due to the non-uniform internal  $\text{Hg}^0$   
 153 concentration gradient, measured  $\text{Hg}^0$  flux from substrates may change unpredictably when flushing flow rate  
 154 varies (Eckley et al., 2010; Lin et al., 2012), which should be taken into consideration when flux obtained by  
 155 DFCs of different designs and flushing flow rates cannot be directly compared. Another limitation of DFCs is the  
 156 isolation of chamber internal surfaces from ambient condition. This excludes the effect of atmospheric  
 157 turbulence and therefore may cause a large uncertainty when using DFC data as in-put for scale-up estimation.  
 158 Lin et al. (2012) proposed an aerodynamic designed chamber (NDFC) which enables producing a uniform  
 159 surface friction velocity to link with ambient shear condition to rescale to the ambient flux using Eq. (2), which  
 160 allows to utilize ambient surface shear condition rather than artificial steady flushing flow rate to calculate flux:

$$161 \quad F = \frac{Q(C_{out} - C_{in})}{A} \cdot \frac{k_{mass(a)}}{k_{mass(DFC)}} \quad (2)$$

162 where  $k_{mass(a)}$  is the overall mass transfer coefficient under ambient condition, and  $k_{mass(DFC)}$  is overall mass  
 163 transfer coefficient in the DFC measurement area.

164 In addition to the uncertainties caused by varying flushing flow rates, altered short and long wave radiation  
 165 balance within DFCs resulting in a modified micro-environment were found to bias the observed flux (Zhu et al.,  
 166 2015a). DFC flux is measured through intermittent sampling of ambient and chamber air for  $\text{Hg}^0$  analysis using  
 167 a single detector (Lindberg et al., 2002c), which assumed that ambient  $\text{Hg}^0$  variability was negligible during air  
 168 sampling. At locations where significant variation in  $\text{Hg}^0$  concentration exist (e.g., sites with anthropogenic  
 169 emission sources), Eckley et al. (2011a) proposed a data assimilation protocol:  $|\Delta C_{oi}| > |\Delta C_{ii}|$  should be valid  
 170 for each calculated flux, otherwise the flux should be rejected ( $\Delta C_{oi}$  is the difference between  $C_{out}$  and the  
 171 average of two  $C_{in}$  which before and after taking  $C_{out}$ , while  $\Delta C_{ii}$  is the difference between above two  $C_{in}$ ).  
 172 The concern about influencing plant physiology restricts the deployment of small DFCs to short term field



173 measurements over the same vegetated plot. Given the small footprint and that  $\text{Hg}^0$  fluxes over terrestrial  
174 surfaces are profoundly variable in space and time, replication DFC measurements are thus preferred but often  
175 not carried out.

176

## 177 2.2 Micrometeorological methods

178 MM methods differ in measurement principles and spatial scale of flux footprint compared to DFCs and  
179 have the capability of measuring ecosystem-scale (typically hectare scale) flux under undisturbed conditions and  
180 represent a preferred flux quantification techniques over vegetated landscapes. MM techniques for background  
181  $\text{Hg}^0$  flux measurements currently comprises of relaxed eddy accumulation method (REA), aerodynamic gradient  
182 method (AGM), and modified Bowen-ratio method (MBR). The preferred MM technique, eddy covariance (EC),  
183 a direct flux measurement method without any applications of empirical constants, requires a fast response ( $\sim 10$   
184 Hz) gas analyzer, and has not been realized for regular  $\text{Hg}^0$  flux measurements (Aubinet et al., 2012). Recently,  
185 Pierce et al. (2015) reported the first field trial of CRDS-EC flux measurement over Hg enriched soils with a  
186 minimum flux detection limit of  $32 \text{ ng m}^{-2} \text{ h}^{-1}$ , insufficient for  $\text{Hg}^0$  flux measurement at most, if not all,  
187 background sites. Sommar et al. (2013a) and Zhu et al. (2015b) detailed the theory, computation, and existing  
188 MM approaches for measuring  $\text{Hg}^0$  fluxes. Gradient methods rely on quantifying the vertical concentration  
189 gradient (two or more heights sampling), turbulent parameters (AGM) or scalar concentration gradient (MBR),  
190 and scalar EC-fluxes. A major advantage of REA method is that REA up- and down-draft sampling conducted at  
191 one height, which overcomes the uncertainties associated with: (1) footprint differences due to two heights  
192 sampling in gradient methods, and (2) possible oxidation/reduction introduced forming or loss of  $\text{Hg}^0$  between  
193 the two heights. On the other hand, the analytical requirement for REA is more stringent than for the gradient  
194 methods, especially under windy conditions, increasing the demand on the precision of the sampling and  
195 chemical analysis (Zhu et al., 2015a).

196 REA method has been deployed for flux measurement for agricultural lands, forest canopies, wetlands, and  
197 urban settings (Cobos et al., 2002; Olofsson et al., 2005; Bash and Miller, 2009; Osterwalder et al., 2015;  
198 Sommar et al., 2013b). AGM method has been used over grasslands, agricultural lands, saltmarsh, landfills, and  
199 snow (Lee et al., 2000; Kim et al., 2001; Kim et al., 2003; Cobbett et al., 2007; Cobbett and Van Heyst, 2007;





200 Fritsche et al., 2008c; Fritsche et al., 2008b; Baya and Van Heyst, 2010). MBR method has been set up in  
201 grasslands, forest floor, agricultural lands, lakes, wetlands, and snow (Lindberg et al., 1992; Lindberg et al.,  
202 1995b; Lindberg et al., 1998; Lindberg and Meyers, 2001; Lindberg et al., 2002b; Brooks et al., 2006; Fritsche et  
203 al., 2008b; Converse et al., 2010). The theoretical and application requirement of micrometeorology is less  
204 restricted for large areas of uniform vegetation (or soil) in flat landscapes, where an atmospheric surface layer  
205 develops and the horizontal flux variability is low in the absence of pollution plumes and the flux above the  
206 surface remains constant with height (Wesely and Hicks, 2000). Under these turbulent exchange conditions, the  
207 flux acquired at the measurement height resembles the actual flux at the surfaces under measurement. There are  
208 several potential causes that can invalidate the above assumptions. For instance, the advection of  $\text{Hg}^0$  from the  
209 nearby sources to the measurement site may occur. It is known that local point sources of  $\text{Hg}^0$  can affect MM  
210 measurements downwind (Bash and Miller, 2007). Loubet et al. (2009) estimated such advection errors in  $\text{NH}_3$   
211 gradient flux to result in 2.1% to 52% of vertical flux at a monitoring site at 810m downwind of  $\text{NH}_3$  source (a  
212 farm building) implying a significant error contribution from advection. Large variation of  $\text{Hg}^0$  fluxes measured  
213 by MBR methods were also reported at nighttime as a result of advection in Nevada STORM project, however,  
214 the error have not been quantified (Gustin et al., 1999). For  $\text{Hg}^0$  flux over forest canopies, the influence of  
215 within-canopy source and sink terms on net ecosystem flux has not been evaluated. A multiple heights  
216 gradients/REA measurements is needed to resolve the true flux. Since there is not a reliable sensitive  $\text{Hg}^0$  sensor  
217 at high measurement frequency, an empirical multiplication factor or proxy scalar is required for computing all  
218 MM- $\text{Hg}^0$  flux (e.g., relaxation coefficient  $\beta$  derived from a selected proxy scalar for REA, eddy diffusivity  
219  $K_H$  derived from sensible heat for AGM, and proxy scalar such as sensible heat,  $\text{CO}_2$ , and  $\text{H}_2\text{O}$  flux for MBR)  
220 (Lindberg et al., 1995a; Edwards et al., 2005; Baya and Van Heyst, 2010; Zhu et al., 2015b). These empirical  
221 factors may introduce uncertainties when the proxy scalar value is small, which frequently occur during dawn  
222 and dusk and under the condition of low atmospheric turbulence. Proxy scalar inferred relaxation coefficient  
223 ( $\beta_{\text{CO}_2}$ ,  $\beta_T$ ,  $\beta_{\text{H}_2\text{O}}$ ) is typically not significantly different ( $\sim 0.56$ ) during a campaign above wheat agricultural  
224 land, while all  $\beta$  values were highly variable when the corresponding scalar flux was close to zero (Gronholm  
225 et al., 2008; Sommar et al., 2013b). Converse et al. (2010) reported  $\text{Hg}^0$  flux over a wetland meadow using



226 collocated AGM and MBR methods for four campaigns during an entire year. They found comparable fluxes in  
227 summer, while source/sink characteristics reversed between the two methods in fall and winter. Zhu et al. (2015b)  
228 found that AGM and MBR observed similar  $\text{Hg}^0$  fluxes when absolute sensible heat flux was  $>20 \text{ W m}^{-2}$ ; and the  
229 agreement is not satisfactory when the absolute sensible heat flux was  $<20 \text{ W m}^{-2}$ . Rejecting flux data collected  
230 under low turbulence conditions can bias the integrated flux over time (Mauder and Foken, 2004); and adequate  
231 data rejection and correction approaches need to be developed (Aubinet et al., 2012).

232

### 233 **2.3 Comparability of flux measured by micrometeorological and chamber methods**

234 Limited efforts have been devoted to understand the flux disparity caused by different flux measurement  
235 techniques. The Nevada STORMS project was the first attempt using eleven collocated measurements (7 DFC  
236 methods and 4 gradient-based MM methods) to simultaneously quantify  $\text{Hg}^0$  flux from Hg-enriched bare soils in  
237 September 1997 (Gustin et al., 1999; Lindberg et al., 1999; Poissant et al., 1999; Wallschläger et al., 1999). In the  
238 campaign, the mean fluxes obtained using MM methods were three times greater than those obtained by DFCs  
239 (Fig. 2a). One possible reason for the low observed flux by DFC was the small flushing flow rates  
240 (corresponding TOT: 1.1-24 min) that were not sufficient to eliminate the accumulated  $\text{Hg}^0$  in the DFC and  
241 subsequently suppressed  $\text{Hg}^0$  evasion. Later, Gustin and coworkers extended the study at the same site using a  
242 1-L polycarbonate DFC (TOT: 0.2 min) (Engle et al., 2001) and a MBR method (Gustin et al., 1999) in October  
243 1998 (Gustin, 2011). Although MBR show substantial flux variability, DFC and MM fluxes were not  
244 significantly different ( $p>0.05$ ) for dry and wet diel flux cycles (Fig. 2b). Two challenges in comparing MM and  
245 DFCs fluxes in these studies were the site heterogeneity ( $1.2\text{-}14.6 \mu\text{g Hg g}^{-1}$  in soil) and the footprint differences.  
246 The footprint of MM methods was estimated to be 40-70 m upwind the sampling sites ( $50\text{-}200 \text{ m}^2$ ) while DFC  
247 covered only  $0.12\text{-}0.3 \text{ m}^2$  (Gustin et al., 1999). Recently, an integrated field  $\text{Hg}^0$  flux methods intercomparison  
248 project measured  $\text{Hg}^0$  flux from a background homogenized agricultural field ( $\sim 45 \text{ ng Hg g}^{-1}$ ) using REA, AGM,  
249 MBR, a polycarbonate NDFC (TOT: 0.47 min), and a traditional quartz DFC (TDFC, TOT: 0.32 min) (Fu et al.,  
250 2008a; Zhu et al., 2015a, b). Overall, MM fluxes showed highly dynamic temporal variability while DFCs  
251 followed a gradual diel cycle similar to those temperature and solar irradiance. REA observed a broader flux  
252 distribution similar to  $\text{NH}_3$  and  $\text{CH}_4$  fluxes observed by MM techniques (Beverland et al., 1996; Moncrieff et al.,



253 1998; Nemitz et al., 2001). The median fluxes obtained by REA, AGM, and MBR were not significantly  
254 different (Friedman two-way analysis,  $\chi^2 = 1.29 < \chi^2_{p=0.05} = 5.99$ ). Over a three-week period, NDFC obtained a  
255 comparable mean flux with AGM and MBR which are approximately three times of the TDFC flux, implying  
256 that NDFC potentially reduced uncertainty using real atmospheric boundary shear condition to rescale (Lin et al.,  
257 2012). However, the correlation between NDFC/TDFC and MBR flux are weak because of high variability of  
258 MM flux (Fig. 2c). Pierce et al. (2015) observed comparable mean flux from simultaneous measurement using  
259 CRDS-EC, MBR, and DFC ( $849 \text{ ng m}^{-2} \text{ h}^{-1}$ ,  $1309 \text{ ng m}^{-2} \text{ h}^{-1}$ , and  $1105 \text{ ng m}^{-2} \text{ h}^{-1}$ , respectively) over Hg-enriched  
260 soils, similar flux patterns were recorded from CRDS-EC and MBR.

261 Fig. 3 showed the comparisons of  $\text{Hg}^0$  fluxes measured by MM methods and DFCs from relative  
262 homogeneous landscapes reported in the literature (cf. Section 4, substrate total Hg  $< 0.3 \mu\text{g Hg g}^{-1}$ ). MM  
263 methods yield a broader  $\text{Hg}^0$  flux range compared to DFCs methods, consistent with the field campaigns using  
264 collocated measurements (Zhu et al., 2015b). MM mean flux is higher than DFCs flux by a factor of two  
265 approximately, which may be a result by the fact that a large fraction of DFC measurements utilized a relative  
266 low TOT underestimating surface flux. However, Mann-Whitney  $U$  test indicated that the differences between  
267 the two methods are not significant ( $p=0.16$ , one-tailed). Probability of the two data sets showed positive  
268 skewness (4.2 and 3.9 for MM and DFCs, respectively) and kurtosis (19.6 and 27.2) caused by those high flux  
269 observations, likely resulting from asymmetrical data distribution as well as the differences in measurement site  
270 and periods. The flux data of MM methods in Fig. 3 were mostly obtained from agricultural fields (33%) and  
271 grasslands (36%) while the data of DFC methods were mainly from background sites (68%); and MM  
272 measurement generally covered a longer period (weeks to year) compared DFC measurements lasted a much  
273 shorter period (hours, days to a few weeks). Typically, significant  $\text{Hg}^0$  evasion is observed during daytime, while  
274 deposition, bi-directional exchange, or mild emission occurs at nighttime (cf. Section 4). Agnan et al. (2015)  
275 summarized MM and DFC fluxes observed in laboratory and during field campaigns over terrestrial substrates,  
276 and found that observed the median MM flux ( $-0.01 \text{ ng m}^{-2} \text{ h}^{-1}$ ,  $n=51$ ) was statistically smaller than the median  
277 DFC flux ( $0.5 \text{ ng m}^{-2} \text{ h}^{-1}$  and  $1.75 \text{ ng m}^{-2} \text{ h}^{-1}$  for flushing flow rate  $\leq 2 \text{ L min}^{-1}$  and  $> 2 \text{ L min}^{-1}$ ,  $p < 0.05$ ). They  
278 suggest elevated flushing flow rate generated partial vacuum inside DFC created artificial  $\text{Hg}^0$  flux from soil  
279 even at  $< 2 \text{ L min}^{-1}$ , although this is not supported by the large  $\text{Hg}^0$  concentration gradient (inside and outside



280 DFC) formed at low flushing flow rate (Zhang et al., 2002; Eckley et al., 2010). An alternative explanation is that  
281 MM measurements were predominantly deployed for background vegetated surfaces while DFC were mainly  
282 applied for soil surfaces, the difference in the source/sink characteristics over vegetation and bare soils may  
283 cause the difference in median fluxes.

284

### 285 **3. Factors influencing air-surface Hg<sup>0</sup> exchange**

#### 286 **3.1 Air-soil Hg exchange**

287 Meteorological parameters (solar radiation, soil/air temperature, atmospheric turbulence), soil substrate  
288 characteristics (e.g. Hg content, soil moisture, organic matters, porosity, and microbial activity), and ambient air  
289 characteristics (e.g. Hg<sup>0</sup> and O<sub>3</sub> concentration) can influence the air-surface exchange of Hg<sup>0</sup>. Changes of these  
290 factors force two controlling processes: (1) formation of evaporable Hg<sup>0</sup>, and (2) mass transfer of Hg<sup>0</sup>. Solar  
291 radiation has been found highly positively correlated with soil Hg<sup>0</sup> flux (Carpi and Lindberg, 1997; Boudala et  
292 al., 2000; Zhang et al., 2001; Gustin et al., 2002; Poissant et al., 2004a; Bahlmann et al., 2006), which is  
293 generally regarded as enhancing Hg<sup>II</sup> reduction and therefore facilitating Hg<sup>0</sup> evasion (Gustin et al., 2002).  
294 Actinic light spectral analysis suggested UV-B can reduce Hg<sup>II</sup> to Hg<sup>0</sup> over soil, while UV-A and visible light  
295 have a much lower enhancement (Moore and Carpi, 2005; Choi and Holsen, 2009b). Temperature is an  
296 important factor that promotes Hg<sup>0</sup> evasion, typically described by Arrhenius equation (Carpi and Lindberg,  
297 1997; Poissant and Casimir, 1998; Gustin et al., 2002). However, Arrhenius relationship cannot explain Hg<sup>0</sup> flux  
298 spikes at sub-zero temperatures, implying other mechanisms such as the expansion and contraction of liquid  
299 fraction in soil substrates occurred (Corbett-Hains et al., 2012). Atmospheric turbulence (i.e. wind, surface  
300 friction velocity) is another factor in driving the Hg<sup>0</sup> release from soil (Lindberg et al., 1999; Wallschläger et al.,  
301 1999). Increased turbulence enhances Hg<sup>0</sup> mass transfer and promotes Hg<sup>0</sup> desorption from soil (Gustin et al.,  
302 1997; Lindberg et al., 2002c; Zhang et al., 2002; Eckley et al., 2010; Lin et al., 2012).

303 Soil types, soil moisture and Hg content in soil are also important factors influencing observed Hg<sup>0</sup> flux (Xu  
304 et al., 1999; Kocman and Horvat, 2010; Lin et al., 2010a). Lindberg et al. (1999) observed that rainfall and  
305 irrigation enhances soil Hg<sup>0</sup> emission by an order of magnitude. Subsequent studies supported that adding water  
306 to dry soil promotes Hg reduction and that water molecular likely replaces soil Hg<sup>0</sup> binding sites and facilitates



307 Hg<sup>0</sup> emission. In saturated soil, Hg emission is suppressed because the soil pore space is filled with water, which  
308 hampers Hg mass transfer (Gillis and Miller, 2000b; Gustin and Stamenkovic, 2005). Pannu et al. (2014)  
309 investigated Hg<sup>0</sup> flux over boreal soil by manipulating soil moisture, maximum flux was observed at 60% soil  
310 moisture (water filled pore space), whereas flux become inhibited at 80%. Repeated rewetting experiments  
311 showed smaller increase in emission, implying “volatilizable” Hg<sup>0</sup> needs to be resupplied by means of reduction  
312 and dry deposition after a wetting event (Gustin and Stamenkovic, 2005; Song and Van Heyst, 2005; Eckley et al.,  
313 2011b). Soil organic matter (SOM) have a strong affinity with Hg<sup>0</sup> and form stable complexes with Hg<sup>II</sup> (Grigal,  
314 2003; Skyllberg et al., 2006), and therefore diminish soil Hg<sup>0</sup> efflux (Yang et al., 2007). Maclair et al. (2008)  
315 measured Hg<sup>0</sup> flux from sand (0.5 µg Hg g<sup>-1</sup>) spiked with humic substances; and found that Hg<sup>0</sup> flux decreased  
316 sharply by incremental addition of up to 0.1% of humic matter. Higher soil porosity has also been suggested to  
317 facilitate Hg<sup>II</sup> reduction and Hg<sup>0</sup> transfer from soil (Fu et al., 2012a). Microbial induced reduction can enhance  
318 Hg<sup>0</sup> evasion but to a less extent (Fritsche et al., 2008a; Choi and Holsen, 2009b). Higher flux has also been  
319 observed by increasing soil pH value (Yang et al., 2007).

320 Elevated ambient Hg<sup>0</sup> concentration has been found to suppress Hg<sup>0</sup> flux by reducing Hg<sup>0</sup> concentration  
321 gradient at the interfacial surfaces (Xin and Gustin, 2007). At locations where ambient Hg concentration is high  
322 (e.g., mining sites, landfills), deposition is predominately observed despite of the influence of meteorological  
323 factors (Bash and Miller, 2007; Wang et al., 2007b; Zhu et al., 2013c). Atmospheric O<sub>3</sub> was found to induce  
324 not-yet-understood chemical processes that enhance Hg<sup>0</sup> emission from soil in the dark (Zhang et al., 2008).  
325 Laboratory experiments showed that Hg<sup>0</sup> flux from soils with Hg<sup>II</sup> as the dominant species can be enhanced by  
326 1.7 to 51 times in the presence of O<sub>3</sub> (50-70 ppb), and be decreased by >75% over Hg<sup>0</sup>-amended soils (Engle et  
327 al., 2005). Environmental factors interacts naturally (e.g., irradiation and temperature), which can impose  
328 synergistic and antagonistic effects on forcing Hg<sup>0</sup> flux changes (Gustin and Stamenkovic, 2005). Fig. 4 shows  
329 the individual effects and synergism between solar radiation, air temperature, and water content on Hg<sup>0</sup> flux from  
330 a typical low organic content soil (~1.5 wt %) (Lin et al., 2010a). All three individual factors enhance flux by  
331 90%-140%, while two-factor synergetic effect accounts for 20%-30% enhancement.

332

### 333 3.2 Air-vegetation Hg<sup>0</sup> exchange



334 Vegetation alters air-ecosystem  $\text{Hg}^0$  flux through (1) changing environmental variables at ground surfaces  
335 (e.g., reducing solar radiation, temperature, and friction velocity) (Gustin et al., 2004), and (2) provide active  
336 surface for Hg uptake. Carpi et al. (2014) reported forest floor soil fluxes of  $-0.73 \pm 1.84$  and  $0.33 \pm 0.09 \text{ ng m}^{-2} \text{ h}^{-1}$   
337 from intact New England and Amazon forest floors, respectively. Substantial emission fluxes at  $9.13 \pm 2.08$ ,  
338  $21.2 \pm 0.35 \text{ ng m}^{-2} \text{ h}^{-1}$  were observed after deforestation suggested forest coverage effectively reduced ground  
339 floor  $\text{Hg}^0$  emission. More importantly, air-plant interaction increases the complexity of air-terrestrial Hg  
340 exchanges; and the role of vegetation as a source or a sink of atmospheric Hg has been in debates in the literature.  
341 Lindberg et al. (1998) observed a significant  $\text{Hg}^0$  emission from forest canopies in Tennessee and Sweden  
342 ( $10\text{-}300$  and  $1\text{-}4 \text{ ng m}^{-2} \text{ h}^{-1}$ ); estimated annual  $\text{Hg}^0$  emission from global forest to be 800-2000 tons; and  
343 emphasized the need for a re-assessment on this potentially important source. Based on the observed Hg  
344 presence in xylem sap (Bishop et al., 1998), plant has been hypothesized as a conduit for releasing geospheric Hg  
345 to the atmosphere (Leonard et al., 1998a, b). Subsequent models simply treated plant emission as a function of  
346 evapotranspiration rate (Xu et al., 1999; Bash et al., 2004; Gbor et al., 2006; Shetty et al., 2008). However, recent  
347 measurement suggested that air-surface exchange of  $\text{Hg}^0$  is largely bidirectional between air and plant and that  
348 growing plants act as a net sink (Ericksen et al., 2003; Stamenkovic et al., 2008; Hartman et al., 2009). Stable Hg  
349 isotope tracer studies have shown that Hg in soils cannot be translocated from roots to leaf due to the transport  
350 barrier at the root zone (Rutter et al., 2011b; Cui et al., 2014), suggesting that the source of Hg in leaf is of  
351 atmospheric origin.

352 Hg concentration in foliage is generally influenced by the level of air  $\text{Hg}^0$  present in air  $\text{Hg}^0$  (Ericksen et al.,  
353 2003; Frescholtz et al., 2003; Ericksen and Gustin, 2004; Millhollen et al., 2006a; Fay and Gustin, 2007a; Niu et  
354 al., 2011). Climate factors (e.g., solar irradiation, temperature), biological factors (e.g., leaf age, plant species),  
355 and ambient air components (e.g.,  $\text{CO}_2$ ) also significantly influence on foliar  $\text{Hg}^0$  flux (Rea et al., 2002;  
356 Millhollen et al., 2006a; Millhollen et al., 2006b; Fay and Gustin, 2007a; Bushey et al., 2008; Stamenkovic and  
357 Gustin, 2009; Rutter et al., 2011a). For instance, higher Hg concentration found at the bottom aged leaf suggest  
358 the influence of longer exposure time (Bushey et al., 2008) over an immediate source from soil (Frescholtz et al.,  
359 2003). Stomatal and non-stomatal (e.g., cuticle) processes are both viable pathways for bidirectional Hg  
360 exchange (Stamenkovic and Gustin, 2009). Stomatal process may play a predominant role as Hg accumulated on



361 cuticle surface was generally <10% of total Hg content in leaf (Rutter et al., 2011a; Laacouri et al., 2013). Solar  
362 radiation, temperature, and CO<sub>2</sub> concentrations regulating plant stomatal activity may therefore affect Hg uptake  
363 and gas exchange. For instance, high air-vegetation Hg<sup>0</sup> flux observed during daytime show deposition, opposite  
364 to daytime evasion observed over other terrestrial surfaces (cf. Section 4.3) (Stamenkovic et al., 2008). In  
365 addition, Hg in leaf has been shown to be assimilated into leaf biomass during the growing stage (Bash and  
366 Miller, 2009), suggesting Hg uptake occurs with plant assimilation metabolism.

367 It has been proposed that Hg in leaf can be classified as two forms: (1) exchangeable Hg which can be  
368 re-emitted back to the atmosphere, and (2) biological assimilated Hg retained in leaf (Rutter et al., 2011a).  
369 However, whether or not Hg<sup>0</sup> can be oxidized after uptake into tissue, and the possibility of assimilated Hg being  
370 reemitted from leaf (e.g., reduction of leaf retained Hg<sup>II</sup> or un-oxidized Hg<sup>0</sup> originally from ambient air) remain  
371 unclear. Many studies observed a so-called “compensation point” denoting the interfacial concentration of Hg  
372 that drive the concentration gradient for bi-directional air-vegetation exchange of Hg<sup>0</sup> (Hanson et al., 1995;  
373 Poissant et al., 2008; Bash and Miller, 2009). However, the hypothesis of compensation point does not explain  
374 the accumulation of Hg in vegetation pool. Recent Hg isotopic fractionation studies show promise for exploring  
375 air-leaf Hg exchange mechanism. Demers et al. (2013) reported a kinetic mass dependent fractionation (MDF,  
376  $\delta^{202}\text{Hg}$ ) of -2.89‰ during air-leaf Hg exchange from air to leaf. The result indicated that uptake of atmospheric  
377 Hg by leaf occurs, and the deposited Hg is likely to be chemically bonded in leaf with sulfur and nitrogen  
378 functional groups in enzymes within stomatal cavities (Rutter et al., 2011a), rather than with carboxylic ligands  
379 on leaf surface. Another important finding is the negative mass independent fractionation (MIF,  $\Delta^{199}\text{Hg}$ ) of Hg of  
380 -0.19‰ to -0.29‰, correlated well with Hg<sup>II</sup> photochemical reduction by low molecular mass organic matter  
381 with sulfur-containing ligands (Zheng and Hintelmann, 2010). This implies that the Hg reemission may result  
382 from revolatilization of chemical bounded Hg in leaf. However, they did not rule out the potential influence of  
383 PBM and GOM that deposit on the leaf, which may undergo partial uptake by plant with the remaining being  
384 reemitted back to the atmosphere.

385

### 386 3.3 Air-water Hg exchange

387 Bulk method, DFC and MM methods have been utilized in air-water Hg<sup>0</sup> flux measurement. Bulk methods

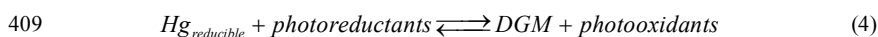


388 is the most widely utilized approach for oceanic surface (>80% of the field data, Table 1). Sommar et al. (2013a)  
 389 summarized the methodologies of the bulk method, which generally controlled by both kinetic (overall mass  
 390 transfer coefficient,  $k$ ) and thermodynamic (partial pressure related concentration gradients) forcing  
 391 (Wanninkhof, 1992; Wanninkhof et al., 2009; Kuss et al., 2009; Kuss, 2014):

$$392 \quad F = k \times (DGM - GEM/H'_T) = 0.31 \times U_{10}^2 \times \left( \frac{\nu}{600 \times D_{Hg^0}} \right)^{-0.5} \times (DGM - GEM/H'_T) \quad (3)$$

393 where DGM is dissolved gaseous Hg concentration in the surface water film, GEM is near surface gas  $Hg^0$   
 394 concentration,  $H'_T$  is dimensions Henry's law constant,  $U_{10}$  is wind speed at 10m,  $\nu$  is the water kinematic  
 395 viscosity, and  $D_{Hg^0}$  is  $Hg^0$  diffusion coefficient in water. Fig. 5 shows air-surface exchange processes and  
 396 transformation of DGM in water phase. From a kinetic point of view, the overall mass transfer coefficient of  $Hg^0$   
 397 is described by a molecular diffusivity in the water and gas film. Since the mass transfer boundary layer of water  
 398 has much higher resistance than the gaseous layer for sparingly soluble  $Hg^0$ , the overall mass transfer coefficient  
 399 is limited by water transfer velocity (Eq. 5) (Kim and Fitzgerald, 1986). Surface wind speed is an important  
 400 driving force enhancing the mass transfer coefficient in water (Qureshi et al., 2011b),  $D_{Hg^0}$  has been  
 401 experimentally determined as a function of temperature ( $T$ , Kelvin) for freshwater ( $D_{Hg^0}^{fresh} = 0.0335e^{-18.63/RT}$ ,  $R$   
 402 represents gas constant) and seawater ( $D_{Hg^0}^{sea} = 0.0011e^{-11.06/RT}$ ) (Kuss, 2014).

403 Processes controlled the concentration of DGM in surface water directly regulated air-water  $Hg^0$  flux.  
 404 Photochemically induced  $Hg^{II}$  reduction is the predominant pathway of DGM formation in surface water (Amyot  
 405 et al., 1994; Amyot et al., 1997a; Amyot et al., 1997b; Costa and Liss, 1999; Lalonde et al., 2001; Zhang and  
 406 Lindberg, 2001; Feng et al., 2004). Zhang (2006) summarized Hg photochemical redox chemical process. Eq. (6)  
 407 resembling a simplified scheme of gross photo-reactions governing the DGM pool in surface waters (O'Driscoll  
 408 et al., 2006; O'Driscoll et al., 2008; Qureshi et al., 2010):



410  $Fe^{III}$  has been reported to enhance sunlit photo-reduction in natural water (Lin and Pehkonen, 1997; Zhang and





411 Lindberg, 2001). Complexes of  $\text{Fe}^{\text{III}}$ -natural organic ligands was hypothesized to undergo photolysis to form  
412 reactive intermediates (e.g., organic free radicals) capable of reducing  $\text{Hg}^{\text{II}}$ . Dissolved organic matter (DOM)  
413 serving as electron donor and complexation agent in the natural water is the most important precursor for  
414 formation of photo-reductants (Ravichandran, 2004; Vost et al., 2011; Zhang et al., 2011). Similarly, irradiation  
415 derived photo-oxidant may oxidize DGM simultaneously and reduce Hg evasion from water. Reactive radicals  
416 (e.g.,  $\cdot\text{O}_2$ ,  $\cdot\text{OH}$ ) produced through DOM,  $\text{NO}_3^-$  photolysis have been identified as possible oxidants (Lin and  
417 Pehkonen, 1997; Zhang and Lindberg, 2001; Zhang et al., 2012b). In addition,  $\text{Cl}^-$  was reported to enhance  
418 photo-oxidation by stabilizing the oxidative products ( $\text{HgCl}_n^{2-n}$ ) and facilitating oxidation via formation of  
419 highly oxidizing ligand ( $\text{Cl}_2^{\ominus}$ ) (Yamamoto, 1996; Lalonde et al., 2001; Sun et al., 2014). Secondary radicals (e.g.,  
420  $\text{CO}_3^{\cdot-}$ ) can sometimes act as a photo-oxidant (He et al., 2014). Field studies also observed DGM and  $\text{Hg}^0$  flux  
421 peaks in the nighttime, suggesting the importance of dark reduction (O'Driscoll et al., 2003; Zhang et al., 2006b;  
422 Fu et al., 2013b). Dark abiotic redox transformation is the most important pathway (Fig. 5). Although dark  
423 abiotic reduction takes place mainly in the anoxic environment (Gu et al., 2011; Zheng et al., 2012), it also occurs  
424 in the oxic condition at a lower reaction rate (Allard and Arsenie, 1991). Natural organic matter shows reducing,  
425 oxidizing, and complexing properties with Hg in the anoxic environment due to its diversity functional groups  
426 (e.g., thiols group, quinones and non-quinoid structures, carboxyl group) (Gu et al., 2011; Zheng et al., 2012;  
427 Zheng et al., 2013). Although aqueous liquid Hg droplet can be rapidly oxidized in oxygenated chloric water,  
428 DGM is unable to be oxidized under such conditions (Amyot et al., 2005).

429 Biological redox transformation is another important DGM cycling pathway. Ariya et al. (2015) reviewed  
430 the biological processes in Hg redox transformation, which contains phototrophic and chemotrophic Hg redox  
431 processes. Aquatic algae, cyanobacteria, and diatoms involved phototrophic Hg reduction was positively  
432 correlated with photosynthetic activities, which is likely a bio-detoxification process (Ben-Bassat and Mayer,  
433 1975; Kuss et al., 2015). In addition, photo-reactivation of DOM and  $\text{Fe}^{\text{III}}$  facilitates  $\text{Hg}^{\text{II}}$  reduction through algae  
434 (Deng et al., 2009). Kuss et al. (2015) reported that cyanobacteria-light synergetic and photochemical  
435 transformation equally contributed to  $\sim 30\%$  DGM production in Baltic Sea, while low-light production  
436 contributed  $\sim 40\%$ , highlighting the importance of biotic reduction. Two pathways have been identified for  $\text{Hg}^{\text{II}}$



437 reduction by bacteria. The first is reduction by Hg-resistant microorganisms where  $\text{Hg}^{\text{II}}$  is reduced in cell's  
438 cytoplasm by mercuric reductase and transported out as  $\text{Hg}^0$  (Barkay et al., 2003); the other is  $\text{Hg}^{\text{II}}$  reduced by  
439 Hg-sensitive dissimilatory metal-reducing bacteria utilizing iron and/or manganese as terminal electron acceptor  
440 during respiration (Wiatrowski et al., 2006). Intracellular oxidation was supposed to be mediated by oxidase  
441 (Siciliano et al., 2002), while extracellular thiol functional groups on cell membrane also shows capability to  
442 oxidize  $\text{Hg}^0$  under anoxic environment (Colombo et al., 2013; Hu et al., 2013). A review of genetic-based  
443 microbial Hg redox transformation can be found in Lin et al. (2011).

444

#### 445 **3.4 Air-snow Hg exchange**

446 Schroeder et al. (1998) reported episodes of unexpected low  $\text{Hg}^0$  concentrations in the Arctic air during  
447 spring time, so-called atmospheric mercury depletion events (AMDEs), through an arrays of photochemically  
448 initiated oxidation by halogens (Lindberg et al., 2002a; Sommar et al., 2007; Moore et al., 2014). The  
449 phenomena was finally confirmed widespread in the coastal Polar Regions. During AMDEs, a large amount of  
450 surface layer  $\text{Hg}^0$  is oxidized and deposited in snowpack via GOM and PBM dry deposition (Steffen et al., 2008).  
451 The deposited Hg onto snow can be rapidly re-volatilized back to the atmosphere via photochemical  $\text{Hg}^{\text{II}}$   
452 reduction on snow or in melted snow (Dommergue et al., 2003; Faïn et al., 2007; Kirk et al., 2006).  
453 Photo-reduction is the predominant pathway for Hg reemission from snow as inferred by Hg isotope  
454 fractionation signatures (Sherman et al., 2010). The reduction rate was found to be linearly correlated with UV  
455 intensity (Lalonde et al., 2002; Mann et al., 2015b), while  $\text{Cl}^-$  showed an inhibiting effect on the photo-reduction  
456 (Section 3.3) (Steffen et al., 2013). Oxidation and reemission of  $\text{Hg}^0$  occurred simultaneously with the presence  
457 of oxidants (e.g.,  $\cdot\text{OH}$ ,  $\text{Cl}$ , and  $\text{Br}$ ) formed through photolysis (Poulain et al., 2004). Nighttime elevated GEM in  
458 snow air was observed at Station Nord, Greenland, likely a result from dark formation of reducing radicals (e.g.,  
459  $\text{HO}_2\cdot$ ) (Ferrari et al., 2004). Temperature is another factor enhancing Hg emission from snow by changing the  
460 solid and liquid water ratio (Mann et al., 2015a).  $\text{Hg}^0$  flux from snow surface in the temperate regions has rarely  
461 been investigated (Faïn et al., 2007). Field data collected in Ontario and Northern New York confirmed that  
462 photo-reduction is the predominant pathway in enhancing  $\text{Hg}^0$  emission (Lalonde et al., 2003; Maxwell et al.,  
463 2013). A positive correlation between  $\text{Hg}^0$  fluxes and temperature has also been found (Maxwell et al., 2013).



464 Hg<sup>0</sup> flux over snow cover under forest canopy was found to be smaller compared to those found in open field,  
465 possibly caused by lower light under canopy (Poulain et al., 2007).

466

#### 467 **4. Global observation of atmosphere-biosphere Hg exchange**

##### 468 **4.1 Data sources, extraction and processing**

469 A comprehensive database of global observation of Hg<sup>0</sup> flux over terrestrial and oceanic surfaces is  
470 compiled from the field observed data reported in peer-reviewed literatures; and the fluxes over water surfaces  
471 calculated using two-film gas exchange model based on *in-situ* measured DGM are also included. For those  
472 studies that measured TGM (Hg<sup>0</sup> + GOM) got flux calculation, the measured flux is regarded as Hg<sup>0</sup> flux  
473 because of the small fraction of GOM in TGM measurement (GOM/GEM < 2% in general, Gustin and Jaffe,  
474 2010, Sprovieri et al., 2010; Fu et al., 2015), therefore Hg<sup>0</sup> and TGM are not discriminable for Hg vapor analyzer  
475 during a typical concentration measurement period (5 mins sampling, 1.0-1.5 L min<sup>-1</sup>) in flux sampling. As  
476 complete time-series flux datasets are not available in literature, each data point included in the database  
477 corresponds to the arithmetic mean of the flux observed during each campaign, with the campaign period lasting  
478 up to one year. For those studies periodically (e.g. weekly) measured seasonal flux at the same site, the average  
479 fluxes of all campaigns was used. A summary of Hg<sup>0</sup> flux data documented in a total of 172 peer reviewed  
480 articles are presented in Table 1, which were obtained using DFCs (85.6%), MM (7.9%), Hg<sup>0</sup>/<sup>222</sup>Rn flux ratio  
481 (0.3%), and enriched isotope tracers (0.1%), or estimated using two-film gas exchange model (6.1%). Based on  
482 the landscapes characteristics and surface Hg contents, the flux datasets are assigned into 11 categories.  
483 Classification of background soils (e.g., open field bare soil and forest ground soils with little perturbation by  
484 human activities) follows the corresponding literature definition. Soil Hg content of ≤ 0.3 μg g<sup>-1</sup> was applied as  
485 the threshold for background soil in case no classification was assigned in the original article. Hg contaminated  
486 sites are divided into natural enriched and anthropogenic contaminated sites based on the Hg sources. The  
487 remaining flux data were categorized into 9 classes according to the land uses and ecosystem types (Table 1). It is  
488 important to recognize that the Hg<sup>0</sup> fluxes represent the experimental and modeling results using diverse  
489 methodologies with campaign periods of different durations. Given the reasonably large flux sample sizes, the  
490 flux statistics (e.g., mean, median) from multiple studies for different landscapes are compared. It should be



491 noted that flux reported in laboratory controlled and field manipulated experimental studies utilizing  
492 treated/untreated substrates are *not* included in the database. Instead, the implications of those studies are  
493 discussed in terms of the environmental effects of  $\text{Hg}^0$  exchange mechanisms (cf. Section 3).

494

#### 495 **4.2 Global database of earth surfaces-atmosphere $\text{Hg}^0$ flux**

496 Table 1 summarizes the statistics of  $\text{Hg}^0$  fluxes measured to date. The site characteristics where  $\text{Hg}^0$  flux  
497 measurements were performed are highly diverse. Most studies were devoted to flux investigation over natural  
498 Hg-enriched sites (~38.2%) and background surfaces (~18.4%). Direct field measurements over terrestrial  
499 surfaces accounts for 94.1% (n=811) of the data, only 5.9% (n=51) of the data represents oceanic fluxes. In terms  
500 of substrate Hg contents, measurements at contaminated sites (natural Hg-enriched and anthropogenic polluted)  
501 consisted of 44.9% of the datasets, motivated by extensive emission at these sites caused by local and regional  
502 atmospheric pollution. For unpolluted terrestrial surfaces, most measurements were carried out over background  
503 soils (37%, n=159), while only a few studies directed to the forest foliage and above canopy flux (n=8). DFC  
504 methods are suitable for bare soil and low vegetated surface, covering 97% of the data over background soils.  
505 The remaining datasets are observations of ecosystem flux using MM methods, which require relatively more  
506 complex instrumentation and experimental efforts in the field (Gustin, 2011; Aubinet et al., 2012; Sommar et al.,  
507 2013a).

508 Fig. 6 shows the box and whisker plots of  $\text{Hg}^0$  fluxes. As seen, the categorized data exhibit substantial data  
509 variability and positive skewness. Many campaigns focus only on daytime flux (cf. Section 4.3.2) and therefore  
510 the median of mean flux in each category is a more appropriate statistics for comparison. The medians of  $\text{Hg}^0$   
511 fluxes for the 11 site categories follow the order: grasslands < forest foliage & canopy level < background soils <  
512 wetlands < seawater < snow < freshwater < urban settings < agricultural fields < anthropogenically contaminated  
513 surfaces < natural Hg-enriched surfaces (Table 1). A clear increase in flux from background to contaminated  
514 sites suggests the strong influence of substrate Hg contents on  $\text{Hg}^0$  flux. Median fluxes from contaminated sites  
515 are two orders of magnitude greater than those over other surfaces; such source strength significantly enhances  
516 local and regional atmospheric Hg concentration. Fluxes over vegetative surfaces (grasslands, forest foliage and  
517 canopy level), mixed vegetated waters (wetlands) are lower than those over background soils and open water



518 (freshwater and seawater), supporting that vegetation reduces Hg emission by masking ground floor evasion  
519 and/or plant uptake. The fluxes at human perturbed urban settings and over agricultural fields were higher than  
520 the flux over undisturbed earth surfaces, likely a result of reemission of legacy Hg deposition. Most surfaces  
521 showed net Hg<sup>0</sup> emission; approximately 25% of measurements over vegetated surfaces showed net Hg  
522 deposition (Fig. 6).

523 Results of frequency analysis of the mean Hg<sup>0</sup> fluxes for each land cover are presented in Fig. 7. While the  
524 mean Hg<sup>0</sup> flux from background soils have a large range (-51.7 – 33.3 ng m<sup>-2</sup> h<sup>-1</sup>), ~90% of the flux data ranges  
525 from -5 to 10 ng m<sup>-2</sup> h<sup>-1</sup>. Similar patterns are also evident for freshwater, oceans, grasslands, and wetlands. The  
526 occasional high emission and deposition fluxes are mainly due to short sampling duration (e.g. mid-day flux) or  
527 extreme atmospheric Hg<sup>0</sup> concentration events caused by local/regional sources. Comparatively, fluxes over  
528 agricultural fields and in urban settings show a much larger range and a lower kurtosis. Strong Hg<sup>0</sup> evasion was  
529 observed at contaminated sites (>97% of total observations showed evasion), although extremely high  
530 deposition also occurred in the presence of high ambient Hg<sup>0</sup> and atmospheric subsidence (Bash and Miller, 2007;  
531 Zhu et al., 2013c). Most measurements over snow (87%) show evasions; these studies were carried out in the  
532 Polar Regions and focused on Hg reemission from snow after AMDEs. The distribution of Hg<sup>0</sup> fluxes of  
533 air-foliage and canopy level exchange showed that half of the measurements (n=4) gave a net emission, while the  
534 mean flux is not significantly different from zero ( $p=0.24$ , ANOVA).

535

### 536 **4.3 Spatial distribution and temporal variation of global Hg<sup>0</sup> flux data**

#### 537 *4.3.1 Spatial distribution*

538 Fig. 8 shows the box and whisker plots of Hg<sup>0</sup> flux from four relatively homogenized surfaces (background  
539 soils, agricultural fields, grasslands, and freshwater) observed in different regions. Worldwide flux measurement  
540 was unevenly distributed, most studies were conducted in North American and East Asia, which limits global  
541 representativeness. Hg<sup>0</sup> flux observed in East Asia is consistently higher compared to those measured in Europe,  
542 North and South America, Australia, and South Africa ( $p < 0.05$ , ANOVA, except freshwater). This can be  
543 explained by the greater anthropogenic emission and re-emission of Hg deposition (Selin et al., 2007; Selin et al.,  
544 2008; Lin et al., 2010b; Smith-Downey et al., 2010). The flux over freshwater in Europe is somewhat higher than



545 those measured in East Asia ( $6.5$  vs.  $4.6$   $\text{ng m}^{-2} \text{h}^{-1}$ ,  $p=0.40$ , ANOVA). These data were obtained mostly prior to  
546 2002 ( $n=9$ ) or during summer time and daytime ( $n=8$ ) (Schroeder et al., 1989; Xiao et al., 1991; Lindberg et al.,  
547 1995b; Gårdfeldt et al., 2001; Feng et al., 2002), which could have yielded higher fluxes.

548

#### 549 *4.3.2 Diurnal and seasonal patterns*

550 Fig. 9 displays the general diel variation of  $\text{Hg}^0$  flux measured by DFC and DFB methods. Fluxes were  
551 typically higher during daytime and lower at nighttime from soil, mine, water and snow surfaces, where  $\text{Hg}^0$  can  
552 be formed through photo-reduction. As discussed in Section 3, the observed diel variations are in agreement with  
553 results from laboratory controlled studies: higher irradiance and temperature promoted  $\text{Hg}^0$  reduction and  
554 evasion at daytime, which formed a “dome-shaped” diel flux pattern from most earth surfaces (e.g., soils, mine,  
555 water, and snow). On the contrary, greater deposition during daytime and evasion/near-zero-flux at nighttime  
556 have been frequently observed from foliage, possibly facilitated by the uptake through stomata that exhibit  
557 higher stomatal conductivity during daytime.

558 Seasonally, higher evasion flux occurs in warm season and smaller exchange is observed in cold season. For  
559 example, seasonal data from Choi and Holsen (2009a) showed a higher evasion from forest floor soil in  
560 Adirondack Mountain (New York, USA) in summer ( $1.46$   $\text{ng m}^{-2} \text{h}^{-1}$ ) shifted to insignificant exchange in winter  
561 ( $0.19$   $\text{ng m}^{-2} \text{h}^{-1}$ ). Similar trends were also found in agricultural soils, freshwater, and mine surfaces (Fu et al.,  
562 2010a; Eckley et al., 2011b; Zhu et al., 2011). Observed diurnal and seasonal patterns may also be influenced by  
563 vegetative surface changes and meteorological characteristics. For example, Sommar et al. (2015) reported  
564 seasonal flux observation over a wheat-corn rotation cropland using REA measurement, an unexpected low flux  
565 was observed in summer during corn growing stage (median:  $-6.1$   $\text{ng m}^{-2} \text{h}^{-1}$ ) due to the uptake by corn leaf (leaf  
566 area index 2.7-3.6), which is similar to the flux ( $-6.7$   $\text{ng m}^{-2} \text{h}^{-1}$ ) observed in winter and much lower than the  
567 wheat canopy flux ( $13.4$   $\text{ng m}^{-2} \text{h}^{-1}$ ) in early spring. The limited availability of seasonal data in peer-reviewed  
568 literature does not allow a thorough assessment of seasonal characteristics of different terrestrial surfaces. It is  
569 important to recognize that the modified landscapes and vegetative biomass growing cycle caused by seasonal  
570 changes (e.g., change of LAI in deciduous forest, growing season of forest ecosystem, etc.) may significantly  
571 modify the flux characteristics. More data, especially measurements using consistent quantification techniques



572 over a longer campaign period (e.g., 1 year or longer), are needed for addressing the seasonal variability of  $\text{Hg}^0$   
573 exchange flux and better estimating the annual exchange from vegetative surfaces. To accomplish such  
574 measurements, automation of flux quantification apparatus is also required.

575

#### 576 **4.4 Source and sink characteristics of natural surfaces in the context of global Hg budget**

##### 577 *4.4.1 Background soils and water are important diffuse sources of $\text{Hg}^0$*

578 Although  $\text{Hg}^0$  flux observed over background soil ( $1.3 \text{ ng m}^{-2} \text{ h}^{-1}$ ) and unpolluted water bodies ( $2.8$  and  $2.5$   
579  $\text{ ng m}^{-2} \text{ h}^{-1}$  for fresh and seawater) may appear mild (Table 1), the annual emission from these two types surfaces  
580 accounted for 64% of total atmospheric Hg emission because of their large areal coverage globally (Pirrone et al.,  
581 2010). For example, it has been estimated that bare soil releases  $\sim 550 \text{ Mg yr}^{-1}$  (Selin et al., 2008; Pirrone et al.,  
582 2010) and surface ocean releases  $2000\text{-}2900 \text{ Mg yr}^{-1}$  of  $\text{Hg}^0$  globally (Fig. 1) (Mason et al., 2012; AMAP/UNEP,  
583 2013). Constraining the uncertainties on  $\text{Hg}^0$  emission from these diffuse sources will greatly improve the  
584 accuracy of global Hg budget. Global  $\text{Hg}^0$  evasion from soil is mainly based on empirical relationship between  
585 flux, temperature and irradiation (cf., Section 5), which needs mechanistic refinement. Air-seawater exchange  
586 estimated by global models is subject to the uncertainty in (1) mechanisms of aqueous redox transformation and  
587 the associated kinetic parameters, and (2)  $\text{Hg}^0$  mass transfer rates as determined by surface friction velocity  
588 (Qureshi et al., 2011a). Kinetic parameters of these processes largely rely on limited field data without  
589 experimental verification (AMAP/UNEP, 2013) and require further investigation. Parameterization of  $\text{Hg}^0$  flux  
590 using field data and redox transformation rate constants in soil and water are critical to reduce the uncertainty in  
591 future studies.

592

##### 593 *4.4.2 Contaminated surfaces are intensive local $\text{Hg}^0$ sources*

594 Hg evasion from contaminated surfaces (Fig. 6 and Fig. 7) has been recognized as an important input  
595 contributing to regional atmospheric Hg budget (Ferrara et al., 1998b; Kotnik et al., 2005).  $\text{Hg}^0$  flux from  
596 contaminated point sources have been extensively investigated by using LIDAR technique, which is by far the  
597 most effective experimental approach to spatially resolve the  $\text{Hg}^0$  air-surface exchange at contaminated sites.  
598 Ferrara et al. (1998a) measured the spatial distribution TGM concentration and TGM flux from the world's



599 largest Hg mine, Almadén Hg mine, in Spain. TGM concentration and flux were estimated to be  $0.1 - 5 \mu\text{g m}^{-3}$ ,  
600  $600 - 1200 \text{ g h}^{-1}$  in fall, 1993, above the village of Almadén. Several attempts have been made to quantitatively  
601 estimate atmospheric Hg input in mining areas. Gustin et al. (2003) and Wang et al., (2005) applied a log-linear  
602 correlation between the flux and substrate Hg contents and solar irradiance. Eckley et al. (2011b) computed  
603 annual Hg emission from two active gold mines (up to  $109 \text{ kg year}^{-1}$ ) using flux measurement of flux and  
604 statistically derived the empirical relationship between flux and meteorological variables based on Geographical  
605 Information System (GIS) data. Similarly, Kocman and Horvat (2011) obtained  $\sim 51 \text{ kg year}^{-1}$  emission from  
606 Idrijca River catchment, a former Hg mine, using field measurement and GIS data. In total, annual Hg emission  
607 from global contaminated surfaces was estimated to be  $\sim 82 \text{ Mg}$  via modeling of flux from more than 3000 Hg  
608 contaminated sites comprising Hg mining, non-ferrous metal production, precious metal processing, and various  
609 polluted industrial sites (Kocman et al., 2013), which is emitted from a very limited surface areas thus can pose a  
610 strong environmental impact to the local area surrounding the contaminated sites.

611

#### 612 4.4.3 Areas impacted by human activities exhibit elevated $\text{Hg}^0$ reemission

613 The median evasion flux over human urban settings and agricultural fields is 5-10 times higher than the  
614 value over background soils (Table 1). Direct anthropogenic Hg input and atmospheric Hg deposition explain the  
615 enhanced reemission. Natural surfaces nearby the anthropogenic point sources (e.g. power plant, Pb-Zn smelter,  
616 chlor-alkali plant) generally showed higher soil Hg content due to atmospheric Hg deposition (Lodenius and  
617 Tulisalo, 1984; Li et al., 2011; Zheng et al., 2011; Guédron et al., 2013). A fraction of these deposited Hg can be  
618 swiftly reemitted back to the atmosphere (Fu et al., 2012a; Eckley et al., 2015). Newly deposited Hg to soil,  
619 aquatic system and snow pack in the Polar Regions can also be readily converted to  $\text{Hg}^0$  and reemitted (Amyot et  
620 al., 2004; Poulain et al., 2004; Ericksen et al., 2005). Eckley et al. (2015) observed soil  $\text{Hg}^0$  flux near a large  
621 base-metal smelter (Flin Flon, Manitoba, Canada) and reported a net deposition during operation ( $-3.8 \text{ ng m}^{-2} \text{ h}^{-1}$ )  
622 and elevated emission ( $108 \text{ ng m}^{-2} \text{ h}^{-1}$ ) after operation ceased. To date, the source and sink characteristics of  
623 surfaces impacted by human activities have not been adequately investigated. Future investigation should be  
624 coordinated toward spatially resolving the  $\text{Hg}^0$  exchange over human impacted surfaces for better quantifying  
625 the emission budget of legacy Hg.





626

627 *4.4.4 Flux over vegetated surfaces likely a sink but large uncertainties remains*

628 Data of  $\text{Hg}^0$  flux over foliage and forest canopy showed a small net emission (median:  $0.7 \text{ ng m}^{-2} \text{ h}^{-1}$ ) with  
629 substantial variability (Figs. 6 and 7). There have been conflicting reports regarding the role of forest ecosystems  
630 as Hg source or sink at global scale (Lindqvist et al., 1991; Lindberg et al., 1998; Frescholtz and Gustin, 2004;  
631 Fay and Gustin, 2007a; Fay and Gustin, 2007b; Hartman et al., 2009; Cui et al., 2014). Laboratory studies  
632 suggested that plant is a net sink atmospheric Hg through leaf assimilation (Millhollen et al., 2006a;  
633 Stamenkovic and Gustin, 2009; Rutter et al., 2011b; Cui et al., 2014). Using Hg concentration in plant tissues and  
634 net primary productivity as a proxy for atmospheric Hg deposition, Obrist (2007) estimated plants remove  
635  $\sim 1024.2 \text{ Mg yr}^{-1}$  Hg globally (foliage contributed  $237.6 \text{ Mg/yr}$ ). Fu et al. (2015b) estimated that global litterfall  
636 contributes to  $1232 \text{ Mg yr}^{-1}$  of Hg deposition, throughfall contributes to  $1338 \text{ yr}^{-1}$  of Hg deposition, and forest  
637 floor evades  $\sim 381 \text{ Mg yr}^{-1}$  of Hg into the atmosphere. Hg content in forest soil is comparatively higher than the  
638 concentration found in bare soil due to the input via litterfall and wet Hg deposition (Blackwell and Driscoll,  
639 2015a, b; Obrist et al., 2011); and  $\sim 90\%$  boreal forest soil Hg was believed to be originated from litterfall input  
640 (Jiskra et al., 2015). These studies suggested forest ecosystem is likely a large atmospheric Hg sink, although  
641 these bulk proxy methods are not sufficiently sophisticated to resolve the global Hg mass balances.  
642 Synchronized, long-term observation of air canopy flux and litterfall/throughfall deposition is useful to  
643 understand the source and sink characteristics of forest.

644

645 **5. Modeling of air-surface  $\text{Hg}^0$  exchange flux**

646 A summary of recent modeling efforts on estimating natural emission was presented in Table 2. For  
647 air-foliage  $\text{Hg}^0$  exchange, earlier parameterization (S1, Table 2) calculates the flux as a function of the  
648 evapotranspiration rate based on soil-root-stem-foliage transpiration stream. It is assumed that Hg passed  
649 through the soil-root interface and then is transferred into foliage in as complexes with organic ligands (Moreno  
650 et al., 2005a; Moreno et al., 2005b; Wang et al., 2012). However, root uptake is unlikely to occur (Cui et al.,  
651 2014). Hg isotopic signatures between air and foliage (Demers et al., 2013; Yin et al., 2013), and air-foliage flux  
652 measurements (Graydon et al., 2006; Gustin et al., 2008) suggest that: (1) the exchange is bi-directional, and (2)



653 atmospheric Hg uptake by foliage is the major pathway for Hg accumulation. Therefore, a bidirectional flux  
654 scheme building on the compensation point (S2, Table 2) is perhaps more scientifically sound and  
655 mathematically robust. For air-soil Hg<sup>0</sup> exchange, in addition to the bidirectional resistance scheme (S3),  
656 statistical relationships have been developed based on measured flux and observed environmental factors such as  
657 air/soil temperature, solar radiation, soil moisture and soil Hg content (S1-S2, Table 2), which tends to be  
658 site-specific and oversimplifies the influence of environmental factors (Wang et al., 2014). For air-water flux  
659 simulation, the two-film diffusion model is widely used by incorporating surface storage and aqueous Hg redox  
660 chemistry (Bash et al., 2007; Strode et al., 2007). Bash (2010) suggested a pseudo-first kinetic water photo-redox  
661 scheme in CMAQ simulation with bidirectional Hg exchange. Strode et al. (2007) parameterized the reduction  
662 rate as the product of local shortwave solar radiation, net primary productivity, and a scaling parameter in  
663 GEOS-Chem. Soerensen et al. (2010) updated the surface ocean redox reactions in GEOS-Chem, and added a  
664 term for dark oxidation, and suggested new linear relationships between the total solar radiation, net primary  
665 productivity, and photo-oxidation rate coefficient, photoreduction coefficient, and biotic reduction coefficient.

666 Using the S1 scheme (Table 2), the range of simulated air-foliage fluxes were 0 to 5 ng m<sup>-2</sup> h<sup>-1</sup> in North  
667 America (Bash et al., 2004) and 0 to 80 ng m<sup>-2</sup> h<sup>-1</sup> in East Asia (Shetty et al., 2008). Change the modeling  
668 approach to resistance based models with compensation point assumption (S2 scheme), the range was -2.2 to  
669 -0.7 ng m<sup>-2</sup> h<sup>-1</sup> (Wang et al., 2014). Zhang et al. (2012a) reported the annual Hg<sup>0</sup> uptake by foliage was 5-33 μg  
670 m<sup>-2</sup> with the S2 scheme, similar to the litterfall Hg flux measured at Mercury Deposition Network Sites. For  
671 air-soil exchange, model-estimated fluxes ranged from 0 to 25 ng m<sup>-2</sup> h<sup>-1</sup> using the S1 and S2 scheme (Bash et al.,  
672 2004; Gbor et al., 2006; Shetty et al., 2008; Kikuchi et al., 2013), comparable to the 0-20 ng m<sup>-2</sup> h<sup>-1</sup> using the S3  
673 scheme (Wang et al., 2014). For air-water exchange, the model-estimated flux was 1-12 ng m<sup>-2</sup> h<sup>-1</sup>, consistent  
674 with measured fluxes (Bash et al., 2004; Shetty et al., 2008; Bash, 2010; Wang et al., 2014).

675 Future development of Hg<sup>0</sup> flux model requires mechanistic understanding of air-surface exchange  
676 processes. Presently, bidirectional resistance scheme, the stomatal compensation point is treated as a constant  
677 value (Bash, 2010; Wang et al., 2014) or calculated as following in Wright and Zhang (2015):

$$678 \quad \chi_{st} = 8.204 \frac{8.9803 \times 10^9}{T} \cdot \Gamma_{st} \cdot e^{-\frac{8353.8}{T}} \quad (5)$$



679 where  $T$  is the temperature of stomata/surface, and  $\Gamma_{st}$  is the emission potential of the stomata.  $\Gamma_{st}$  is an empirical  
680 input value and suggested in  $5\text{--}25\text{ ng m}^{-3}$  depending on the specific land use. Battke et al., 2005; Heaton et al.,  
681 2005; and Battke et al., 2008 reported that plants have the ability to reduce the  $\text{Hg}^{\text{II}}$  to  $\text{Hg}^0$  in foliar cell through  
682 reducing ligands (e.g., NADPH). To propose a more physically robust modeling scheme, the redox processes in  
683 foliage and the role of ligands on Hg uptake need to be better understood. The finding that  $\text{Hg}^0$  can pass through  
684 the soil-root interface under artificial laboratory conditions (Moreno et al., 2005b) needs to be carefully verified  
685 in the field.

686 Another area that requires advancement is the determination of  $\text{Hg}^{\text{II}}$  reduction rate (Scholtz et al.,  
687 2003; Bash, 2010; Wang et al., 2014) and the hypothetical parameter  $\Gamma_{st}$  (Wright and Zhang, 2015) in soil. It is  
688 well known that  $\text{Hg}^{\text{II}}$  can be reduced by natural organic acids via biotic/abiotic reduction (Zhang and Lindberg,  
689 1999; Zheng et al., 2012). Experimental investigations showed that  $\text{O}_3$  is important in controlling Hg emissions  
690 from substrates (Engle et al., 2005). However, the kinetic description of these process is fundamentally unknown.  
691 The pseudo-first reduction rate constant of  $\text{Hg}^{\text{II}}$  has been assumed to be in the range of  $10^{-11}$  to  $10^{-10}\text{ s}^{-1}$  (Scholtz  
692 et al., 2003; Qureshi et al., 2011a). Under laboratory conditions at  $100\text{ W m}^{-2}$  and  $32\pm 7\text{ }^\circ\text{C}$ , the pseudo-first  
693 reduction rate was estimated to be  $2\text{--}8\times 10^{-10}\text{ m}^2\text{ s}^{-1}\text{ w}^{-1}$  basing on 2 mm soil depth (the maximum depth for light  
694 penetration in soil) (Quinones and Carpi, 2011). Si and Ariya (2015) reported a photo-reduction rate of  $\text{Hg}^{\text{II}}$  in  
695 presence of alkanethiols to be  $3\text{--}9\times 10^{-9}\text{ m}^2\text{ s}^{-1}\text{ w}^{-1}$ . Other than these kinetic information, kinetic measurements for  
696  $\text{Hg}^{\text{II}}$  reduction in the absence of light will enable additional mechanistic parameterization of Hg evasion model  
697 for soil and vegetative surface.

698

## 699 **6. Conclusions and future perspectives**

700 Understanding in the air-surface exchange of  $\text{Hg}^0$  has been steadily advancing since mid-1980s. Substantial  
701 amount of data exists, but with large uncertainty and data gaps in Africa, South and Central Asia, Middle East,  
702 South America and Australia. Fundamentally, flux measurement approaches (e.g., MM and DFCs) are different  
703 and individual flux measurement data are not directly comparable. The  $\text{Hg}^0$  flux data compiled in this study  
704 represent the current state of understanding that requires continuous updates.  $\text{Hg}^0$  flux in East Asia is statistically  
705 higher than the values observed in other world regions, suggesting reemission of atmospheric deposition or



706 strong anthropogenic influence.  $\text{Hg}^0$  exchange over weak diffuse sources (e.g., background soil and water) and  
707 vegetation need better constrains for global analysis of atmospheric Hg budget through extensive on-site  
708 measurement and fundamental mechanical studies (e.g., redox transformation rate constant, mass transfer  
709 diffusivity). Although predominate factors in controlling  $\text{Hg}^0$  flux have been identified, the effects of those  
710 factors on flux have not been fundamentally and quantitatively determined for different surfaces, which limited  
711 the accuracy of flux modeling. Based on the data synthesis in this study, the following knowledge gaps need to be  
712 addressed:

713 **(1) Improving temporal resolution and sensitivity of  $\text{Hg}^0$  flux measurements.** Insufficient temporal  
714 resolution and sensitivity in the detection of ambient Hg has limited our capability in accurately determining the  
715 air-surface exchange of  $\text{Hg}^0$ . Development of high temporal resolution and sensitive sensor for determining  $\text{Hg}^0$   
716 concentration gradient is of prime importance to improve flux data quality and to reduce uncertainty in the global  
717 assessment of Hg budget. Such advancement will also open up new opportunities to explore fundamental  
718 exchange mechanism in response to the changes in environmental factors.

719 **(2) Standardization of  $\text{Hg}^0$  flux measurement techniques and establish data comparison strategy.**  $\text{Hg}^0$  flux  
720 measurement uncertainties from using different techniques remains large, standardized method is useful to  
721 compare flux obtained from various techniques. Fundamental study is needed to compare current  $\text{Hg}^0$  flux  
722 quantification methods, synchronized measuring flux from various methods using varied operation parameters is  
723 suggested to build potential empirical data comparison strategy and correction methods, this will largely reduce  
724 the gross uncertainty in the Hg budget estimation and greatly improve comparability of flux data reported by  
725 different research groups.

726 **(3) Fundamental investigation on the environmental processes driving Hg exchange.** Although flux  
727 response to environmental parameters (e.g., irradiance, precipitation, temperature rising) are qualitatively  
728 defined in statistical sense, the processes driving  $\text{Hg}^0$  exchange need to be understood fundamentally. Recent  
729 advancement on isotopic tracing techniques (e.g., enriched Hg isotope tracers and stable Hg isotopic  
730 fractionation data) may offer mechanistic insights and new data should be incorporated into new modeling  
731 analysis.

732 **(4) Long-term measurement of  $\text{Hg}^0$  flux at representative sites.** There is a substantial data gap in the current



733 Hg<sup>0</sup> flux database in terms of geographical coverage and land use type. Forest is most likely an overlooked sink  
734 for atmospheric Hg<sup>0</sup>, however, few field campaigns have been conducted at forest sites. In addition, current flux  
735 database are mainly from short-term campaigns. It is presently unclear how global changes (e.g. climate change,  
736 global anthropogenic Hg reduction) will force Hg<sup>0</sup> flux changes over different surfaces. There is presently no  
737 network of flux measurements at global monitoring sites. Continuous observation of flux is also useful for  
738 providing better database for scale-up estimation.

739 **(5) Development and improvement of air-surface exchange models for Hg.** The present state of development  
740 of air-surface exchange model does not allow appropriate process analysis due to a lack of fundamental  
741 understanding in the chemical and mass transfer processes of evasion and deposition. Existing air-surface Hg<sup>0</sup>  
742 flux schemes incorporate over-simplified chemical schemes with not-yet verified kinetic parameters. In addition,  
743 the interactions between Hg<sup>II</sup> and organic matters in the natural environment, as well as the interfacial transfer of  
744 different Hg species over various surfaces, have significant knowledge gaps. Studies address these gaps are  
745 critically needed and will benefits not only the measurement approaches but also the model parameterization in  
746 estimating the global air-surface exchange of Hg.

747

#### 748 **Acknowledgements**

749 This research was supported by 973 Program (2013CB430002) and the National Science Foundation of China  
750 (41503122).

751


 752 **Table 1:** A statistical summary of field *in situ* observed Hg<sup>0</sup> flux reported in the literatures.

753

Landscapes	Hg <sup>0</sup> flux (ng m <sup>-2</sup> h <sup>-1</sup> )				N	References <sup>b</sup>
	Mean	Median	Min ( <i>min</i> ) <sup>a</sup>	Max ( <i>max</i> ) <sup>a</sup>		
Background soil	2.1	1.3	-51.7 (-51.7)	33.3 (97.8)	159	(1)
Urban settings	16.4	6.2	0.2 (-318)	129.5 (437)	29	(2)
Agricultural fields	25.1	15.3	-4.1 (-1051)	183 (1071)	59	(3)
Forest foliage & canopy level	6.3	0.7	-9.6 (-4111)	37.0 (1000)	8	(4)
Grasslands	5.5	0.4	-18.7 (-989.6)	41.5 (870)	38	(5)
Wetlands	12.5	1.4	-0.3 (-375)	85 (677)	23	(6)
Freshwater	4.0	2.8	-0.3 (-18.2)	74.0 (88.9)	93	(7)
Sea water	5.9	2.5	0.1 (-2.7)	40.5 (46.0)	51	(8)
Snow	5.7	2.7	-10.8 (-2160)	40 (720)	15	(9)
Natural enriched surfaces	5618	226	-5493 (-9434)	239200 (420000)	329	(10)
Anthropogenically contaminated surfaces	595	184	-1.4 (-286.2)	13700 (13700)	58	(11)

 754 Notes: [a]. Min/Max are campaign/site-based average flux, while (*min*)/(*max*) represent lowest/largest instantaneous flux; [b] References: see **Appendix A**.

755

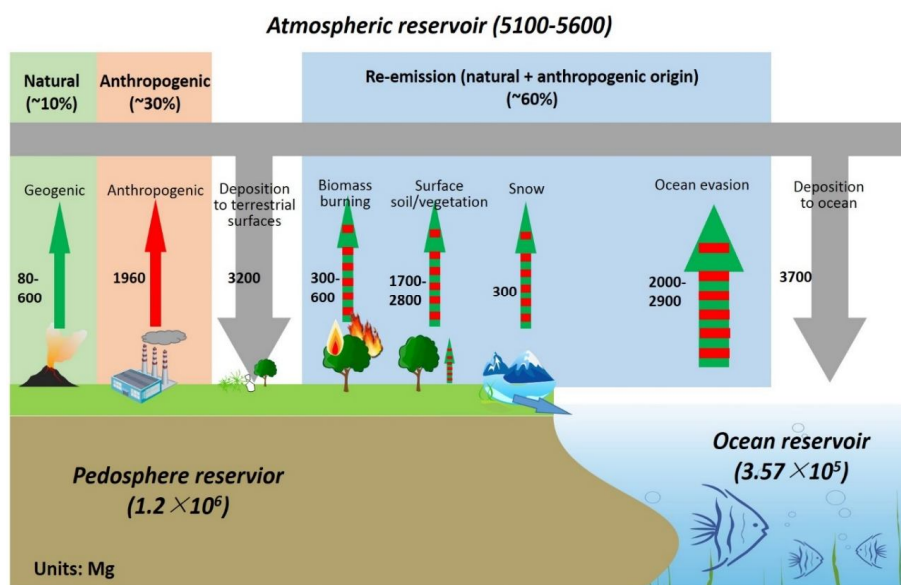
756

757 **Table 2:** A comparison of natural surface mercury flux models

	General models	Description	References
Foliage	S1: $F = ECs$	E: transpiration rate ( $\text{g m}^{-2} \text{s}^{-1}$ ) Cs: $\text{Hg}^0$ in soil water ( $\text{ng g}^{-1}$ )	Xu et al., 1999; Bash et al., 2004; Shetty et al., 2008; Gbor et al., 2006
	S2: $F_{st/cu} = \frac{\chi_{st/cu} - \chi_c}{R_{st/cu}}$	$\chi_{st/cu}$ : stomatal/cuticular compensation point ( $\text{ng m}^{-3}$ )	Zhang et al., 2009; Bash, 2010; Wang et al., 2014; Wright and Zhang, 2015
		$F_{st/cu}$ : air-cuticular/stomatal flux ( $\text{ng m}^{-2} \text{s}^{-1}$ )	
		$\chi_c$ : compensation point at the air-canopy ( $\text{ng m}^{-3}$ )	
		$R_{st/cu}$ : resistance between air-cuticular/stomatal ( $\text{m s}^{-1}$ )	
Soil	S1: $\log F = -\frac{\alpha}{T} + \beta \log(C) + \gamma R + \varepsilon$	T: soil temperature ( $^{\circ}$ )	Xu et al., 1999; Bash et al., 2004; Gbor et al., 2006; Shetty et al., 2008; Selin et al., 2008
		C: soil $\text{Hg}$ concentration ( $\text{ng g}^{-1}$ )	
		R: solar radiation ( $\text{W m}^{-2}$ )	
	S2: $\frac{F}{C} = \alpha T + \beta R + \delta \Theta + \delta TR + \dots$	T: soil temperature ( $^{\circ}$ )	Lin et al., 2010a; Kikuchi et al., 2013
		C: soil $\text{Hg}$ concentration ( $\text{ng g}^{-1}$ )	
		R: solar radiation ( $\text{W m}^{-2}$ )	
		$\Theta$ : soil moisture (%)	
	S3: $F = \frac{\chi_s - \chi_c}{R_g + R_{ac}}$	$\chi_s$ : soil compensation point ( $\text{ng m}^{-3}$ )	Zhang et al., 2009; Bash, 2010; Wang et al., 2014; Wright and Zhang, 2015
		$\chi_c$ : compensation point at the air-soil ( $\text{ng m}^{-3}$ )	
		$R_g$ : resistance between air-soil ( $\text{m s}^{-1}$ )	
$R_{ac}$ : In-canopy aerodynamic resistance ( $\text{m s}^{-1}$ )			
Water	$F = \frac{\chi_w - \chi_c}{R_w + R_a}$	$\chi_w$ : water compensation point ( $\text{ng m}^{-3}$ )	Xu et al., 1999; Bash et al., 2004; Gbor et al., 2006; Shetty et al., 2008; Bash, 2010; Wang et al., 2014
		$\chi_c$ : air $\text{Hg}^0$ concentration ( $\text{ng m}^{-3}$ )	
		$R_w$ : liquid side resistance ( $\text{m s}^{-1}$ )	
		$R_a$ : air side resistance ( $\text{m s}^{-1}$ )	



761 **Fig. 1.** The most recent Hg reservoirs and global atmosphere Hg inventory illustrating the exchange flux  
762 between atmosphere and earth surfaces. Adapted from Selin, 2009; Gustin and Jaffe, 2010; Soerensen et al.,  
763 2010; Corbitt et al., 2011; Mason et al., 2012; AMAP/UNEP, 2013.  
764

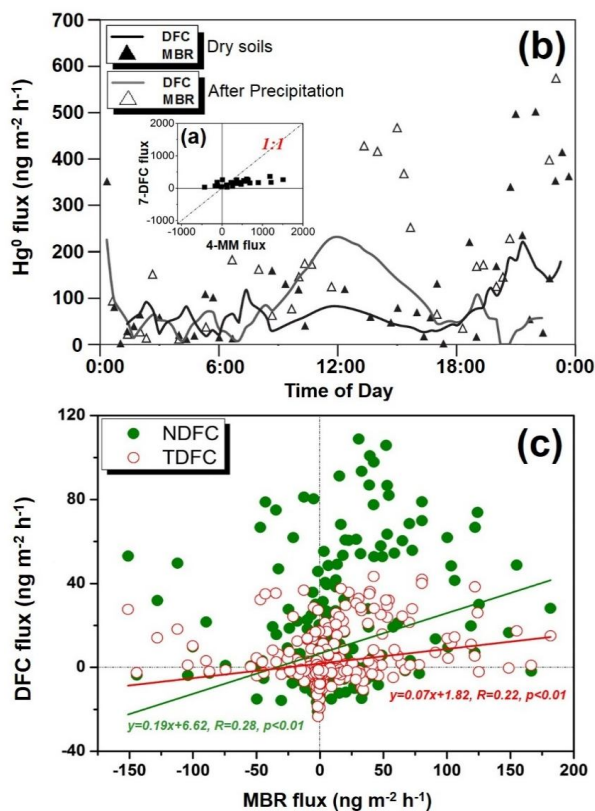


765  
766  
767





768 **Fig. 2.** Field collocated DFCs and MM techniques observed fluxes from two intercomparison studies: (a).  
769 Inlaid scatter plot of averaged 4-MM flux vs. averaged 7-DFC flux (TOT: 1.1-24 min) in Hg-enriched  
770 Nevada STORMS site in September, 1997 (Gustin et al., 1999); (b). Diel evolution of  $\text{Hg}^0$  flux measured  
771 using a 1L polycarbonate-DFC (TOT: 0.2 min) and MBR method at same Nevada STORMS site in October,  
772 1998 (Gustin, 2011); (b). Scatter plot of DFC with traditional/novel designs (TDFC/NDFC) vs. MBR  $\text{Hg}^0$   
773 flux obtained in Yucheng Intercomparison project (Zhu et al., 2015b).  
774



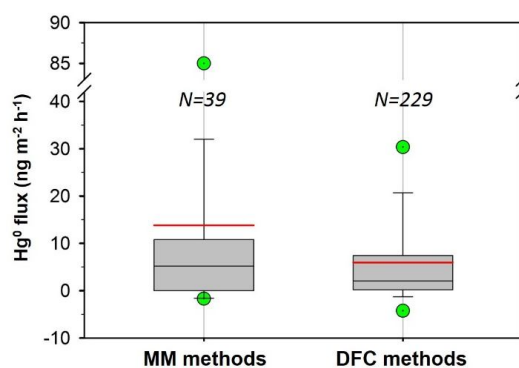
775

776

777



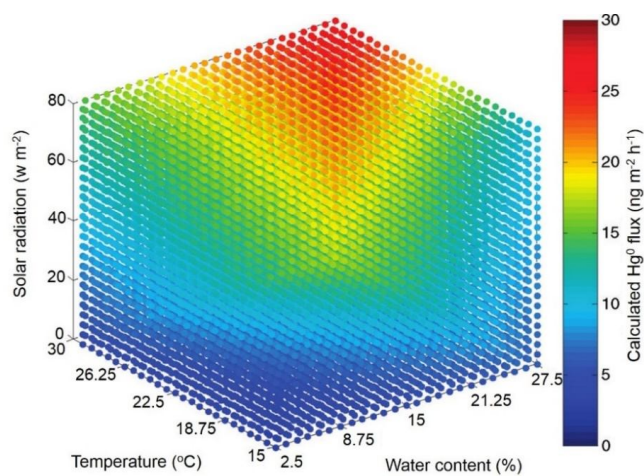
778 **Fig 3.** Box and whisker plots of  $\text{Hg}^0$  fluxes measured by MM methods and DFC methods. (Flux data  
779 including measurements from background soils, agricultural fields, grasslands, and wetlands at substrate  
780 total Hg lower than  $0.3 \mu\text{g Hg g}^{-1}$ , data source: Table 1. The two box horizontal border lines indicate 25th and  
781 75th percentiles, whiskers represent 10th and 90th percentiles, and outliers (green circles) indicate 5th and  
782 95th percentiles from bottom to top. Red line and black line indicate mean and median flux).  
783



784  
785  
786



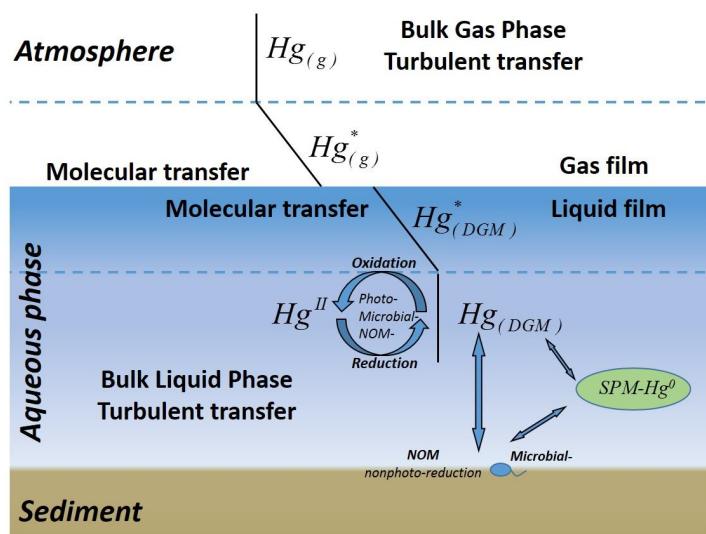
787 **Fig. 4.** 4-D graphical visualization of the effect of air temperature, soil water content, and solar radiation on  
788 the measured  $\text{Hg}^0$  flux from soil (Lin et al., 2010a).  
789



790  
791  
792



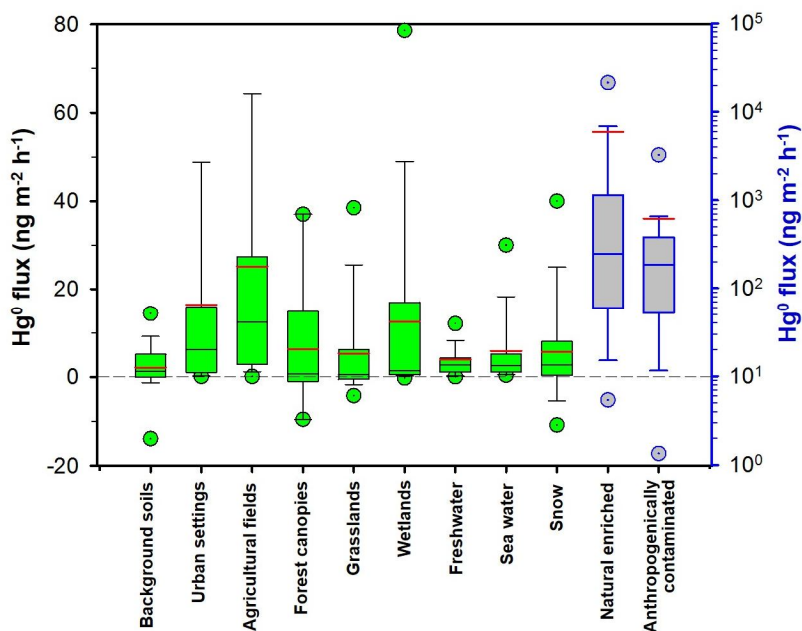
793 **Fig. 5.** Conceptual view of DGM cycling in water and mass transfer process across the atmosphere-water  
794 interface.  
795



796  
797  
798



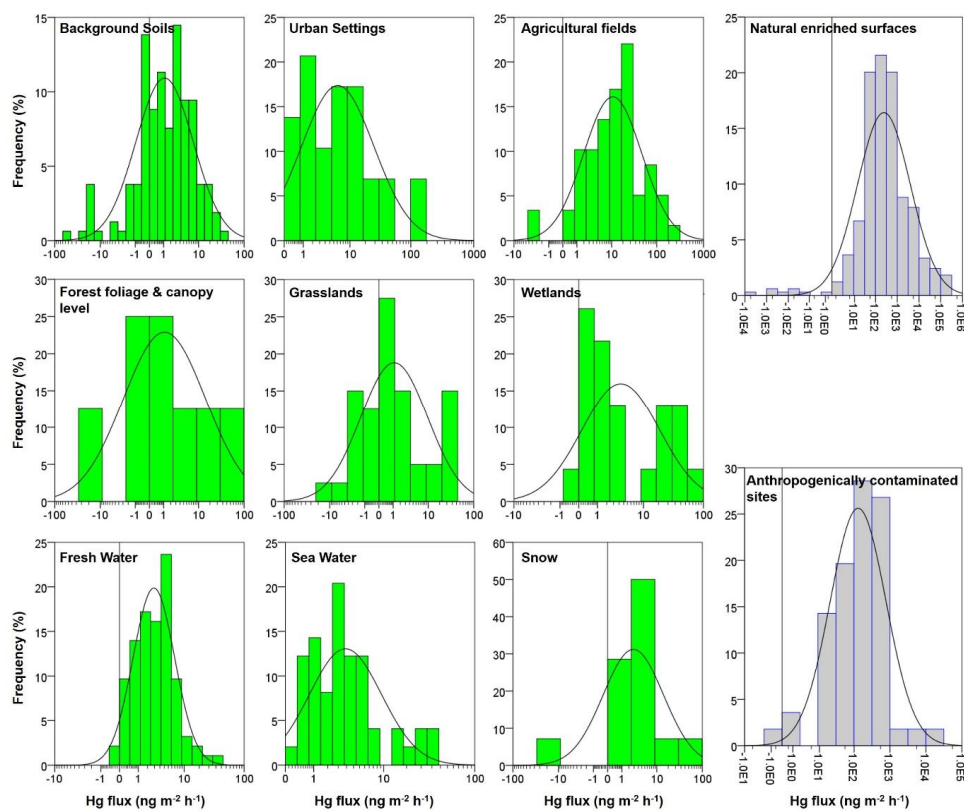
799 Fig. 6. Box and whisker plots of global field observed  $\text{Hg}^0$  flux obtained from various landscapes. (Data  
800 Source: Table 1. Red line and black line indicate mean and median flux).  
801



802  
803  
804



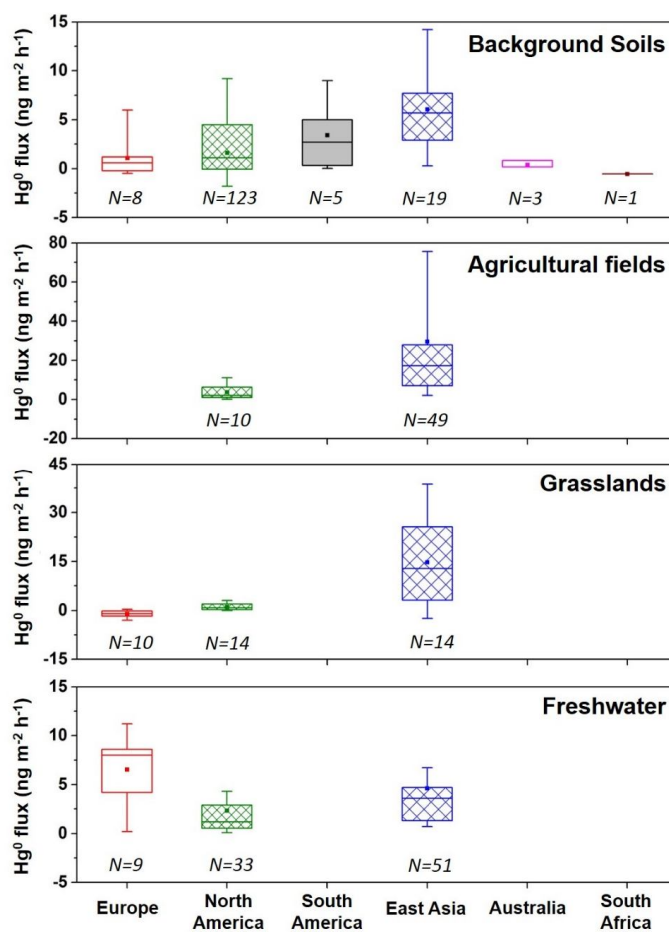
805 **Fig. 7.** Histograms of  $\text{Hg}^0$  flux frequency distribution obtained from various earth surfaces. (Data source:  
806 Table 1).  
807



808  
809  
810



811 **Fig. 8.** Box and whisker plots of continents segregated  $\text{Hg}^0$  flux obtained from four homogeneous surfaces  
812 (Background soils, agricultural fields, grasslands, and freshwater. Filled square block and horizontal line in  
813 box indicate mean and median flux).  
814



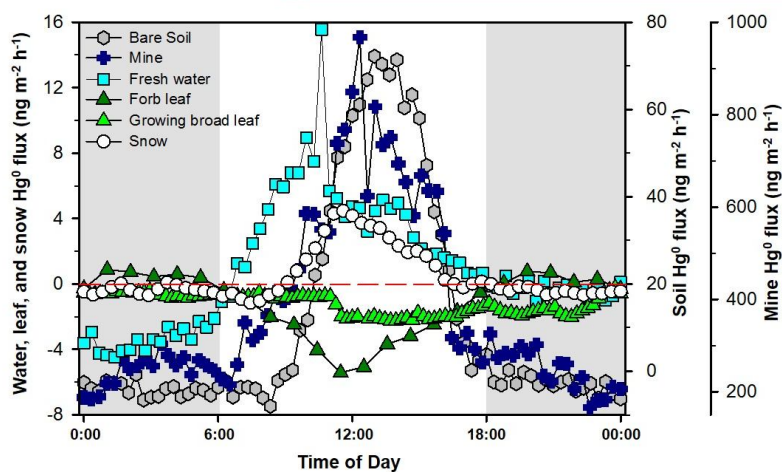
815

816

817



818 **Fig. 9.** Diurnal patterns of  $\text{Hg}^0$  flux from various environmental compartments (soil, mine, freshwater, forb  
819 leaf, growing broad leaf, and snow) measured using DFC methods. (Data obtained from soil: Zhu et al.,  
820 2015b; mine: Eckley et al., 2011a; fresh water: O'Driscoll et al., 2003; forb leaf: Stamenkovic et al., 2008;  
821 growing broad leaf: Fu et al., 2015c; and snow: Maxwell et al., 2013)  
822



823

824

825



826 **Appendix A: References for Table 1**

- 827 (1). Schroeder et al., 1989; Xiao et al., 1991; Kim et al., 1995; Carpi and Lindberg, 1998; Ferrara et al., 1998a; Lindberg et al., 1998; Poissant  
828 and Casimir, 1998; Engle et al., 2001; Zhang et al., 2001; Coolbaugh et al., 2002; Hintelmann et al., 2002; Zehner and Gustin, 2002; Fang et al.,  
829 2003; Nacht and Gustin, 2004; Poissant et al., 2004b; Edwards et al., 2005; Ericksen et al., 2005; Magarelli and Fostier, 2005; Schroeder et al.,  
830 2005; Ericksen et al., 2006; Gustin et al., 2006; Sigler and Lee, 2006; Wang et al., 2006; Fu et al., 2008a; Kuiken et al., 2008a; Kuiken et al.,  
831 2008b; Almeida et al., 2009; Choi and Holsen, 2009a; Fu et al., 2012a; Kyllonen et al., 2012; Demers et al., 2013; Edwards and Howard, 2013;  
832 Ma et al., 2013; Slemr et al., 2013; Zhu et al., 2013b; Blackwell et al., 2014; Carpi et al., 2014; Du et al., 2014; Fu et al., 2015c;  
833 (2). Kim and Kim, 1999; Fang et al., 2003; Feng et al., 2005; Gabriel et al., 2005; Gabriel et al., 2006; Obrist et al., 2006; Wang et al., 2006;  
834 Eckley and Branfireun, 2008; Liu et al., 2014; Osterwalder et al., 2015;  
835 (3). Feng et al., 1997; Carpi and Lindberg, 1998; Cobos et al., 2002; Kim et al., 2002; Kim et al., 2003; Wang et al., 2004; Feng et al., 2005;  
836 Schroeder et al., 2005; Ericksen et al., 2006; Xin et al., 2006; Cobbett and Van Heyst, 2007; Fu et al., 2008a; Baya and Van Heyst, 2010; Zhu  
837 et al., 2011; Fu et al., 2012a; Sommar et al., 2013b; Zhu et al., 2013a; Zhu et al., 2015b; Sommar et al., 2015;  
838 (4). Lindberg et al., 1998; Graydon et al., 2006; Bash and Miller, 2008; Poissant et al., 2008; Bash and Miller, 2009; Fu et al., 2015c;  
839 (5). Poissant and Casimir, 1998; Schroeder et al., 2005; Ericksen et al., 2006; Obrist et al., 2006; Fu et al., 2008a; Fu et al., 2008b; Fritsche et  
840 al., 2008b; Fritsche et al., 2008c; Converse et al., 2010;  
841 (6). Lee et al., 2000; Lindberg and Zhang, 2000; Lindberg and Meyers, 2001; Lindberg et al., 2002b; Wallschläger et al., 2002; Poissant et al.,  
842 2004a; Poissant et al., 2004b; Marsik et al., 2005; Schroeder et al., 2005; Zhang et al., 2005; Zhang et al., 2006b; Smith and Reinfeldt, 2009;  
843 Kyllonen et al., 2012; Fritsche et al., 2014; Osterwalder et al., 2015;  
844 (7). Schroeder et al., 1989; Xiao et al., 1991; Schroeder et al., 1992; Lindberg et al., 1995b; Amyot et al., 1997a; Amyot et al., 1997b; Mason  
845 and Sullivan, 1997; Poissant and Casimir, 1998; Boudala et al., 2000; Poissant et al., 2000; Gärdfeldt et al., 2001; Feng et al., 2002; Feng et al.,  
846 2003; O'Driscoll et al., 2003; Feng et al., 2004; Hines and Brezoni, 2004; Tseng et al., 2004; Schroeder et al., 2005; Wang et al., 2006; Zhang  
847 et al., 2006a; Southworth et al., 2007; O'Driscoll et al., 2007; Feng et al., 2008b; O'Driscoll et al., 2008; Fu et al., 2010a; Fu et al., 2013a; Fu et  
848 al., 2013b;  
849 (8). Kim and Fitzgerald, 1986; Mason and Fitzgerald, 1993; Mason et al., 1993; Baeyens and Leermakers, 1998; Mason et al., 1998; Mason et  
850 al., 1999; Ferrara and Mazzolai, 1998; Ferrara et al., 2001; Gärdfeldt et al., 2001; Mason et al., 2001; Rolfhus and Fitzgerald, 2001; Wängberg  
851 et al., 2001a; Wängberg et al., 2001b; Feng et al., 2002; Conaway et al., 2003; Gärdfeldt et al., 2003; Laurier et al., 2003; Schroeder et al., 2005;  
852 St. Louis et al., 2005; Temme et al., 2005; Narukawa et al., 2006; Andersson et al., 2007; Kuss and Schneider, 2007; Sommar et al., 2007;  
853 Andersson et al., 2008; Castelle et al., 2009; Fu et al., 2010b; Bouchet et al., 2011; Andersson et al., 2011; Ci et al., 2011a; Ci et al., 2011b; Xu  
854 et al., 2012; Fantozzi et al., 2013; Ci et al., 2015; Marumoto and Imai, 2015;  
855 (9). Schroeder et al., 2003; Ferrari et al., 2005; Schroeder et al., 2005; Brooks et al., 2006; Cobbett et al., 2007; Faïn et al., 2007; Sommar et al.,  
856 2007; Fritsche et al., 2008c; Steen et al., 2009; Maxwell et al., 2013;  
857 (10). Ferrara et al., 1997; Feng et al., 1997; Ferrara et al., 1998a; Ferrara and Mazzolai, 1998; He et al., 1998; Gustin et al., 1999; Lindberg et  
858 al., 1999; Poissant et al., 1999; Wallschläger et al., 1999; Edwards et al., 2001; Engle et al., 2001; Coolbaugh et al., 2002; Engle and Gustin,  
859 2002; Zehner and Gustin, 2002; Gustin et al., 2003; Nacht and Gustin, 2004; Nacht et al., 2004; Edwards et al., 2005; Kotnik et al., 2005;  
860 Schroeder et al., 2005; Wang et al., 2005; Engle et al., 2006; García-Sánchez et al., 2006; Wang et al., 2007a; Wang et al., 2007b; Eckley et al.,  
861 2011a; Edwards and Howard, 2013; Fantozzi et al., 2013; Dalziel and Tordon, 2014;  
862 (11). Lindberg et al., 1995a; Carpi and Lindberg, 1997; Lindberg and Price, 1999; Kim et al., 2001; Wängberg et al., 2003; Goodrow et al.,  
863 2005; Lindberg et al., 2005; Olofsson et al., 2005; Wang et al., 2006; Xin et al., 2006; Nguyen et al., 2008; Rinklebe et al., 2009; Li et al., 2010;  
864 Zhu et al., 2013b; Eckley et al., 2015.  
865  
866

867 **References**

- 868 Agnan, Y., Le Dantec, T., Moore, C. W., Edwards, G. C., and Obrist, D.: New constraints on terrestrial  
869 surface-atmosphere fluxes of gaseous elemental mercury using a global database, *Environ. Sci. Technol.*,  
870 10.1021/acs.est.5b04013, 2015.
- 871 Aldén, M., Edner, H., and Svanberg, S.: Remote measurement of atmospheric mercury using differential  
872 absorption lidar, *Opt. Lett.*, 7, 221-223, 1982.
- 873 Allard, B., and Arsenie, I.: Abiotic reduction of mercury by humic substances in aquatic system — an important  
874 process for the mercury cycle, *Water Air Soil Poll.*, 56, 457-464, 1991.
- 875 Almeida, M. D., Marins, R. V., Paraquetti, H. H. M., Bastos, W. R., and Lacerda, L. D.: Mercury degassing from  
876 forested and open field soils in Rondonia, Western Amazon, Brazil, *Chemosphere*, 77, 60-66, 2009.
- 877 Amyot, M., Mierle, G., Lean, D. R. S., and McQueen, D. J.: Sunlight-induced formation of dissolved gaseous  
878 mercury in lake waters, *Environ. Sci. Technol.*, 28, 2366-2371, 1994.
- 879 Amyot, M., Lean, D., and Mierle, G.: Photochemical formation of volatile mercury in high Arctic lakes, *Environ.*  
880 *Toxicol. Chem.*, 16, 2054-2063, 1997a.
- 881 Amyot, M., Mierle, G., Lean, D., and McQueen, D. J.: Effect of solar radiation on the formation of dissolved  
882 gaseous mercury in temperate lakes, *Geochim. Cosmochim. Ac.*, 61, 975-987, 1997b.
- 883 Amyot, M., Southworth, G., Lindberg, S. E., Hintelmann, H., Lalonde, J. D., Ogrinc, N., Poulain, A. J., and  
884 Sandilands, K. A.: Formation and evasion of dissolved gaseous mercury in large enclosures amended with  
885 <sup>200</sup>HgCl<sub>2</sub>, *Atmos. Environ.*, 38, 4279-4289, 2004.
- 886 Amyot, M., Morel, F. M. M., and Ariya, P. A.: Dark oxidation of dissolved and liquid elemental mercury in aquatic  
887 environments, *Environ. Sci. Technol.*, 39, 110-114, 2005.
- 888 Andersson, M. E., Gårdfeldt, K., Wängberg, I., Sprovieri, F., Pirrone, N., and Lindqvist, O.: Seasonal and daily  
889 variation of mercury evasion at coastal and off shore sites from the Mediterranean Sea, *Mar. Chem.*, 104, 214-226,  
890 2007.
- 891 Andersson, M. E., Sommar, J., Gårdfeldt, K., and Lindqvist, O.: Enhanced concentrations of dissolved gaseous  
892 mercury in the surface waters of the Arctic Ocean, *Mar. Chem.*, 110, 190-194, 2008.
- 893 Andersson, M. E., Sommar, J., Gårdfeldt, K., and Jutterstrom, S.: Air-sea exchange of volatile mercury in the  
894 North Atlantic Ocean, *Mar. Chem.*, 125, 1-7, 2011.
- 895 Ariya, P. A., Amyot, M., Dastoor, A., Deeds, D., Feinberg, A., Kos, G., Poulain, A., Ryjkov, A., Semeniuk, K.,  
896 Subir, M., and Toyota, K.: Mercury physicochemical and biogeochemical transformation in the atmosphere and at  
897 atmospheric interfaces: a review and future directions, *Chem. Rev.*, 115, 3760-3802, 2015.
- 898 Aubinet, M., Vesala, T., and Papale, D.: Eddy covariance: a practical guide to measurement and data analysis,  
899 Springer, 2012.
- 900 Baeyens, W., and Leermakers, M.: Elemental mercury concentrations and formation rates in the Scheldt estuary  
901 and the North Sea, *Mar. Chem.*, 60, 257-266, 1998.
- 902 Bahlmann, E., Ebinghaus, R., and Ruck, W.: Development and application of a laboratory flux measurement  
903 system (LFMS) for the investigation of the kinetics of mercury emissions from soils, *J. Environ. Manage.*, 81,  
904 114-125, 2006.
- 905 Barkay, T., Miller, S. M., and Summers, A. O.: Bacterial mercury resistance from atoms to ecosystems, *FEMS*  
906 *Microbiol. Rev.*, 27, 355-384, 2003.
- 907 Bash, J. O., Miller, D. R., Meyer, T. H., and Bresnahan, P. A.: Northeast United States and Southeast Canada  
908 natural mercury emissions estimated with a surface emission model, *Atmos. Environ.*, 38, 5683-5692, 2004.
- 909 Bash, J. O., Bresnahan, P., and Miller, D. R.: Dynamic surface interface exchanges of mercury: A review and  
910 compartmentalized modeling framework, *Journal of Applied Meteorology and Climatology*, 46, 1606-1618,  
911 2007.
- 912 Bash, J. O., and Miller, D. R.: A note on elevated total gaseous mercury concentrations downwind from an  
913 agriculture field during tilling, *Sci. Total Environ.*, 388, 379-388, 2007.
- 914 Bash, J. O., and Miller, D. R.: A relaxed eddy accumulation system for measuring surface fluxes of total gaseous  
915 mercury, *J. Atmos. Ocean. Tech.*, 25, 244-257, 2008.
- 916 Bash, J. O., and Miller, D. R.: Growing season total gaseous mercury (TGM) flux measurements over an *Acer*  
917 *rubrum* L. stand, *Atmos. Environ.*, 43, 5953-5961, 2009.
- 918 Bash, J. O.: Description and initial simulation of a dynamic bidirectional air-surface exchange model for mercury  
919 in Community Multiscale Air Quality (CMAQ) model, *J. Geophys. Res.-Atmos.*, 115, D06305,  
920 doi:10.1029/2009JD012834, 2010.
- 921 Battke, F., Ernst, D., and Halbach, S.: Ascorbate promotes emission of mercury vapour from plants, *Plant Cell*  
922 *Environ.*, 28, 1487-1495, 2005.
- 923 Battke, F., Ernst, D., Fleischmann, F., and Halbach, S.: Phytoreduction and volatilization of mercury by ascorbate  
924 in *Arabidopsis thaliana*, European beech and Norway spruce, *Appl. Geochem.*, 23, 494-502, 2008.
- 925 Bauer, D., Campuzano-Jost, P., and Hynes, A. J.: Rapid, ultra-sensitive detection of gas phase elemental mercury



- 926 under atmospheric conditions using sequential two-photon laser induced fluorescence, *J. Environ. Monitor.*, 4,  
927 339-343, 2002.
- 928 Bauer, D., Everhart, S., Remeika, J., Tatum Ernest, C., and Hynes, A. J.: Deployment of a sequential two-photon  
929 laser-induced fluorescence sensor for the detection of gaseous elemental mercury at ambient levels: fast, specific,  
930 ultrasensitive detection with parts-per-quadrillion sensitivity, *Atmos. Meas. Tech.*, 7, 4251-4265, 2014.
- 931 Baya, A. P., and Van Heyst, B.: Assessing the trends and effects of environmental parameters on the behaviour of  
932 mercury in the lower atmosphere over cropped land over four seasons, *Atmos. Chem. Phys.*, 10, 8617-8628, 2010.
- 933 Ben-Bassat, D., and Mayer, A. M.: Volatilization of Mercury by Algae, *Physiol. Plant.*, 33, 128-132, 1975.
- 934 Beverland, I. J., Oneill, D. H., Scott, S. L., and Moncrieff, J. B.: Design, construction and operation of flux  
935 measurement systems using the conditional sampling technique, *Atmos. Environ.*, 30, 3209-3220, 1996.
- 936 Bishop, K. H., Lee, Y. H., Munthe, J., and Dambrine, E.: Xylem sap as a pathway for total mercury and  
937 methylmercury transport from soils to tree canopy in the boreal forest, *Biogeochemistry*, 40, 101-113, 1998.
- 938 Blackwell, B., Driscoll, C., Maxwell, J., and Holsen, T.: Changing climate alters inputs and pathways of mercury  
939 deposition to forested ecosystems, *Biogeochemistry*, 119, 215-228, 2014.
- 940 Blackwell, B. D., and Driscoll, C. T.: Deposition of Mercury in Forests along a Montane Elevation Gradient,  
941 *Environ. Sci. Technol.*, 49, 5363-5370, 2015a.
- 942 Blackwell, B. D., and Driscoll, C. T.: Using foliar and forest floor mercury concentrations to assess spatial patterns  
943 of mercury deposition, *Environ. Poll.*, 202, 126-134, 2015b.
- 944 Bouchet, S., Tessier, E., Monperrus, M., Bridou, R., Clavier, J., Thouzeau, G., and Amouroux, D.: Measurements  
945 of gaseous mercury exchanges at the sediment-water, water-atmosphere and sediment-atmosphere interfaces of a  
946 tidal environment (Arcachon Bay, France), *J. Environ. Monitor.*, 13, 1351-1359, 2011.
- 947 Boudala, F. S., Folkens, I., Beauchamp, S., Tordon, R., Neima, J., and Johnson, B.: Mercury Flux Measurements  
948 over Air and Water in Kejimikujik National Park, Nova Scotia, *Water Air Soil Poll.*, 122, 183-202, 2000.
- 949 Brooks, S. B., Saiz-Lopez, A., Skov, H., Lindberg, S. E., Plane, J. M. C., and Goodsite, M. E.: The mass balance of  
950 mercury in the springtime arctic environment, *Geophys. Res. Lett.*, 33, 13, 10.1029/2005GL025525, 2006.
- 951 Bushey, J. T., Nallana, A. G., Montesdeoca, M. R., and Driscoll, C. T.: Mercury dynamics of a northern hardwood  
952 canopy, *Atmos. Environ.*, 42, 6905-6914, 2008.
- 953 Carpi, A., and Lindberg, S. E.: Sunlight-mediated emission of elemental mercury from soil amended with  
954 municipal sewage sludge, *Environ. Sci. Technol.*, 31, 2085-2091, 1997.
- 955 Carpi, A., and Lindberg, S. E.: Application of a Teflon (TM) dynamic flux chamber for quantifying soil mercury  
956 flux: Tests and results over background soil, *Atmos. Environ.*, 32, 873-882, 1998.
- 957 Carpi, A., Frei, A., Cocris, D., McCloskey, R., Contreras, E., and Ferguson, K.: Analytical artifacts produced by a  
958 polycarbonate chamber compared to a Teflon chamber for measuring surface mercury fluxes, *Anal. Bioanal.*  
959 *Chem.*, 388, 361-365, 2007.
- 960 Carpi, A., Fostier, A. H., Orta, O. R., dos Santos, J. C., and Gittings, M.: Gaseous mercury emissions from soil  
961 following forest loss and land use changes: Field experiments in the United States and Brazil, *Atmos. Environ.*, 96,  
962 423-429, 2014.
- 963 Castelle, S., Schäfer, J., Blanc, G., Dabrin, A., Lancelour, L., and Masson, M.: Gaseous mercury at the air-water  
964 interface of a highly turbid estuary (Gironde Estuary, France), *Mar. Chem.*, 117, 42-51, 2009.
- 965 Choi, H. D., and Holsen, T. M.: Gaseous mercury fluxes from the forest floor of the Adirondacks, *Environ. Poll.*,  
966 157, 592-600, 2009a.
- 967 Choi, H. D., and Holsen, T. M.: Gaseous mercury emissions from unsterilized and sterilized soils: The effect of  
968 temperature and UV radiation, *Environ. Poll.*, 157, 1673-1678, 2009b.
- 969 Ci, Z., Wang, C., Wang, Z., and Zhang, X.: Elemental mercury (Hg(0)) in air and surface waters of the Yellow Sea  
970 during late spring and late fall 2012: Concentration, spatial-temporal distribution and air/sea flux, *Chemosphere*,  
971 119, 199-208, 2015.
- 972 Ci, Z. J., Zhang, X. S., and Wang, Z. W.: Elemental mercury in coastal seawater of Yellow Sea, China: Temporal  
973 variation and air-sea exchange, *Atmos. Environ.*, 45, 183-190, 2011a.
- 974 Ci, Z. J., Zhang, X. S., Wang, Z. W., Niu, Z. C., Diao, X. Y., and Wang, S. W.: Distribution and air-sea exchange of  
975 mercury (Hg) in the Yellow Sea, *Atmos. Chem. Phys.*, 11, 2881-2892, 2011b.
- 976 Clarkson, T. W., and Magos, L.: The toxicology of mercury and its chemical compounds, *Crit. Rev. Toxicol.*, 36,  
977 609-662, 2006.
- 978 Cobbett, F. D., Steffen, A., Lawson, G., and Van Heyst, B. J.: GEM fluxes and atmospheric mercury  
979 concentrations (GEM, RGM and Hg-P) in the Canadian Arctic at Alert, Nunavut, Canada (February-June 2005),  
980 *Atmos. Environ.*, 41, 6527-6543, 2007.
- 981 Cobbett, F. D., and Van Heyst, B. J.: Measurements of GEM fluxes and atmospheric mercury concentrations  
982 (GEM, RGM and Hg-P) from an agricultural field amended with biosolids in Southern Ont., Canada (October  
983 2004-November 2004), *Atmos. Environ.*, 41, 2270-2282, 2007.
- 984 Cobos, D. R., Baker, J. M., and Nater, E. A.: Conditional sampling for measuring mercury vapor fluxes, *Atmos.*  
985 *Environ.*, 36, 4309-4321, 2002.



- 986 Colombo, M. J., Ha, J., Reinfelder, J. R., Barkay, T., and Yee, N.: Anaerobic oxidation of Hg (0) and  
 987 methylmercury formation by *Desulfovibrio desulfuricans* ND132, *Geochim. Cosmochim. Ac.*, 112, 166-177,  
 988 2013.
- 989 Conaway, C. H., Squire, S., Mason, R. P., and Flegal, A. R.: Mercury speciation in the San Francisco Bay estuary,  
 990 *Mar. Chem.*, 80, 199-225, 2003.
- 991 Converse, A. D., Riscassi, A. L., and Scanlon, T. M.: Seasonal variability in gaseous mercury fluxes measured in a  
 992 high-elevation meadow, *Atmos. Environ.*, 44, 2176-2185, 2010.
- 993 Coolbaugh, M. F., Gustin, M. S., and Rytuba, J. J.: Annual emissions of mercury to the atmosphere from natural  
 994 sources in Nevada and California, *Environ. Geol.*, 42, 338-349, 2002.
- 995 Corbett-Hains, H., Walters, N. E., and Van Heyst, B. J.: Evaluating the effects of sub-zero temperature cycling on  
 996 mercury flux from soils, *Atmos. Environ.*, 102, 102-108, 2012.
- 997 Corbitt, E. S., Jacob, D. J., Holmes, C. D., Streets, D. G., and Sunderland, E. M.: Global source-receptor  
 998 relationships for mercury deposition under present-day and 2050 emissions scenarios, *Environ. Sci. Technol.*, 45,  
 999 10477-10484, 2011.
- 1000 Costa, M., and Liss, P. S.: Photoreduction of mercury in sea water and its possible implications for Hg-0 air-sea  
 1001 fluxes, *Mar. Chem.*, 68, 87-95, 1999.
- 1002 Cui, L., Feng, X., Lin, C.-J., Wang, X., Meng, B., Wang, X., and Wang, H.: Accumulation and translocation of  
 1003 <sup>198</sup>Hg in four crop species, *Environ. Toxicol. Chem.*, 33, 334-340, 2014.
- 1004 Dalziel, J., and Tordon, R.: Gaseous mercury flux measurements from two mine tailing sites in the Seal Harbour  
 1005 area of Nova Scotia, *Geochem. Explor. Env. A.*, 14, 17-24, 2014.
- 1006 Demers, J. D., Blum, J. D., and Zak, D. R.: Mercury isotopes in a forested ecosystem: Implications for air-surface  
 1007 exchange dynamics and the global mercury cycle, *Global Biogeochem. Cy.*, 27, 222-238, 2013.
- 1008 Deng, L., Fu, D., and Deng, N.: Photo-induced transformations of mercury(II) species in the presence of algae,  
 1009 *Chlorella vulgaris*, *J. Hazard. Mater.*, 164, 798-805, 2009.
- 1010 Dommergue, A., Ferrari, C. P., Gauchard, P.-A., Boutron, C. F., Poissant, L., Pilote, M., Jitaru, P., and Adams, F.  
 1011 C.: The fate of mercury species in a sub-arctic snowpack during snowmelt, *Geophys. Res. Lett.*, 30, 12,  
 1012 10.1029/2003GL017308, 2003.
- 1013 Driscoll, C. T., Mason, R. P., Chan, H. M., Jacob, D. J., and Pirrone, N.: Mercury as a global pollutant: Sources,  
 1014 pathways, and effects, *Environ. Sci. Technol.*, 47, 4967-4983, 2013.
- 1015 Du, B., Wang, Q., Luo, Y., and Duan, L.: Field measurements of soil Hg emission in a masson pine forest in  
 1016 Tieshanping, Chongqing in Southwestern China, *Huanjing Kexue*, 10, 35, 3830-3835, 2014. (In Chinese with  
 1017 English Abstract)
- 1018 Eckley, C. S., and Branfireun, B.: Gaseous mercury emissions from urban surfaces: Controls and spatiotemporal  
 1019 trends, *Appl. Geochem.*, 23, 369-383, 2008.
- 1020 Eckley, C. S., Gustin, M., Lin, C. J., Li, X., and Miller, M. B.: The influence of dynamic chamber design and  
 1021 operating parameters on calculated surface-to-air mercury fluxes, *Atmospheric Environment*, 44, 194-203, 2010.
- 1022 Eckley, C. S., Gustin, M., Marsik, F., and Miller, M. B.: Measurement of surface mercury fluxes at active  
 1023 industrial gold mines in Nevada (USA), *Sci. Total Environ.*, 409, 514-522, 2011a.
- 1024 Eckley, C. S., Gustin, M., Miller, M. B., and Marsik, F.: Scaling non-point-source mercury emissions from two  
 1025 active industrial gold mines: Influential Variables and Annual Emission Estimates, *Environ. Sci. Technol.*, 45,  
 1026 392-399, 2011b.
- 1027 Eckley, C. S., Blanchard, P., McLennan, D., Mintz, R., and Sekela, M.: Soil-air mercury flux near a large  
 1028 industrial emission source before and after Closure (Flin Flon, Manitoba, Canada), *Environ. Sci. Technol.*, 49,  
 1029 9750-9757, 2015.
- 1030 Edner, H., Faris, G., Sunesson, A., Svanberg, S., Bjarnason, J. Ö., Kristmannsdottir, H., and Sigurdsson, K.: Lidar  
 1031 search for atmospheric atomic mercury in Icelandic geothermal fields, *J. Geophys. Res.-Atmos.*, 96, 2977-2986,  
 1032 1991.
- 1033 Edwards, G. C., Rasmussen, P. E., Schroeder, W. H., Kemp, R. J., Dias, G. M., Fitzgerald-Hubble, C. R., Wong, E.  
 1034 K., Halfpenny-Mitchell, L., and Gustin, M. S.: Sources of variability in mercury flux measurements, *J. Geophys.*  
 1035 *Res.-Atmos.*, 106, 5421-5435, 2001.
- 1036 Edwards, G. C., Rasmussen, P. E., Schroeder, W. H., Wallace, D. M., Halfpenny-Mitchell, L., Dias, G. M., Kemp,  
 1037 R. J., and Ausma, S.: Development and evaluation of a sampling system to determine gaseous mercury fluxes  
 1038 using an aerodynamic micrometeorological gradient method, *J. Geophys. Res.-Atmos.*, 110, D10306,  
 1039 doi:10.1029/2004jd005187, 2005.
- 1040 Edwards, G. C., and Howard, D. A.: Air-surface exchange measurements of gaseous elemental mercury over  
 1041 naturally enriched and background terrestrial landscapes in Australia, *Atmos. Chem. Phys.*, 13, 5325-5336, 2013.
- 1042 Engle, M. A., Gustin, M. S., and Zhang, H.: Quantifying natural source mercury emissions from the Ivanhoe  
 1043 Mining District, north-central Nevada, USA, *Atmos. Environ.*, 35, 3987-3997, 2001.
- 1044 Engle, M. A., and Gustin, M. S.: Scaling of atmospheric mercury emissions from three naturally enriched areas:  
 1045 Flowery Peak, Nevada; Peavine Peak, Nevada; and Long Valley Caldera, California, *Sci. Total Environ.*, 290,



- 1046 91-104, 2002.
- 1047 Engle, M. A., Gustin, M. S., Lindberg, S. E., Gertler, A. W., and Ariya, P. A.: The influence of ozone on  
1048 atmospheric emissions of gaseous elemental mercury and reactive gaseous mercury from substrates, Atmos.  
1049 Environ., 39, 7506-7517, 2005.
- 1050 Engle, M. A., Gustin, M. S., Goff, F., Counce, D. A., Janik, C. J., Bergfeld, D., and Rytuba, J. J.: Atmospheric  
1051 mercury emissions from substrates and fumaroles associated with three hydrothermal systems in the western  
1052 United States, J. Geophys. Res.-Atmos., 111, D17304, doi:10.1029/2005JD006563, 2006.
- 1053 Erickson, J. A., Gustin, M. S., Schorran, D. E., Johnson, D. W., Lindberg, S. E., and Coleman, J. S.: Accumulation  
1054 of atmospheric mercury in forest foliage, Atmos. Environ., 37, 1613-1622, 2003.
- 1055 Erickson, J. A., and Gustin, M. S.: Foliar exchange of mercury as a function of soil and air mercury concentrations,  
1056 Sci. Total Environ., 324, 271-279, 2004.
- 1057 Erickson, J. A., Gustin, M. S., Lindberg, S. E., Olund, S. D., and Krabbenhoft, D. P.: Assessing the potential for  
1058 re-emission of mercury deposited in precipitation from arid soils using a stable isotope, Environ. Sci. Technol., 39,  
1059 8001-8007, 2005.
- 1060 Erickson, J. A., Gustin, M. S., Xin, M., Weisberg, P. J., and Fernandez, G. C. J.: Air-soil exchange of mercury from  
1061 background soils in the United States, Sci. Total Environ., 366, 851-863, 2006.
- 1062 Fain, X., Moosmuller, H., and Obrist, D.: Toward real-time measurement of atmospheric mercury concentrations  
1063 using cavity ring-down spectroscopy, Atmos. Chem. Phys., 10, 2879-2892, 2010.
- 1064 Fain, X., Grangeon, S., Bahlmann, E., Fritsche, J., Obrist, D., Dommergue, A., Ferrari, C. P., Cairns, W.,  
1065 Ebinghaus, R., and Barbante, C.: Diurnal production of gaseous mercury in the alpine snowpack before snowmelt,  
1066 J. Geophys. Res.-Atmos., 112, D21311, doi:10.1029/2007JD008520, 2007.
- 1067 Fang, F., Wang, Q., and Luo, J.: Mercury concentration, emission flux in urban land surface and its factors,  
1068 Shengtai Huanjing, 12, 260-262, 2003. (In Chinese with English Abstract)
- 1069 Fantozzi, L., Ferrara, R., Dini, F., Tamburello, L., Pirrone, N., and Sprovieri, F.: Study on the reduction of  
1070 atmospheric mercury emissions from mine waste enriched soils through native grass cover in the Mt. Amiata  
1071 region of Italy, Environ. Res., 125, 69-74, 2013.
- 1072 Fay, L., and Gustin, M.: Assessing the influence of different atmospheric and soil mercury concentrations on foliar  
1073 mercury concentrations in a controlled environment, Water Air Soil Poll., 181, 373-384, 2007a.
- 1074 Fay, L., and Gustin, M. S.: Investigation of mercury accumulation in cattails growing in constructed wetland  
1075 mesocosms, Wetlands, 27, 1056-1065, 2007b.
- 1076 Feng, X., Chen, Y., and Zhu, W.: Vertical fluxes of volatile mercury over soil surfaces in Guizhou Province, China,  
1077 J. Environ. Sci., 9, 241-245, 1997.
- 1078 Feng, X., Shang, L., Tang, S., Yan, H., and Liu, C.: Gaseous mercury exchange rate between air and water over  
1079 Baihua reservoir, Guizhou, China during cold season, J. Phys. IV, 107, 451-454, 2003.
- 1080 Feng, X. B., Sommar, J., Gärdfeldt, K., and Lindqvist, O.: Exchange flux of total gaseous mercury between air and  
1081 natural water surfaces in summer season, Sci. China Ser. D, 45, 211-220, 2002.
- 1082 Feng, X. B., Yan, H. Y., Wang, S. F., Qiu, G. L., Tang, S. L., Shang, L. H., Dai, Q. J., and Hou, Y. M.: Seasonal  
1083 variation of gaseous mercury exchange rate between air and water surface over Baihua reservoir, Guizhou, China,  
1084 Atmos. Environ., 38, 4721-4732, 2004.
- 1085 Feng, X. B., Wang, S. F., Qiu, G. L., Hou, Y. M., and Tang, S. L.: Total gaseous mercury emissions from soil in  
1086 Guiyang, Guizhou, China, J. Geophys. Res.-Atmos., 110, D14306, doi:10.1029/2004JD005643, 2005.
- 1087 Feng, X. B., Li, P., Qiu, G. L., Wang, S., Li, G. H., Shang, L. H., Meng, B., Jiang, H. M., Bai, W. Y., Li, Z. G., and  
1088 Fu, X. W.: Human exposure to methylmercury through rice intake in mercury mining areas, guizhou province,  
1089 china, Environ. Sci. Technol., 42, 326-332, 2008a.
- 1090 Feng, X. B., Wang, S. F., Qiu, G. G., He, T. R., Li, G. H., Li, Z. G., and Shang, L. H.: Total gaseous mercury  
1091 exchange between water and air during cloudy weather conditions over Hongfeng Reservoir, Guizhou, China, J.  
1092 Geophys. Res.-Atmos., 113, D15309, doi:10.1029/2007JD009600, 2008b.
- 1093 Ferrara, R., Maserti, B. E., Andersson, M., Edner, H., Ragnarson, P., and Svanberg, S.: Mercury degassing rate  
1094 from mineralized areas in the Mediterranean basin, Water Air Soil Poll., 93, 59-66, 1997.
- 1095 Ferrara, R., Maserti, B. E., Andersson, M., Edner, H., Ragnarson, P., Svanberg, S., and Hernandez, A.:  
1096 Atmospheric mercury concentrations and fluxes in the Almadén district (Spain), Atmos. Environ., 32, 3897-3904,  
1097 1998a.
- 1098 Ferrara, R., and Mazzolai, B.: A dynamic flux chamber to measure mercury emission from aquatic systems, Sci.  
1099 Total Environ., 215, 51-57, 1998.
- 1100 Ferrara, R., Mazzolai, B., Edner, H., Svanberg, S., and Wallinder, E.: Atmospheric mercury sources in the Mt.  
1101 Amiata area, Italy, Sci. Total Environ., 213, 13-23, 1998b.
- 1102 Ferrara, R., Lanzillotta, E., and Ceccarini, C.: Dissolved gaseous mercury concentration and mercury evasion  
1103 flux from seawater in front of a chlor-alkali plant, Environ. Technol., 22, 971-978, 2001.
- 1104 Ferrari, C. P., Dommergue, A., Boutron, C. F., Skov, H., Goodsite, M., and Jensen, B.: Nighttime production of  
1105 elemental gaseous mercury in interstitial air of snow at Station Nord, Greenland, Atmos. Environ., 38, 2727-2735,



- 1106 2004.
- 1107 Ferrari, C. P., Gauchard, P. A., Aspmo, K., Dommergue, A., Magand, O., Bahlmann, E., Nagorski, S., Temme, C.,  
 1108 Ebinghaus, R., and Steffen, A.: Snow-to-air exchanges of mercury in an Arctic seasonal snow pack in Ny-Ålesund,  
 1109 Svalbard, *Atmos. Environ.*, 39, 7633-7645, 2005.
- 1110 Fitzgerald, W. F., and Gill, G. A.: Subnanogram determination of mercury by two-stage gold amalgamation and  
 1111 gas phase detection applied to atmospheric analysis, *Anal Chem*, 51, 1714-1720, 10.1021/ac50047a030, 1979.
- 1112 Frescholtz, T. F., Gustin, M. S., Schorran, D. E., and Fernandez, G. C. J.: Assessing the source of mercury in foliar  
 1113 tissue of quaking aspen, *Environ. Toxicol. Chem.*, 22, 2114-2119, 2003.
- 1114 Frescholtz, T. F., and Gustin, M. S.: Soil and foliar mercury emission as a function of soil concentration, *Water Air  
 1115 Soil Poll.*, 155, 223-237, 2004.
- 1116 Fritsche, J., Obrist, D., and Alewell, C.: Evidence of microbial control of Hg<sup>0</sup> emissions from uncontaminated  
 1117 terrestrial soils, *J. Plant Nutr. Soil Sc.*, 171, 200-209, 2008a.
- 1118 Fritsche, J., Obrist, D., Zeeman, M. J., Conen, F., Eugster, W., and Alewell, C.: Elemental mercury fluxes over a  
 1119 sub-alpine grassland determined with two micrometeorological methods, *Atmos. Environ.*, 42, 2922-2933, 2008b.
- 1120 Fritsche, J., Wohlfahrt, G., Ammann, C., Zeeman, M., Hammerle, A., Obrist, D., and Alewell, C.: Summertime  
 1121 elemental mercury exchange of temperate grasslands on an ecosystem-scale, *Atmos. Chem. Phys.*, 8, 7709-7722,  
 1122 2008c.
- 1123 Fritsche, J., Osterwalder, S., Nilsson, M. B., Sagerfors, J., Åkerblom, S., Bishop, K., and Alewell, C.: Evasion of  
 1124 Elemental Mercury from a Boreal Peatland Suppressed by Long-Term Sulfate Addition, *Environ. Sci. Technol.  
 1125 Lett.*, 1, 421-425, 10.1021/ez500223a, 2014.
- 1126 Fu, X., Feng, X., Zhang, H., Yu, B., and Chen, L.: Mercury emissions from natural surfaces highly impacted by  
 1127 human activities in Guangzhou province, South China, *Atmos. Environ.*, 54, 185-193, 2012a.
- 1128 Fu, X., Feng, X., Guo, Y., Meng, B., Yin, R., and Yao, H.: Distribution and production of reactive mercury and  
 1129 dissolved gaseous mercury in surface waters and water/air mercury flux in reservoirs on Wujiang River,  
 1130 Southwest China, *J. Geophys. Res.-Atmos.*, 118, 3905-3917, 2013a.
- 1131 Fu, X., Feng, X., Yin, R., and Zhang, H.: Diurnal variations of total mercury, reactive mercury, and dissolved  
 1132 gaseous mercury concentrations and water/air mercury flux in warm and cold seasons from freshwaters of  
 1133 southwestern China, *Environ. Toxicol. Chem.*, 32, 2256-2265, 2013b.
- 1134 Fu, X. W., Feng, X. B., and Wang, S. F.: Exchange fluxes of Hg between surfaces and atmosphere in the eastern  
 1135 flank of Mount Gongga, Sichuan province, southwestern China, *J. Geophys. Res.-Atmos.*, 113, D20306,  
 1136 doi:10.1029/2008JD009814, 2008a.
- 1137 Fu, X. W., Feng, X. B., Wang, S. F., Qiu, G. L., and Li, P.: Mercury flux rate of two types of grasslands in Guiyang,  
 1138 *Huanjing Kexue Yanjiu*, 20, 33-37, 2008b. (In Chinese with English Abstract)
- 1139 Fu, X. W., Feng, X. B., Wan, Q., Meng, B., Yan, H. Y., and Guo, Y. N.: Probing Hg evasion from surface waters of  
 1140 two Chinese hyper/meso-eutrophic reservoirs, *Sci. Total Environ.*, 408, 5887-5896, 2010a.
- 1141 Fu, X. W., Feng, X. B., Zhang, G., Xu, W. H., Li, X. D., Yao, H., Liang, P., Li, J., Sommar, J., Yin, R. S., and Liu,  
 1142 N.: Mercury in the marine boundary layer and seawater of the South China Sea: Concentrations, sea/air flux, and  
 1143 implication for land outflow, *J. Geophys. Res.-Atmos.*, 115, D06303, doi:10.1029/2009JD012958, 2010b.
- 1144 Fu, X. W., Feng, X., Liang, P., Deliger, Zhang, H., Ji, J., and Liu, P.: Temporal trend and sources of speciated  
 1145 atmospheric mercury at Waliguan GAW station, Northwestern China, *Atmos. Chem. Phys.*, 12, 1951-1964,  
 1146 2012b.
- 1147 Fu, X. W., Zhang, H., Lin, C. J., Feng, X. B., Zhou, L. X., and Fang, S. X.: Correlation slopes of GEM/CO,  
 1148 GEM/CO<sub>2</sub>, and GEM/CH<sub>4</sub> and estimated mercury emissions in China, South Asia, the Indochinese Peninsula, and  
 1149 Central Asia derived from observations in northwestern and southwestern China, *Atmos. Chem. Phys.*, 15,  
 1150 1013-1028, 2015a.
- 1151 Fu, X. W., Zhang, H., Yu, B., Wang, X., Lin, C. J., and Feng, X. B.: Observations of atmospheric mercury in China:  
 1152 a critical review, *Atmos. Chem. Phys.*, 15, 9455-9476, 2015b.
- 1153 Fu, X. W., Zhu, W., Zhang, H., Wang, X., Sommar, J., Xu, Y., Lin, C. J., and Feng, X. B.: Depletion of atmospheric  
 1154 gaseous elemental mercury by plant uptake at Mt. Changbai, Northeast China, Submitted to *Environ. Sci.  
 1155 Technol.*, 2015c.
- 1156 Gabriel, M. C., Williamson, D. G., Brooks, S., Zhang, H., and Lindberg, S.: Spatial variability of mercury  
 1157 emissions from soils in a southeastern US urban environment, *Environ. Geol.*, 48, 955-964, 2005.
- 1158 Gabriel, M. C., Williamson, D. G., Zhang, H., Brooks, S., and Lindberg, S.: Diurnal and seasonal trends in total  
 1159 gaseous mercury flux from three urban ground surfaces, *Atmos. Environ.*, 40, 4269-4284, 2006.
- 1160 García-Sánchez, A., Contreras, F., Adams, M., and Santos, F.: Atmospheric mercury emissions from polluted gold  
 1161 mining areas (Venezuela), *Environ. Geochem. Hlth.*, 28, 529-540, 2006.
- 1162 Gärdfeldt, K., Feng, X., Sommar, J., and Lindqvist, O.: Total gaseous mercury exchange between air and water at  
 1163 river and sea surfaces in Swedish coastal regions, *Atmos. Environ.*, 35, 3027-3038, 2001.
- 1164 Gärdfeldt, K., Sommar, J., Ferrara, R., Ceccarini, C., Lanzillotta, E., Munthe, J., Wängberg, I., Lindqvist, O.,  
 1165 Pirone, N., Sprovieri, F., Pesenti, E., and Strömberg, D.: Evasion of mercury from coastal and open waters of the



- 1166 Atlantic Ocean and the Mediterranean Sea, *Atmos. Environ.*, **37**, 73-84, 2003.
- 1167 Gbor, P., Wen, D., Meng, F., Yang, F., Zhang, B., and Sloan, J.: Improved model for mercury emission, transport  
 1168 and deposition, *Atmos. Environ.*, **40**, 973-983, 2006.
- 1169 Gillis, A., and Miller, D. R.: Some potential errors in the measurement of mercury gas exchange at the soil surface  
 1170 using a dynamic flux chamber, *Sci. Total Environ.*, **260**, 181-189, 2000a.
- 1171 Gillis, A. A., and Miller, D. R.: Some local environmental effects on mercury emission and absorption at a soil  
 1172 surface, *Sci. Total Environ.*, **260**, 191-200, 2000b.
- 1173 Goodrow, S. M., Miskewitz, R., Hires, R. I., Eisenreich, S. J., Douglas, W. S., and Reinfeld, J. R.: Mercury  
 1174 emissions from cement-stabilized dredged material, *Environ. Sci. Technol.*, **39**, 8185-8190, 2005.
- 1175 Graydon, J. A., St Louis, V. L., Lindberg, S. E., Hintelmann, H., and Krabbenhoft, D. P.: Investigation of mercury  
 1176 exchange between forest canopy vegetation and the atmosphere using a new dynamic chamber, *Environ. Sci.  
 1177 Technol.*, **40**, 4680-4688, 2006.
- 1178 Grigal, D. F.: Mercury sequestration in forests and peatlands: A review, *J. Environ. Qual.*, **32**, 393-405, 2003.
- 1179 Gronholm, T., Haapanala, S., Launiainen, S., Rinne, J., Vesala, T., and Rannik, U.: The dependence of the beta  
 1180 coefficient of REA system with dynamic deadband on atmospheric conditions, *Environ. Poll.*, **152**, 597-603,  
 1181 2008.
- 1182 Gu, B. H., Bian, Y. R., Miller, C. L., Dong, W. M., Jiang, X., and Liang, L. Y.: Mercury reduction and  
 1183 complexation by natural organic matter in anoxic environments, *P. Natl. Acad. Sci. USA*, **108**, 1479-1483, 2011.
- 1184 Guédron, S., Grangeon, S., Jouravel, G., Charlet, L., and Sarret, G.: Atmospheric mercury incorporation in soils of  
 1185 an area impacted by a chlor-alkali plant (Grenoble, France): Contribution of canopy uptake, *Sci. Total Environ.*,  
 1186 **445**, 356-364, 2013.
- 1187 Gustin, M., and Jaffe, D.: Reducing the Uncertainty in Measurement and Understanding of Mercury in the  
 1188 Atmosphere, *Environ. Sci. Technol.*, **44**, 2222-2227, 2010.
- 1189 Gustin, M. S., Taylor, G. E., and Maxey, R. A.: Effect of temperature and air movement on the flux of elemental  
 1190 mercury from substrate to the atmosphere, *J. Geophys. Res.-Atmos.*, **102**, 3891-3898, 1997.
- 1191 Gustin, M. S., Lindberg, S., Marsik, F., Casimir, A., Ebinghaus, R., Edwards, G., Hubble-Fitzgerald, C., Kemp, R.,  
 1192 Kock, H., Leonard, T., London, J., Majewski, M., Montecinos, C., Owens, J., Pilote, M., Poissant, L., Rasmussen,  
 1193 P., Schaedlich, F., Schneeberger, D., Schroeder, W., Sommar, J., Turner, R., Vette, A., Wallschlaeger, D., Xiao, Z.,  
 1194 and Zhang, H.: Nevada STORMS project: Measurement of mercury emissions from naturally enriched surfaces, *J.  
 1195 Geophys. Res.-Atmos.*, **104**, 21831-21844, 1999.
- 1196 Gustin, M. S., Biester, H., and Kim, C. S.: Investigation of the light-enhanced emission of mercury from naturally  
 1197 enriched substrates, *Atmos. Environ.*, **36**, 3241-3254, 2002.
- 1198 Gustin, M. S., Coolbaugh, M. F., Engle, M. A., Fitzgerald, B. C., Keislar, R. E., Lindberg, S. E., Nacht, D. M.,  
 1199 Quashnick, J., Rytuba, J. J., Sladek, C., Zhang, H., and Zehner, R. E.: Atmospheric mercury emissions from mine  
 1200 wastes and surrounding geologically enriched terrains, *Environ. Geol.*, **43**, 339-351, 2003.
- 1201 Gustin, M. S., Ericksen, J. A., Schorran, D. E., Johnson, D. W., Lindberg, S. E., and Coleman, J. S.: Application of  
 1202 controlled mesocosms for understanding mercury air-soil-plant exchange, *Environ. Sci. Technol.*, **38**, 6044-6050,  
 1203 2004.
- 1204 Gustin, M. S., and Stamenkovic, J.: Effect of watering and soil moisture on mercury emissions from soils,  
 1205 *Biogeochemistry*, **76**, 215-232, 2005.
- 1206 Gustin, M. S., Engle, M., Ericksen, J., Lyman, S., Stamenkovic, J., and Xin, M.: Mercury exchange between the  
 1207 atmosphere and low mercury containing substrates, *Appl. Geochem.*, **21**, 1913-1923, 2006.
- 1208 Gustin, M. S., Lindberg, S. E., and Weisberg, P. J.: An update on the natural sources and sinks of atmospheric  
 1209 mercury, *Appl. Geochem.*, **23**, 482-493, 2008.
- 1210 Gustin, M. S.: Exchange of mercury between the atmosphere and terrestrial ecosystems, in: *Environmental  
 1211 Chemistry and Toxicology of Mercury*, edited by: Liu, G. L., Cai, Y., and O'Driscoll, N., 423-451, 2011.
- 1212 Gustin, M. S., Huang, J., Miller, M. B., Peterson, C., Jaffe, D. A., Ambrose, J., Finley, B. D., Lyman, S. N., Call,  
 1213 K., Talbot, R., Feddersen, D., Mao, H., and Lindberg, S. E.: Do we understand what the mercury speciation  
 1214 instruments are actually measuring? Results of RAMIX, *Environ. Sci. Technol.*, **47**, 7295-7306, 2013.
- 1215 Gustin, M. S., Amos, H. M., Huang, J., Miller, M. B., and Heidecorn, K.: Measuring and modeling mercury in the  
 1216 atmosphere: a critical review, *Atmos. Chem. Phys.*, **15**, 5697-5713, 2015.
- 1217 Hanson, P. J., Lindberg, S. E., Tabberer, T. A., Owens, J. G., and Kim, K. H.: Foliar exchange of mercury-vapor -  
 1218 evidence for a compensation point, *Water Air Soil Poll.*, **80**, 373-382, 1995.
- 1219 Hartman, J. S., Weisberg, P. J., Pillai, R., Ericksen, J. A., Kuiken, T., Lindberg, S. E., Zhang, H., Rytuba, J. J., and  
 1220 Gustin, M. S.: Application of a rule-based model to estimate mercury exchange for three background biomes in  
 1221 the Continental United States, *Environ. Sci. Technol.*, **43**, 4989-4994, 2009.
- 1222 He, F., Zhao, W., Liang, L., and Gu, B.: Photochemical oxidation of dissolved elemental mercury by carbonate  
 1223 radicals in water, *Environ. Sci. Technol. Lett.*, **1**, 499-503, 2014.
- 1224 He, J., Tan, H., Sommar, J., Xiao, Z., and Lindqvist, O.: Mercury pollution in a mining area of Guizhou, China:  
 1225 Fluxes over contaminated surfaces and concentrations in air, biological and geological samples, *Toxicol. Environ.*



- 1226 Chem., 67, 225-236, 1998.
- 1227 Heaton, A. P., Rugh, C., Wang, N.-J., and Meagher, R.: Physiological responses of transgenic *merA-tobacco*
- 1228 (*Nicotiana tabacum*) to foliar and root mercury exposure, *Water Air Soil Poll.*, 161, 137-155, 2005.
- 1229 Hines, N. A., and Brezonik, P. L.: Mercury dynamics in a small Northern Minnesota lake: water to air exchange
- 1230 and photoreactions of mercury, *Mar. Chem.*, 90, 137-149, 2004.
- 1231 Hintelmann, H., Harris, R., Heyes, A., Hurley, J. P., Kelly, C. A., Krabbenhoft, D. P., Lindberg, S., Rudd, J. W. M.,
- 1232 Scott, K. J., and St Louis, V. L.: Reactivity and mobility of new and old mercury deposition in a Boreal forest
- 1233 ecosystem during the first year of the METAALICUS study, *Environ. Sci. Technol.*, 36, 5034-5040, 2002.
- 1234 Holland K. 2005. Standard operation procedures: Ohio lumex mercury analyzer (Lumex RA 915). Available at
- 1235 [http://www.renewnyc.com/content/pdfs/130liberty/SeptemberDeconstruction/B\\_SOP\\_for\\_OhioLumex.pdf](http://www.renewnyc.com/content/pdfs/130liberty/SeptemberDeconstruction/B_SOP_for_OhioLumex.pdf). Last
- 1236 accessed December 25<sup>th</sup>, 2015.
- 1237 Hu, H., Lin, H., Zheng, W., Tomanicek, S. J., Johs, A., Feng, X., Elias, D. A., Liang, L., and Gu, B.: Oxidation and
- 1238 methylation of dissolved elemental mercury by anaerobic bacteria, *Nat. Geosci.*, 6, 751-754, 2013.
- 1239 Jaffe, D., Prestbo, E., Swartzendruber, P., Weiss-Penzias, P., Kato, S., Takami, A., Hatakeyama, S., and Kajii, Y.:
- 1240 Export of atmospheric mercury from Asia, *Atmos. Environ.*, 39, 3029-3038, 2005.
- 1241 Jiskra, M., Wiederhold, J. G., Skyllberg, U., Kronberg, R.-M., Hajdas, I., and Kretzschmar, R.: Mercury
- 1242 deposition and re-emission pathways in boreal forest soils investigated with Hg isotope signatures, *Environ. Sci.*
- 1243 *Technol.*, 49, 7188-7196, 2015.
- 1244 Kikuchi, T., Ikemoto, H., Takahashi, K., Hasome, H., and Ueda, H.: Parameterizing soil emission and atmospheric
- 1245 oxidation-reduction in a model of the global biogeochemical cycle of mercury, *Environ. Sci. Technol.*, 47,
- 1246 12266-12274, 2013.
- 1247 Kim, J. P., and Fitzgerald, W. F.: Sea-air partitioning of mercury in the Equatorial Pacific Ocean, *Science*, 231,
- 1248 1131-1133, 1986.
- 1249 Kim, K.-H., Kim, M.-Y., Kim, J., and Lee, G.: The concentrations and fluxes of total gaseous mercury in a western
- 1250 coastal area of Korea during late March 2001, *Atmos. Environ.*, 36, 3413-3427, 2002.
- 1251 Kim, K. H., and Lindberg, S. E.: Design and initial tests of a dynamic enclosure chamber for measurements of
- 1252 vapor-phase mercury fluxes over soils, *Water Air Soil Poll.*, 80, 1059-1068, 1995.
- 1253 Kim, K. H., Lindberg, S. E., and Meyers, T. P.: Micrometeorological measurements of mercury-vapor fluxes over
- 1254 background forest soils in eastern Tennessee, *Atmos. Environ.*, 29, 267-282, 1995.
- 1255 Kim, K. H., and Kim, M. Y.: The exchange of gaseous mercury across soil-air interface in a residential area of
- 1256 Seoul, Korea, *Atmos. Environ.*, 33, 3153-3165, 1999.
- 1257 Kim, K. H., Kim, M. Y., and Lee, G.: The soil-air exchange characteristics of total gaseous mercury from a
- 1258 large-scale municipal landfill area, *Atmos. Environ.*, 35, 3475-3493, 2001.
- 1259 Kim, K. H., Kim, M. Y., Kim, J., and Lee, G.: Effects of changes in environmental conditions on atmospheric
- 1260 mercury exchange: Comparative analysis from a rice paddy field during the two spring periods of 2001 and 2002,
- 1261 *J. Geophys. Res.-Atmos.*, 108, 4607, doi:10.1029/2003JD003375, 2003.
- 1262 Kirk, J. L., St. Louis, V. L., and Sharp, M. J.: Rapid reduction and reemission of mercury deposited into
- 1263 snowpacks during atmospheric mercury depletion events at Churchill, Manitoba, Canada, *Environ. Sci. Technol.*,
- 1264 40, 7590-7596, 2006.
- 1265 Kocman, D., and Horvat, M.: A laboratory based experimental study of mercury emission from contaminated soils
- 1266 in the River Idrija catchment, *Atmos. Chem. Phys.*, 10, 1417-1426, 2010.
- 1267 Kocman, D., and Horvat, M.: Non-point source mercury emission from the Idrija Hg-mine region: GIS mercury
- 1268 emission model, *J. Environ. Manage.*, 92, 2038-2046, 2011.
- 1269 Kocman, D., Horvat, M., Pirrone, N., and Cinnirella, S.: Contribution of contaminated sites to the global mercury
- 1270 budget, *Environ. Res.*, 125, 160-170, 2013.
- 1271 Kotnik, J., Horvat, M., and Dizdarevic, T.: Current and past mercury distribution in air over the Idrija Hg mine
- 1272 region, Slovenia, *Atmos. Environ.*, 39, 7570-7579, 2005.
- 1273 Kuiken, T., Gustin, M., Zhang, H., Lindberg, S., and Sedinger, B.: Mercury emission from terrestrial background
- 1274 surfaces in the eastern USA. II: Air/surface exchange of mercury within forests from South Carolina to New
- 1275 England, *Appl. Geochem.*, 23, 356-368, 2008a.
- 1276 Kuiken, T., Zhang, H., Gustin, M., and Lindberg, S.: Mercury emission from terrestrial background surfaces in the
- 1277 eastern USA. Part I: Air/surface exchange of mercury within a southeastern deciduous forest (Tennessee) over one
- 1278 year, *Appl. Geochem.*, 23, 345-355, 2008b.
- 1279 Kuss, J., and Schneider, B.: Variability of the gaseous elemental mercury sea-air flux of the Baltic Sea, *Environ.*
- 1280 *Sci. Technol.*, 41, 8018-8023, 2007.
- 1281 Kuss, J., Holzmann, J., and Ludwig, R.: An elemental mercury diffusion coefficient for natural waters determined
- 1282 by molecular dynamics simulation, *Environ. Sci. Technol.*, 43, 3183-3186, 2009.
- 1283 Kuss, J.: Water—air gas exchange of elemental mercury: An experimentally determined mercury diffusion
- 1284 coefficient for Hg<sup>0</sup> water—air flux calculations, *Limnol. Oceanogr.*, 59, 1461-1467, 2014.
- 1285 Kuss, J., Wasmund, N., Nausch, G., and Labrenz, M.: Mercury Emission by the Baltic Sea: A consequence of





- 1286 cyanobacterial activity, photochemistry, and low-light mercury Transformation, *Environ. Sci. Technol.*, 49,  
1287 11449-11457, 2015.
- 1288 Kyllonen, K., Hakola, H., Hellen, H., Korhonen, M., and Verta, M.: Atmospheric mercury fluxes in a southern  
1289 boreal forest and wetland, *Water Air Soil Poll.*, 223, 1171-1182, 2012.
- 1290 Laacouri, A., Nater, E. A., and Kolka, R. K.: Distribution and uptake dynamics of mercury in leaves of common  
1291 deciduous tree species in Minnesota, U.S.A, *Environ. Sci. Technol.*, 47, 10462-10470, 2013.
- 1292 Lalonde, J. D., Amyot, M., Kraepiel, A. M. L., and Morel, F. M. M.: Photooxidation of Hg(0) in artificial and  
1293 natural waters, *Environ. Sci. Technol.*, 35, 1367-1372, 2001.
- 1294 Lalonde, J. D., Poulain, A. J., and Amyot, M.: The role of mercury redox reactions in snow on snow-to-air  
1295 mercury transfer, *Environ. Sci. Technol.*, 36, 174-178, 2002.
- 1296 Lalonde, J. D., Amyot, M., Doyon, M.-R., and Auclair, J.-C.: Photo-induced Hg(II) reduction in snow from the  
1297 remote and temperate Experimental Lakes Area (Ontario, Canada), *J. Geophys. Res.-Atmos.*, 108(D6), 4200,  
1298 10.1029/2001JD001534, 2003.
- 1299 Laurier, F. J. G., Mason, R. P., Whalin, L., and Kato, S.: Reactive gaseous mercury formation in the North Pacific  
1300 Ocean's marine boundary layer: A potential role of halogen chemistry, *J. Geophys. Res.-Atmos.*, 108, 4529,  
1301 doi:10.1029/2003JD003625, 2003.
- 1302 Lee, X., Benoit, G., and Hu, X. Z.: Total gaseous mercury concentration and flux over a coastal saltmarsh  
1303 vegetation in Connecticut, USA, *Atmos. Environ.*, 34, 4205-4213, 2000.
- 1304 Leonard, T. L., Taylor, G. E., Gustin, M. S., and Fernandez, G. C. J.: Mercury and plants in contaminated soils: 1.  
1305 Uptake, partitioning, and emission to the atmosphere, *Environ. Toxicol. Chem.*, 17, 2063-2071, 1998a.
- 1306 Leonard, T. L., Taylor, G. E., Gustin, M. S., and Fernandez, G. C. J.: Mercury and plants in contaminated soils: 2.  
1307 Environmental and physiological factors governing mercury flux to the atmosphere, *Environ. Toxicol. Chem.*, 17,  
1308 2072-2079, 1998b.
- 1309 Li, Z. G., Feng, X., Li, P., Liang, L., Tang, S. L., Wang, S. F., Fu, X. W., Qiu, G. L., and Shang, L. H.: Emissions of  
1310 air-borne mercury from five municipal solid waste landfills in Guiyang and Wuhan, China, *Atmos. Chem. Phys.*,  
1311 10, 3353-3364, 2010.
- 1312 Li, Z. G., Feng, X. B., Li, G. H., Bi, X. Y., Sun, G. Y., Zhu, J. M., Qin, H. B., and Wang, J. X.: Mercury and other  
1313 metal and metalloid soil contamination near a Pb/Zn smelter in east Hunan province, China, *Appl. Geochem.*, 26,  
1314 160-166, 2011.
- 1315 Lin, C.-C., Yee, N., and Barkay, T.: Microbial Transformations in the Mercury Cycle, in: *Environmental  
1316 Chemistry and Toxicology of Mercury*, John Wiley & Sons, Inc., 155-191, 2011.
- 1317 Lin, C.-J., and Pehkonen, S. O.: Aqueous free radical chemistry of mercury in the presence of iron oxides and  
1318 ambient aerosol, *Atmos. Environ.*, 31, 4125-4137, 1997.
- 1319 Lin, C.-J., Zhu, W., Li, X., Feng, X., Sommar, J., and Shang, L.: Novel dynamic flux chamber for measuring  
1320 air-surface exchange of Hg<sup>0</sup> from soils, *Environ. Sci. Technol.*, 46, 8910-8920, 2012.
- 1321 Lin, C. J., and Pehkonen, S. O.: The chemistry of atmospheric mercury: a review, *Atmos. Environ.*, 33, 2067-2079,  
1322 1999.
- 1323 Lin, C. J., Gustin, M. S., Singhasuk, P., Eckley, C., and Miller, M.: Empirical models for estimating mercury flux  
1324 from soils, *Environ. Sci. Technol.*, 44, 8522-8528, 2010a.
- 1325 Lin, C. J., Pan, L., Streets, D. G., Shetty, S. K., Jang, C., Feng, X., Chu, H. W., and Ho, T. C.: Estimating mercury  
1326 emission outflow from East Asia using CMAQ-Hg, *Atmos. Chem. Phys.*, 10, 1853-1864, 2010b.
- 1327 Lindberg, S., Meyers, T., Taylor Jr, G., Turner, R., and Schroeder, W.: Atmosphere-surface exchange of mercury  
1328 in a forest: results of modeling and gradient approaches, *J. Geophys. Res.-Atmos.*, 97, 2519-2528, 1992.
- 1329 Lindberg, S., and Meyers, T.: Development of an automated micrometeorological method for measuring the  
1330 emission of mercury vapor from wetland vegetation, *Wetl. Ecol. Manag.*, 9, 333-347, 2001.
- 1331 Lindberg, S., Bullock, R., Ebinghaus, R., Engstrom, D., Feng, X. B., Fitzgerald, W., Pirrone, N., Prestbo, E., and  
1332 Seigneur, C.: A synthesis of progress and uncertainties in attributing the sources of mercury in deposition, *Ambio*,  
1333 36, 19-32, 2007.
- 1334 Lindberg, S. E., Kim, K. H., Meyers, T. P., and Owens, J. G.: Micrometeorological gradient approach for  
1335 quantifying air-surface exchange of mercury-vapor - tests over contaminated soils, *Environ. Sci. Technol.*, 29,  
1336 126-135, 1995a.
- 1337 Lindberg, S. E., Meyers, T. P., and Munthe, J.: Evasion of mercury vapor from the surface of a recently limed acid  
1338 forest lake in Sweden, *Water Air Soil Poll.*, 85, 725-730, 1995b.
- 1339 Lindberg, S. E., Hanson, P. J., Meyers, T. P., and Kim, K. H.: Air/surface exchange of mercury vapor over forests  
1340 - The need for a reassessment of continental biogenic emissions, *Atmos. Environ.*, 32, 895-908, 1998.
- 1341 Lindberg, S. E., and Price, J. L.: Airborne Emissions of Mercury from Municipal Landfill Operations: A  
1342 Short-Term Measurement Study in Florida, *J. Air Waste Manage.*, 49, 520-532, 1999.
- 1343 Lindberg, S. E., Zhang, H., Gustin, M., Vette, A., Marsik, F., Owens, J., Casimir, A., Ebinghaus, R., Edwards, G.,  
1344 Fitzgerald, C., Kemp, J., Kock, H. H., London, J., Majewski, M., Poissant, L., Pilote, M., Rasmussen, P.,  
1345 Schaedlich, F., Schneeberger, D., Sommar, J., Turner, R., Wallschläger, D., and Xiao, Z.: Increases in mercury



- 1346 emissions from desert soils in response to rainfall and irrigation, *J. Geophys. Res.-Atmos.*, 104, 21879-21888,  
1347 1999.
- 1348 Lindberg, S. E., and Zhang, H.: Air/water exchange of mercury in the Everglades II: measuring and modeling  
1349 evasion of mercury from surface waters in the Everglades Nutrient Removal Project, *Sci. Total Environ.*, 259,  
1350 135-143, 2000.
- 1351 Lindberg, S. E., Brooks, S., Lin, C. J., Scott, K. J., Landis, M. S., Stevens, R. K., Goodsite, M., and Richter, A.:  
1352 Dynamic oxidation of gaseous mercury in the Arctic troposphere at polar sunrise, *Environ. Sci. Technol.*, 36,  
1353 1245-1256, 2002a.
- 1354 Lindberg, S. E., Dong, W. J., and Meyers, T.: Transpiration of gaseous elemental mercury through vegetation in a  
1355 subtropical wetland in Florida, *Atmos. Environ.*, 36, 5207-5219, 2002b.
- 1356 Lindberg, S. E., Zhang, H., Vette, A. F., Gustin, M. S., Barnett, M. O., and Kuiken, T.: Dynamic flux chamber  
1357 measurement of gaseous mercury emission fluxes over soils: Part 2 - effect of flushing flow rate and verification  
1358 of a two-resistance exchange interface simulation model, *Atmos. Environ.*, 36, 847-859, 2002c.
- 1359 Lindberg, S. E., Southworth, G. R., Bogle, M. A., Blasing, T. J., Owens, J., Roy, K., Zhang, H., Kuiken, T., Price,  
1360 J., Reinhart, D., and Sfeir, H.: Airborne emissions of mercury from municipal solid waste. I: New measurements  
1361 from six operating landfills in Florida, *J. Air Waste Manage.*, 55, 859-869, 2005.
- 1362 Lindqvist, O., Johansson, K., Bringmark, L., Timm, B., Aastrup, M., Andersson, A., Hovsenius, G., Håkanson, L.,  
1363 Iverfeldt, Å., and Meili, M.: Mercury in the Swedish environment — Recent research on causes, consequences  
1364 and corrective methods, *Water Air Soil Poll.*, 55, xi-261, 10.1007/BF00542429, 1991.
- 1365 Liu, F., Cheng, H., Yang, K., Zhao, C., Liu, Y., Peng, M., and Li, K.: Characteristics and influencing factors of  
1366 mercury exchange flux between soil and air in Guangzhou City, *J. of Geochem. Explor.*, 139, 115-121, 2014.
- 1367 Lodenius, M., and Tulisalo, E.: Environmental mercury contamination around a chlor-alkali plant, *B. Environ.*  
1368 *Contam. Tox.*, 32, 439-444, 1984.
- 1369 Loubet, B., Milford, C., Hensen, A., Daemmgen, U., Erismann, J. W., Cellier, P., and Sutton, M. A.: Advection of  
1370 NH<sub>3</sub> over a pasture field and its effect on gradient flux measurements, *Biogeosciences*, 6, 1295-1309, 2009.
- 1371 Ma, M., Wang, D., Sun, R., Shen, Y., and Huang, L.: Gaseous mercury emissions from subtropical forested and  
1372 open field soils in a national nature reserve, southwest China, *Atmos. Environ.*, 64, 2013.
- 1373 Magarelli, G., and Fostier, A. H.: Influence of deforestation on the mercury air/soil exchange in the Negro River  
1374 Basin, Amazon, *Atmos. Environ.*, 39, 7518-7528, 2005.
- 1375 Mann, E. A., Mallory, M. L., Ziegler, S. E., Avery, T. S., Tordon, R., and O'Driscoll, N. J.: Photoreducible mercury  
1376 loss from Arctic snow is influenced by temperature and snow age, *Environ. Sci. Technol.*, 49, 12120-12126,  
1377 2015a.
- 1378 Mann, E. A., Mallory, M. L., Ziegler, S. E., Tordon, R., and O'Driscoll, N. J.: Mercury in Arctic snow: Quantifying  
1379 the kinetics of photochemical oxidation and reduction, *Sci. Total Environ.*, 509-510, 115-132, 2015b.
- 1380 Marsik, F. J., Keeler, G. J., Lindberg, S. E., and Zhang, H.: Air-surface exchange of gaseous mercury over a mixed  
1381 sawgrass-cattail stand within the Florida Everglades, *Environ. Sci. Technol.*, 39, 4739-4746, 2005.
- 1382 Marumoto, K., and Imai, S.: Determination of dissolved gaseous mercury in seawater of Minamata Bay and  
1383 estimation for mercury exchange across air-sea interface, *Mar. Chem.*, 168, 9-17, 2015.
- 1384 Mason, R. P., and Fitzgerald, W. F.: The distribution and biogeochemical cycling of mercury in the equatorial  
1385 Pacific Ocean, *Deep-Sea Res. Pt. I*, 40, 1897-1924, 1993.
- 1386 Mason, R. P., Fitzgerald, W. F., Hurley, J., Hanson, A. K., Donaghay, P. L., and Sieburth, J. M.: Mercury  
1387 biogeochemical cycling in a stratified estuary, *Limnol. Oceanogr.*, 38, 1227-1241, 1993.
- 1388 Mason, R. P., and Sullivan, K. A.: Mercury in Lake Michigan, *Environ. Sci. Technol.*, 31, 942-947, 1997.
- 1389 Mason, R. P., Rolffhus, K. R., and Fitzgerald, W. F.: Mercury in the North Atlantic, *Mar Chem*, 61, 37-53, 1998.
- 1390 Mason, R. P., Lawson, N. M., Lawrence, A. L., Leaner, J. J., Lee, J. G., and Sheu, G.-R.: Mercury in the  
1391 Chesapeake Bay, *Mar. Chem.*, 65, 77-96, 1999.
- 1392 Mason, R. P., Lawson, N. M., and Sheu, G. R.: Mercury in the Atlantic Ocean: factors controlling air-sea  
1393 exchange of mercury and its distribution in the upper waters, *Deep-Sea Res. Pt. II.*, 48, 2829-2853, 2001.
- 1394 Mason, R. P., Choi, A. L., Fitzgerald, W. F., Hammerschmidt, C. R., Lamborg, C. H., Soerensen, A. L., and  
1395 Sunderland, E. M.: Mercury biogeochemical cycling in the ocean and policy implications, *Environ. Res.*, 119,  
1396 101-117, 2012.
- 1397 Mauder, M., and Foken, T.: Documentation and instruction manual of EC Software Package TK2, 2004.
- 1398 Maxwell, J. A., Holsen, T. M., and Mondal, S.: Gaseous elemental mercury (GEM) emissions from snow surfaces  
1399 in Northern New York, *PloS One*, 8, 2013.
- 1400 Mergler, D., Anderson, H. A., Chan, L. H. M., Mahaffey, K. R., Murray, M., Sakamoto, M., and Stern, A. H.:  
1401 Methylmercury exposure and health effects in humans: a worldwide concern, *AMBIO*, 36, 3-11, 2007.
- 1402 Millhollen, A. G., Gustin, M. S., and Obrist, D.: Foliar mercury accumulation and exchange for three tree species,  
1403 *Environ. Sci. Technol.*, 40, 6001-6006, 2006a.
- 1404 Millhollen, A. G., Obrist, D., and Gustin, M. S.: Mercury accumulation in grass and forb species as a function of  
1405 atmospheric carbon dioxide concentrations and mercury exposures in air and soil, *Chemosphere*, 65, 889-897,



- 1406 2006b.
- 1407 Moncreiff, J. B., Beverland, I. J., Ó'Neill, D. H., and Cropley, F. D.: Controls on trace gas exchange observed by a  
1408 conditional sampling method, *Atmos. Environ.*, 32, 3265-3274, 1998.
- 1409 Moore, C., and Carpi, A.: Mechanisms of the emission of mercury from soil: Role of UV radiation, *J. Geophys.*  
1410 *Res.-Atmos.*, 110, D24302, doi:10.1029/2004JD005567, 2005.
- 1411 Moore, C. W., Obrist, D., Steffen, A., Staebler, R. M., Douglas, T. A., Richter, A., and Nghiem, S. V.: Convective  
1412 forcing of mercury and ozone in the Arctic boundary layer induced by leads in sea ice, *Nature*, 506, 81-84, 2014.
- 1413 Moreno, F., Anderson, C. N., Stewart, R., Robinson, B., Nomura, R., Ghomshei, M., and Meech, J. A.: Effect of  
1414 thioligands on plant-Hg accumulation and volatilisation from mercury-contaminated mine tailings, *Plant Soil*, 275,  
1415 233-246, 2005a.
- 1416 Moreno, F. N., Anderson, C. W. N., Stewart, R. B., Robinson, B. H., Ghomshei, M., and Meech, J. A.: Induced  
1417 plant uptake and transport of mercury in the presence of sulphur-containing ligands and humic acid, *New Phytol.*,  
1418 166, 445-454, 2005b.
- 1419 Nacht, D. M., and Gustin, M. S.: Mercury emissions from background and altered geologic units throughout  
1420 Nevada, *Water Air Soil Poll.*, 151, 179-193, 2004.
- 1421 Nacht, D. M., Gustin, M. S., Engle, M. A., Zehner, R. E., and Giglioli, A. D.: Atmospheric mercury emissions and  
1422 speciation at the sulphur bank mercury mine superfund site, Northern California, *Environ. Sci. Technol.*, 38,  
1423 1977-1983, 2004.
- 1424 Narukawa, M., Sakata, M., Marumoto, K., and Asakura, K.: Air-sea exchange of mercury in Tokyo Bay, *J.*  
1425 *Oceanogr.*, 62, 249-257, 2006.
- 1426 Nemitz, E., Flynn, M., Williams, P., Milford, C., Theobald, M., Blatter, A., Gallagher, M., and Sutton, M.: A  
1427 relaxed eddy accumulation system for the automated measurement of atmospheric ammonia fluxes, *Water Air*  
1428 *Soil Poll.*, 1, 189-202, 2001.
- 1429 Nguyen, H. T., Kim, K. H., Kim, M. Y., and Shon, Z. H.: Exchange pattern of gaseous elemental mercury in an  
1430 active urban landfill facility, *Chemosphere*, 70, 821-832, 2008.
- 1431 Niu, Z. C., Zhang, X. S., Wang, Z. W., and Ci, Z. J.: Field controlled experiments of mercury accumulation in  
1432 crops from air and soil, *Environ. Poll.*, 159, 2684-2689, 2011.
- 1433 O'Driscoll, N. J., Beauchamp, S., Siciliano, S. D., Rencz, A. N., and Lean, D. R. S.: Continuous analysis of  
1434 dissolved gaseous mercury (DGM) and mercury flux in two freshwater lakes in Kejimikujik Park, Nova Scotia:  
1435 Evaluating mercury flux models with quantitative data, *Environ. Sci. Technol.*, 37, 2226-2235, 2003.
- 1436 O'Driscoll, N. J., Siciliano, S. D., Lean, D. R. S., and Amyot, M.: Gross photoreduction kinetics of mercury in  
1437 temperate freshwater lakes and rivers: Application to a general model of DGM dynamics, *Environ. Sci. Technol.*,  
1438 40, 837-843, 2006.
- 1439 O'Driscoll, N. J., Poissant, L., Canario, J., Ridal, J., and Lean, D. R. S.: Continuous analysis of dissolved gaseous  
1440 mercury and mercury volatilization in the upper St. Lawrence River: Exploring temporal relationships and UV  
1441 attenuation, *Environ. Sci. Technol.*, 41, 5342-5348, 2007.
- 1442 O'Driscoll, N. J., Poissant, L., Canario, J., and Lean, D. R. S.: Dissolved gaseous mercury concentrations and  
1443 mercury volatilization in a frozen freshwater fluvial lake, *Environ. Sci. Technol.*, 42, 5125-5130, 2008.
- 1444 Obrist, D., Gustin, M. S., Arnone, J. A., Johnson, D. W., Schorran, D. E., and Verburg, P. S. J.: Measurements of  
1445 gaseous elemental mercury fluxes over intact tallgrass prairie monoliths during one full year, *Atmos. Environ.*, 39,  
1446 957-965, 2005.
- 1447 Obrist, D., Conen, F., Vogt, R., Siegwolf, R., and Alewell, C.: Estimation of Hg<sup>0</sup> exchange between ecosystems  
1448 and the atmosphere using <sup>222</sup>Rn and Hg<sup>0</sup> concentration changes in the stable nocturnal boundary layer, *Atmos.*  
1449 *Environ.*, 40, 856-866, 2006.
- 1450 Obrist, D.: Atmospheric mercury pollution due to losses of terrestrial carbon pools?, *Biogeochemistry*, 85,  
1451 119-123, 2007.
- 1452 Obrist, D., Johnson, D. W., Lindberg, S. E., Luo, Y., Hararuk, O., Bracho, R., Battles, J. J., Dail, D. B., Edmonds,  
1453 R. L., Monson, R. K., Ollinger, S. V., Pallardy, S. G., Pregitzer, K. S., and Todd, D. E.: Mercury distribution across  
1454 14 U.S. forests. Part I: spatial patterns of concentrations in biomass, litter, and soils, *Environ. Sci. Technol.*, 45,  
1455 3974-3981, 2011.
- 1456 Olofsson, M., Sommar, J., Ljungström, E., Andersson, M., and Wängberg, I.: Application of relaxed eddy  
1457 accumulation technique to quantify Hg<sup>0</sup> fluxes over modified soil surfaces, *Water Air Soil Poll.*, 167, 331-352,  
1458 2005.
- 1459 Osterwalder, S., Fritsche, J., Nilsson, M. B., Alewell, C., Sommar, J., Jocher, G., Schmutz, M., Rinne, J., and  
1460 Bishop, K.: A dual, single detector relaxed eddy accumulation system for long-term measurement of mercury flux,  
1461 *Atmos. Meas. Tech. Discuss.*, 8, 8113-8156, 2015.
- 1462 Pacyna, E. G., Pacyna, J. M., Fudala, J., Strzelecka-Jastrzab, E., Hlawiczka, S., and Panasiuk, D.: Mercury  
1463 emissions to the atmosphere from anthropogenic sources in Europe in 2000 and their scenarios until 2020, *Sci.*  
1464 *Total Environ.*, 370, 147-156, 2006.
- 1465 Pannu, R., Siciliano, S. D., and O'Driscoll, N. J.: Quantifying the effects of soil temperature, moisture and



- 1466 sterilization on elemental mercury formation in boreal soils, *Environ. Poll.*, 193, 138-146, 2014.
- 1467 Pierce, A., Obrist, D., Moosmüller, H., Faïn, X., and Moore, C.: Cavity ring-down spectroscopy sensor
- 1468 development for high-time-resolution measurements of gaseous elemental mercury in ambient air, *Atmos. Meas.*
- 1469 *Tech.*, 6, 1477-1489, 2013.
- 1470 Pierce, A. M., Moore, C. W., Wohlfahrt, G., Hörtnagl, L., Kljun, N., and Obrist, D.: Eddy covariance flux
- 1471 measurements of gaseous elemental mercury using cavity ring-down spectroscopy, *Environ. Sci. Technol.*, 49,
- 1472 1559-1568, 2015.
- 1473 Pirrone, N., Cinnirella, S., Feng, X., Finkelman, R. B., Friedli, H. R., Leaner, J., Mason, R., Mukherjee, A. B.,
- 1474 Stracher, G. B., Streets, D. G., and Telmer, K.: Global mercury emissions to the atmosphere from anthropogenic
- 1475 and natural sources, *Atmos. Chem. Phys.*, 10, 5951-5964, 2010.
- 1476 Poissant, L., and Casimir, A.: Water-air and soil-air exchange rate of total gaseous mercury measured at
- 1477 background sites, *Atmos. Environ.*, 32, 883-893, 1998.
- 1478 Poissant, L., Pilote, M., and Casimir, A.: Mercury flux measurements in a naturally enriched area: Correlation
- 1479 with environmental conditions during the Nevada Study and Tests of the Release of Mercury From Soils
- 1480 (STORMS), *J. Geophys. Res.-Atmos.*, 104, 21845-21857, 1999.
- 1481 Poissant, L., Amyot, M., Pilote, M., and Lean, D.: Mercury water-air exchange over the Upper St. Lawrence River
- 1482 and Lake Ontario, *Environ. Sci. Technol.*, 34, 3069-3078, 2000.
- 1483 Poissant, L., Pilote, M., Constant, P., Beauvais, C., Zhang, H. H., and Xu, X.: Mercury gas exchanges over
- 1484 selected bare soil and flooded sites in the bay St. Francois wetlands (Quebec, Canada), *Atmos. Environ.*, 38,
- 1485 4205-4214, 2004a.
- 1486 Poissant, L., Pilote, M., Xu, X. H., Zhang, H., and Beauvais, C.: Atmospheric mercury speciation and deposition
- 1487 in the Bay St. Francois wetlands, *J. Geophys. Res.-Atmos.*, 109, D11301, doi:10.1029/2003JD004364, 2004b.
- 1488 Poissant, L., Pilote, M., Yumvihoze, E., and Lean, D.: Mercury concentrations and foliage/atmosphere fluxes in a
- 1489 maple forest ecosystem in Quebec, Canada, *J. Geophys. Res.-Atmos.*, 113, D10307, doi:10.1029/2007JD009510,
- 1490 2008.
- 1491 Poulain, A. J., Lalonde, J. D., Amyot, M., Shead, J. A., Raofie, F., and Ariya, P. A.: Redox transformations of
- 1492 mercury in an Arctic snowpack at springtime, *Atmos. Environ.*, 38, 6763-6774, 2004.
- 1493 Poulain, A. J., Roy, V., and Amyot, M.: Influence of temperate mixed and deciduous tree covers on Hg
- 1494 concentrations and photoredox transformations in snow, *Geochim. Cosmochim. Ac.*, 71, 2448-2462, 2007.
- 1495 Quinones, J. L., and Carpi, A.: An Investigation of the kinetic processes influencing mercury emissions from sand
- 1496 and soil samples of varying thickness, *J. Environ. Qual.*, 40, 647-652, 2011.
- 1497 Qureshi, A., O'Driscoll, N. J., MacLeod, M., Neuhold, Y. M., and Hungerbühler, K.: Photoreactions of mercury in
- 1498 surface ocean water: gross reaction kinetics and possible pathways, *Environ. Sci. Technol.*, 44, 644-649, 2010.
- 1499 Qureshi, A., MacLeod, M., and Hungerbühler, K.: Quantifying uncertainties in the global mass balance of
- 1500 mercury, *Global Biogeochem. Cy.*, 25, GB4012, Gb4012, 10.1029/2011gb004068, 2011a.
- 1501 Qureshi, A., MacLeod, M., Sunderland, E., and Hungerbühler, K.: Exchange of elemental mercury between the
- 1502 oceans and the atmosphere, in: *Environmental Chemistry and Toxicology of Mercury*, edited by: Liu, G. L., Cai,
- 1503 Y., and O'Driscoll, N., John Wiley & Sons, Inc: Hoboken, NJ, 389-421, 2011b.
- 1504 Ravichandran, M.: Interactions between mercury and dissolved organic matter - a review, *Chemosphere*, 55,
- 1505 319-331, 2004.
- 1506 Rea, A. W., Lindberg, S. E., Scherbatskoy, T., and Keeler, G. J.: Mercury accumulation in foliage over time in two
- 1507 northern mixed-hardwood forests, *Water Air Soil Poll.*, 133, 49-67, 2002.
- 1508 Rinklebe, J., During, A., Overesch, M., Wennrich, R., Stark, H. J., Mothes, S., and Neue, H. U.: Optimization of a
- 1509 simple field method to determine mercury volatilization from soils-Examples of 13 sites in floodplain ecosystems
- 1510 at the Elbe River (Germany), *Ecol. Eng.*, 35, 319-328, 2009.
- 1511 Rolffhus, K. R., and Fitzgerald, W. F.: The evasion and spatial/temporal distribution of mercury species in Long
- 1512 Island Sound, CT-NY, *Geochim. Cosmochim. Ac.*, 65, 407-418, 2001.
- 1513 Rutter, A. P., Schauer, J. J., Shafer, M. M., Creswell, J., Olson, M. R., Clary, A., Robinson, M., Parman, A. M., and
- 1514 Katzman, T. L.: Climate Sensitivity of Gaseous Elemental Mercury Dry Deposition to Plants: Impacts of
- 1515 Temperature, Light Intensity, and Plant Species, *Environ. Sci. Technol.*, 45, 569-575, 2011a.
- 1516 Rutter, A. P., Schauer, J. J., Shafer, M. M., Creswell, J. E., Olson, M. R., Robinson, M., Collins, R. M., Parman, A.
- 1517 M., Katzman, T. L., and Mallek, J. L.: Dry deposition of gaseous elemental mercury to plants and soils using
- 1518 mercury stable isotopes in a controlled environment, *Atmos. Environ.*, 45, 848-855, 2011b.
- 1519 Scholtz, M. T., Van Heyst, B. J., and Schroeder, W.: Modelling of mercury emissions from background soils, *Sci.*
- 1520 *Total Environ.*, 304, 185-207, 2003.
- 1521 Schroeder, W., Lindqvist, O., Munthe, J., and Xiao, Z. F.: Volatilization of mercury from lake surfaces, *Sci. Total*
- 1522 *Environ.*, 125, 47-66, 1992.
- 1523 Schroeder, W., Anlauf, K., Barrie, L., Lu, J., Steffen, A., Schneeberger, D., and Berg, T.: Arctic springtime
- 1524 depletion of mercury, *Nature*, 394, 331-332, 1998.
- 1525 Schroeder, W. H., Munthe, J., and Lindqvist, O.: Cycling of mercury between water, air, and soil compartments of



- 1526 the environment, *Water Air Soil Poll.*, 48, 337-347, 1989.
- 1527 Schroeder, W. H., Steffen, A., Scott, K., Bender, T., Prestbo, E., Ebinghaus, R., Lu, J. Y., and Lindberg, S. E.:
- 1528 Summary report: first international Arctic atmospheric mercury research workshop, *Atmos. Environ.*, 37,
- 1529 2551-2555, 2003.
- 1530 Schroeder, W. H., Beauchamp, S., Edwards, G., Poissant, L., Rasmussen, P., Tordon, R., Dias, G., Kemp, J., Van
- 1531 Heyst, B., and Banic, C. M.: Gaseous mercury emissions from natural sources in Canadian landscapes, *J. Geophys.*
- 1532 *Res.-Atmos.*, 110, D18302, doi:10.1029/2004JD005699, 2005.
- 1533 Selin, N. E., Jacob, D. J., Park, R. J., Yantosca, R. M., Strode, S., Jaegle, L., and Jaffe, D.: Chemical cycling and
- 1534 deposition of atmospheric mercury: Global constraints from observations, *J. Geophys. Res.-Atmos.*, 112, D02308,
- 1535 doi:10.1029/2006JD007450, 2007.
- 1536 Selin, N. E., Jacob, D. J., Yantosca, R. M., Strode, S., Jaegle, L., and Sunderland, E. M.: Global 3-D
- 1537 land-ocean-atmosphere model for mercury: Present-day versus preindustrial cycles and anthropogenic enrichment
- 1538 factors for deposition, *Global Biogeochem. Cy.*, 22, GB2011, doi:10.1029/2007GB003040, 2008.
- 1539 Selin, N. E.: Global Biogeochemical Cycling of Mercury: A Review, *Annu Rev Env Resour.*, 34, 43-63, 2009.
- 1540 Sherman, L. S., Blum, J. D., Johnson, K. P., Keeler, G. J., Barres, J. A., and Douglas, T. A.: Mass-independent
- 1541 fractionation of mercury isotopes in Arctic snow driven by sunlight, *Nat. Geosci.*, 3, 173-177, 2010.
- 1542 Shetty, S. K., Lin, C. J., Streets, D. G., and Jang, C.: Model estimate of mercury emission from natural sources in
- 1543 East Asia, *Atmos. Environ.*, 42, 8674-8685, 2008.
- 1544 Si, L., and Ariya, P. A.: Photochemical reactions of divalent mercury with thioglycolic acid: Formation of
- 1545 mercuric sulfide particles, *Chemosphere*, 119, 467-472, 2015.
- 1546 Siciliano, S. D., O'Driscoll, N. J., and Lean, D. R. S.: Microbial Reduction and Oxidation of Mercury in
- 1547 Freshwater Lakes, *Environ. Sci. Technol.*, 36, 3064-3068, 2002.
- 1548 Sigler, J. M., and Lee, X.: Gaseous mercury in background forest soil in the northeastern United States, *J. Geophys.*
- 1549 *Res.-Atmos.*, 111, G02007, doi:10.1029/2005JG000106, 2006.
- 1550 Sjöholm, M., Weibring, P., Edner, H., and Svanberg, S.: Atomic mercury flux monitoring using an optical
- 1551 parametric oscillator based lidar system, *Opt. Express*, 12, 551-556, 2004.
- 1552 Skyllberg, U., Bloom, P. R., Qian, J., Lin, C. M., and Bleam, W. F.: Complexation of mercury(II) in soil organic
- 1553 matter: EXAFS evidence for linear two-coordination with reduced sulfur groups, *Environ. Sci. Technol.*, 40,
- 1554 4174-4180, 2006.
- 1555 Slemr, F., Seiler, W., Eberling, C., and Roggendorf, P.: The determination of total gaseous mercury in air at
- 1556 background levels, *Anal. Chim. Acta*, 110, 35-47, 1979.
- 1557 Slemr, F., Brunke, E. G., Whittlestone, S., Zahorowski, W., Ebinghaus, R., Kock, H. H., and Labuschagne, C.:
- 1558 <sup>222</sup>Rn-calibrated mercury fluxes from terrestrial surface of southern Africa, *Atmos. Chem. Phys.*, 13, 6421-6428,
- 1559 2013.
- 1560 Smith-Downey, N. V., Sunderland, E. M., and Jacob, D. J.: Anthropogenic impacts on global storage and
- 1561 emissions of mercury from terrestrial soils: Insights from a new global model, *J. Geophys. Res.-Biogeo.*, 115,
- 1562 G03008, doi:10.1029/2009JG001124, 2010.
- 1563 Smith, L. M., and Reinfelder, J. R.: Mercury volatilization from salt marsh sediments, *J. Geophys. Res.-Biogeo.*,
- 1564 114, G00C09, doi:10.1029/2009JG000979, 2009.
- 1565 Soerensen, A. L., Sunderland, E. M., Holmes, C. D., Jacob, D. J., Yantosca, R. M., Skov, H., Christensen, J. H.,
- 1566 Strode, S. A., and Mason, R. P.: An improved global model for air-sea exchange of mercury: high concentrations
- 1567 over the North Atlantic, *Environ. Sci. Technol.*, 44, 8574-8580, 2010.
- 1568 Sommar, J., Wängberg, I., Berg, T., Gärdfeldt, K., Munthe, J., Richter, A., Urba, A., Wittrock, F., and Schroeder,
- 1569 W. H.: Circumpolar transport and air-surface exchange of atmospheric mercury at Ny-Åringslesund (79° N),
- 1570 Svalbard, spring 2002, *Atmos. Chem. Phys.*, 7, 151-166, 2007.
- 1571 Sommar, J., Zhu, W., Lin, C.-J., and Feng, X.: Field approaches to measure Hg exchange between natural surfaces
- 1572 and the atmosphere - a review, *Critical Reviews in Environmental Science and Technology*, 43, 1657-1739, 2013a.
- 1573 Sommar, J., Zhu, W., Shang, L., Feng, X., and Lin, C.-J.: A whole-air relaxed eddy accumulation measurement
- 1574 system for sampling vertical vapour exchange of elemental mercury, *Tellus B*, 65, 19940,
- 1575 <http://dx.doi.org/10.3402/tellusb.v65i0.19940>, 2013b.
- 1576 Sommar, J., Zhu, W., Shang, L., Lin, C. J., and Feng, X. B.: Seasonal variations in metallic mercury (Hg<sup>0</sup>) vapor
- 1577 exchange over biannual wheat & corn rotation cropland in the North China Plain, *Biogeosciences Discuss.*,
- 1578 12, 16105-16158, 2015.
- 1579 Song, X. X., and Van Heyst, B.: Volatilization of mercury from soils in response to simulated precipitation, *Atmos.*
- 1580 *Environ.*, 39, 7494-7505, 2005.
- 1581 Southworth, G., Lindberg, S., Hintelmann, H., Amyot, M., Poulain, A., Bogle, M., Peterson, M., Rudd, J., Harris,
- 1582 R., Sandilands, K., Krabbenhoft, D., and Olsen, M.: Evasion of added isotopic mercury from a northern temperate
- 1583 lake, *Environ. Toxicol. Chem.*, 26, 53-60, 2007.
- 1584 Sprovieri, F., Pirrone, N., Ebinghaus, R., Kock, H., and Dommergue, A.: A review of worldwide atmospheric
- 1585 mercury measurements, *Atmos. Chem. Phys.*, 10, 8245-8265, 2010.



- 1586 St. Louis, V. L., Sharp, M. J., Steffen, A., May, A., Barker, J., Kirk, J. L., Kelly, D. J. A., Arnott, S. E., Keatley, B.,  
1587 and Smol, J. P.: Some sources and sinks of monomethyl and inorganic mercury on Ellesmere Island in the  
1588 Canadian high Arctic, *Environ. Sci. Technol.*, 39, 2686-2701, 2005.
- 1589 Stamenkovic, J., and Gustin, M. S.: Evaluation of use of EcoCELL technology for quantifying total gaseous  
1590 mercury fluxes over background substrates, *Atmos. Environ.*, 41, 3702-3712, 2007.
- 1591 Stamenkovic, J., Gustin, M. S., Arnone, J. A., Johnson, D. W., Larsen, J. D., and Verburg, P. S. J.: Atmospheric  
1592 mercury exchange with a tallgrass prairie ecosystem housed in mesocosms, *Sci. Total Environ.*, 406, 227-238,  
1593 2008.
- 1594 Stamenkovic, J., and Gustin, M. S.: Nonstomatal versus stomatal uptake of atmospheric mercury, *Environ. Sci.*  
1595 *Technol.*, 43, 1367-1372, 2009.
- 1596 Steen, A. O., Berg, T., Dastoor, A. P., Durnford, D. A., Hole, L. R., and Pfaffhuber, K. A.: Dynamic exchange of  
1597 gaseous elemental mercury during polar night and day, *Atmos. Environ.*, 43, 5604-5610, 2009.
- 1598 Steffen, A., Douglas, T., Amyot, M., Ariya, P., Aspmo, K., Berg, T., Bottenheim, J., Brooks, S., Cobbett, F.,  
1599 Dastoor, A., Dommergue, A., Ebinghaus, R., Ferrari, C., Gärdfeldt, K., Goodsite, M. E., Lean, D., Poulain, A. J.,  
1600 Scherz, C., Skov, H., Sommar, J., and Temme, C.: A synthesis of atmospheric mercury depletion event chemistry  
1601 in the atmosphere and snow, *Atmos. Chem. Phys.*, 8, 1445-1482, 2008.
- 1602 Steffen, A., Bottenheim, J., Cole, A., Douglas, T. A., Ebinghaus, R., Friess, U., Netcheva, S., Nghiem, S., Sihler,  
1603 H., and Staebler, R.: Atmospheric mercury over sea ice during the OASIS-2009 campaign, *Atmos. Chem. Phys.*,  
1604 13, 7007-7021, 2013.
- 1605 Strode, S. A., Jaegle, L., Selin, N. E., Jacob, D. J., Park, R. J., Yantosca, R. M., Mason, R. P., and Slemr, F.: Air-sea  
1606 exchange in the global mercury cycle, *Global Biogeochem. Cy.*, 21, -, 2007.
- 1607 Sun, R., Wang, D., Mao, W., Zhao, S., and Zhang, C.: Roles of chloride ion in photo-reduction/oxidation of  
1608 mercury, *Chinese Sci. Bull.*, 59, 3390-3397, 2014.
- 1609 Sutton, M. A., Nemitz, E., Erisman, J. W., Beier, C., Bahl, K. B., Cellier, P., de Vries, W., Cotrufo, F., Skiba, U., Di  
1610 Marco, C., Jones, S., Laville, P., Soussana, J. F., Loubet, B., Twigg, M., Famulari, D., Whitehead, J., Gallagher, M.  
1611 W., Neftel, A., Flechard, C. R., Herrmann, B., Calanca, P. L., Schjoerring, J. K., Daemmgen, U., Horvath, L., Tang,  
1612 Y. S., Emmett, B. A., Tietema, A., Penuelas, J., Kesik, M., Brueggemann, N., Pilegaard, K., Vesala, T., Campbell,  
1613 C. L., Olesen, J. E., Dragosits, U., Theobald, M. R., Levy, P., Mobbs, D. C., Milne, R., Viovy, N., Vuichard, N.,  
1614 Smith, J. U., Smith, P., Bergamaschi, P., Fowler, D., and Reis, S.: Challenges in quantifying biosphere-atmosphere  
1615 exchange of nitrogen species, *Environ. Pollu.*, 150, 125-139, 2007.
- 1616 Temme, C., Baukau, J., Schneider, B., Aspmo, K., Fain, X., Ferrari, C., Gauchard, P.-A., and Ebinghaus, R.:  
1617 Air/water exchange of mercury in the North Atlantic Ocean during arctic summer, *Proceedings of the XIII*  
1618 *International Conference on Heavy Metals in the Environment, Rio de Janeiro, 2005*,
- 1619 Tseng, C., Lamborg, C., Fitzgerald, W., and Engstrom, D.: Cycling of dissolved elemental mercury in Arctic  
1620 Alaskan lakes, *Geochim. Cosmochim. Ac.*, 68, 1173-1184, 2004.
- 1621 UNEP Minamata Convention on Mercury. Available at <http://www.mercuryconvention.org>, last access: December  
1622 25<sup>th</sup>, 2015.
- 1623 Vost, E. E., Amyot, M., and O'Driscoll, N. J.: Photoreactions of mercury in aquatic systems, in: *Environmental*  
1624 *Chemistry and Toxicology of Mercury*, John Wiley & Sons, Inc., 193-218, 2011.
- 1625 Wallschläger, D., Turner, R. R., London, J., Ebinghaus, R., Kock, H. H., Sommar, J., and Xiao, Z. F.: Factors  
1626 affecting the measurement of mercury emissions from soils with flux chambers, *J. Geophys. Res.-Atmos.*, 104,  
1627 21859-21871, 1999.
- 1628 Wallschläger, D., Kock, H. H., Schroeder, W. H., Lindberg, S. E., Ebinghaus, R., and Wilken, R. D.: Estimating  
1629 gaseous mercury emissions from contaminated floodplain soils to the atmosphere with simple field measurement  
1630 techniques, *Water Air Soil Poll.*, 135, 39-54, 2002.
- 1631 Wang, D. Y., He, L., Shi, X. J., Wei, S. Q., and Feng, X. B.: Release flux of mercury from different environmental  
1632 surfaces in Chongqing, China, *Chemosphere*, 64, 1845-1854, 2006.
- 1633 Wang, J. X., Feng, X. B., Anderson, C. W. N., Wang, H., Zheng, L. R., and Hu, T. D.: Implications of mercury  
1634 speciation in thiosulfate treated plants, *Environ. Sci. Technol.*, 46, 5361-5368, 2012.
- 1635 Wang, S., Feng, X., Qiu, G., and Fu, X.: Comparison of air/soil mercury exchange between warm and cold season  
1636 in Hongfeng Reservoir region, *Huanjing Kexue*, 25, 123-127, 2004. (In Chinese with English Abstract)
- 1637 Wang, S., Feng, X., Qiu, G., Shang, L., Li, P., and Wei, Z.: Mercury concentrations and air/soil fluxes in Wuchuan  
1638 mercury mining district, Guizhou province, China, *Atmos. Environ.*, 41, 5984-5993, 2007a.
- 1639 Wang, S. F., Feng, X. B., Qiu, G. L., Wei, Z. Q., and Xiao, T. F.: Mercury emission to atmosphere from  
1640 Lanmuchang Hg-Tl mining area, Southwestern Guizhou, China, *Atmos. Environ.*, 39, 7459-7473, 2005.
- 1641 Wang, S. F., Feng, X. B., Qiu, G. L., Fu, X. W., and Wei, Z. Q.: Characteristics of mercury exchange flux between  
1642 soil and air in the heavily air-polluted area, eastern Guizhou, China, *Atmos. Environ.*, 41, 5584-5594, 2007b.
- 1643 Wang, X., Lin, C. J., and Feng, X.: Sensitivity analysis of an updated bidirectional air-surface exchange model for  
1644 elemental mercury vapor, *Atmos. Chem. Phys.*, 14, 6273-6287, 2014.
- 1645 Wängberg, I., Munthe, J., Pirrone, N., Iverfeldt, Å., Bahlman, E., Costa, P., Ebinghaus, R., Feng, X., Ferrara, R.,



- 1646 and Gärdfeldt, K.: Atmospheric mercury distribution in Northern Europe and in the Mediterranean region, *Atmos.*  
1647 *Environ.*, 35, 3019-3025, 2001a.
- 1648 Wängberg, I., Schmolke, S., Schager, P., Munthe, J., Ebinghaus, R., and Iverfeldt, A.: Estimates of air-sea  
1649 exchange of mercury in the Baltic Sea, *Atmos. Environ.*, 35, 5477-5484, 2001b.
- 1650 Wängberg, I., Edner, H., Ferrara, R., Lanzillotta, E., Munthe, J., Sommar, J., Sjöholm, M., Svanberg, S., and  
1651 Weibring, P.: Atmospheric mercury near a chlor-alkali plant in Sweden, *Sci. Total Environ.*, 304, 29-41, 2003.
- 1652 Wanninkhof, R.: Relationship between wind-speed and gas-exchange over the Ocean, *J. Geophys. Res.-Oceans.*,  
1653 97, 7373-7382, 1992.
- 1654 Wanninkhof, R., Asher, W. E., Ho, D. T., Sweeney, C., and McGillis, W. R.: Advances in quantifying air-sea gas  
1655 exchange and environmental forcing, *Annu. Rev. Mar. Sci.*, 1, 213-244, 2009.
- 1656 Wesely, M. L., and Hicks, B. B.: A review of the current status of knowledge on dry deposition, *Atmos. Environ.*,  
1657 34, 2261-2282, 2000.
- 1658 Wiatrowski, H. A., Ward, P. M., and Barkay, T.: Novel reduction of mercury(II) by mercury-sensitive  
1659 dissimilatory metal reducing bacteria, *Environ. Sci. Technol.*, 40, 6690-6696, 2006.
- 1660 Wright, L. P., and Zhang, L.: An approach estimating bidirectional air-surface exchange for gaseous elemental  
1661 mercury at AMNet sites, *J. Adv. Model. Earth Sy.*, 7, 35-49, 2015.
- 1662 Xiao, Z. F., Munthe, J., Schroeder, W. H., and Lindqvist, O.: Vertical fluxes of volatile mercury over forest soil and  
1663 lake surfaces in Sweden, *Tellus B*, 43, 267-279, 1991.
- 1664 Xin, M., Gustin, M. S., Ladwig, K., and Pflughoeft-Hassett, D. F.: Air-substrate mercury exchange associated  
1665 with landfill disposal of coal combustion products, *J. Air Waste Manage.*, 56, 1167-1176, 2006.
- 1666 Xin, M., and Gustin, M. S.: Gaseous elemental mercury exchange with low mercury containing soils:  
1667 Investigation of controlling factors, *Appl. Geochem.*, 22, 1451-1466, 2007.
- 1668 Xu, L. Q., Liu, R. H., Wang, J. Y., Tan, H. W., Tang, A. K., and Yu, P.: Mercury emission flux in the Jiaozhou Bay  
1669 measured by flux chamber, *Procedia Environmental Sci.*, 13, 1500-1506, 2012.
- 1670 Xu, X. H., Yang, X. S., Miller, D. R., Helble, J. J., and Carley, R. J.: Formulation of bi-directional  
1671 atmosphere-surface exchanges of elemental mercury, *Atmospheric Environment*, 33, 4345-4355, 1999.
- 1672 Yamamoto, M.: Stimulation of elemental mercury oxidation in the presence of chloride ion in aquatic  
1673 environments, *Chemosphere*, 32, 1217-1224, 1996.
- 1674 Yang, Y. K., Zhang, C., Shi, X. J., Lin, T., and Wang, D. Y.: Effect of organic matter and pH on mercury release  
1675 from soils, *J. Environ. Sci.*, 19, 1349-1354, 2007.
- 1676 Yin, R., Feng, X., and Meng, B.: Stable Hg isotope variation in rice plants (*Oryza sativa* L.) from the Wanshan Hg  
1677 mining district, SW China, *Environ. Sci. Technol.*, 2013.
- 1678 Zehner, R. E., and Gustin, M. S.: Estimation of mercury vapor flux from natural substrate in Nevada, *Environ. Sci.*  
1679 *Technol.*, 36, 4039-4045, 2002.
- 1680 Zhang, H., and Lindberg, S. E.: Processes influencing the emission of mercury from soils: A conceptual model, *J.*  
1681 *Geophys. Res.-Atmos.*, 104, 21889-21896, 1999.
- 1682 Zhang, H., and Lindberg, S. E.: Sunlight and iron(III)-induced photochemical production of dissolved gaseous  
1683 mercury in freshwater, *Environ. Sci. Technol.*, 35, 928-935, 2001.
- 1684 Zhang, H., Lindberg, S. E., Marsik, F. J., and Keeler, G. J.: Mercury air/surface exchange kinetics of background  
1685 soils of the Tahquamenon River watershed in the Michigan Upper Peninsula, *Water Air Soil Poll.*, 126, 151-169,  
1686 2001.
- 1687 Zhang, H., Lindberg, S. E., Barnett, M. O., Vette, A. F., and Gustin, M. S.: Dynamic flux chamber measurement of  
1688 gaseous mercury emission fluxes over soils. Part 1: simulation of gaseous mercury emissions from soils using a  
1689 two-resistance exchange interface model, *Atmos. Environ.*, 36, 835-846, 2002.
- 1690 Zhang, H.: Photochemical redox reactions of mercury, In *Recent Developments in Mercury Science*, pp. 37-79.  
1691 Springer Berlin Heidelberg, 2006.
- 1692 Zhang, H., Dill, C., Kuiken, T., Ensor, M., and Crocker, W. C.: Change of dissolved gaseous mercury  
1693 concentrations in a southern reservoir lake (Tennessee) following seasonal variation of solar radiation, *Environ.*  
1694 *Sci. Technol.*, 40, 2114-2119, 2006a.
- 1695 Zhang, H., Lindberg, S. E., and Kuiken, T.: Mysterious diel cycles of mercury emission from soils held in the dark  
1696 at constant temperature, *Atmos. Environ.*, 42, 5424-5433, 2008.
- 1697 Zhang, H., Feng, X., Larssen, T., Qiu, G., and Vogt, R. D.: In inland China, rice, rather than fish, is the major  
1698 pathway for methylmercury exposure, *Environ. Health Persp.*, 118, 1183-1188, 2010.
- 1699 Zhang, H. H., Poissant, L., Xu, X. H., and Pilote, M.: Explorative and innovative dynamic flux bag method  
1700 development and testing for mercury air-vegetation gas exchange fluxes, *Atmos. Environ.*, 39, 7481-7493, 2005.
- 1701 Zhang, H. H., Poissant, L., Xu, X. H., Pilote, M., Beauvais, C., Amyot, M., Garcia, E., and Laroulandie, J.:  
1702 Air-water gas exchange of mercury in the Bay Saint Francois wetlands: Observation and model parameterization,  
1703 *J. Geophys. Res.-Atmos.*, 111, D17307, doi:10.1029/2005JD006930, 2006b.
- 1704 Zhang, L., Blanchard, P., Gay, D. A., Prestbo, E. M., Risch, M. R., Johnson, D., Narayan, J., Zsolway, R., Holsen,  
1705 T. M., Miller, E. K., Castro, M. S., Graydon, J. A., Louis, V. L. S., and Dalziel, J.: Estimation of speciated and total



- 1706 mercury dry deposition at monitoring locations in eastern and central North America, *Atmos. Chem. Phys.*, 12,  
1707 4327-4340, 2012a.
- 1708 Zhang, L. M., Wright, L. P., and Blanchard, P.: A review of current knowledge concerning dry deposition of  
1709 atmospheric mercury, *Atmos. Environ.*, 43, 5853-5864, 2009.
- 1710 Zhang, Y. T., Chen, X., Yang, Y. K., Wang, D. Y., and Liu, X.: Effect of dissolved organic matter on mercury  
1711 release from water body, *J. Environ. Sci.*, 23, 912-917, 2011.
- 1712 Zhang, Y. T., Sun, R. G., Ma, M., and Wang, D. Y.: Study of inhibition mechanism of  $\text{NO}_3^-$  on photoreduction of  
1713  $\text{Hg(II)}$  in artificial water, *Chemosphere*, 87, 171-176, 2012b.
- 1714 Zheng, N., Liu, J. S., Wang, Q. C., and Liang, Z. Z.: Mercury contamination due to zinc smelting and chlor-alkali  
1715 production in NE China, *Appl. Geochem.*, 26, 188-193, 2011.
- 1716 Zheng, W., and Hintelmann, H.: Isotope fractionation of mercury during its photochemical reduction by  
1717 low-molecular-weight organic compounds, *J. Phys. Chem. A*, 114, 4246-4253, 2010.
- 1718 Zheng, W., Liang, L. Y., and Gu, B. H.: Mercury reduction and oxidation by reduced natural organic matter in  
1719 anoxic environments, *Environ. Sci. Technol.*, 46, 292-299, 2012.
- 1720 Zheng, W., Lin, H., Mann, B. F., Liang, L., and Gu, B.: Oxidation of dissolved elemental mercury by thiol  
1721 compounds under anoxic conditions, *Environ. Sci. Technol.*, 47, 12827-12834, 2013.
- 1722 Zhu, J. S., Wang, D. Y., Liu, X. A., and Zhang, Y. T.: Mercury fluxes from air/surface interfaces in paddy field and  
1723 dry land, *Appl. Geochem*, 26, 249-255, 2011.
- 1724 Zhu, J. S., Wang, D. Y., and Ma, M.: Mercury release flux and its influencing factors at the air-water interface in  
1725 paddy field in Chongqing, China, *Chinese Sci. Bull.*, 58, 266-274, 2013a.
- 1726 Zhu, W., Li, Z., Chai, X., Hao, Y., Lin, C.-J., Sommar, J., and Feng, X.: Emission characteristics and air-surface  
1727 exchange of gaseous mercury at the largest active landfill in Asia, *Atmos. Environ.*, 79, 188-197, 2013b.
- 1728 Zhu, W., Sommar, J., Li, Z., Feng, X., Lin, C.-J., and Li, G.: Highly elevated emission of mercury vapor due to the  
1729 spontaneous combustion of refuse in a landfill, *Atmos. Environ.*, 79, 540-545, 2013c.
- 1730 Zhu, W., Sommar, J., Lin, C. J., and Feng, X.: Mercury vapor air-surface exchange measured by collocated  
1731 micrometeorological and enclosure methods – Part II: Bias and uncertainty analysis, *Atmos. Chem. Phys.*, 15,  
1732 5359-5376, 2015a.
- 1733 Zhu, W., Sommar, J., Lin, C. J., and Feng, X.: Mercury vapor air-surface exchange measured by collocated  
1734 micrometeorological and enclosure methods - Part I: Data comparability and method characteristics, *Atmos.*  
1735 *Chem. Phys.*, 15, 685-702, 2015b.
- 1736